OPTIMIZATION OF DONNAN DIALYSIS FOR ALUM RECOVERY FROM POTABLE WATER TREATMENT RESIDUES

A thesis submitted in fulfilment of the academic requirements for the degree of Master of Engineering in Chemical Engineering in the Faculty of Engineering and The Built Environment at the Durban University of Technology, Durban, South Africa

Dennis Asante-Sackey

Supervisors: Prof. Sudesh Rathilal

Prof. V. L Pillay

Date: February, 2021

ABSTRACT

Treatment of effluent water to meet fresh water discharge limits is very essential. Aluminium sulphate (alum) is the most widely used coagulant during the pre-treatment process, however, it generates a large amount of residue. Subsequent discharge of these residues from potable water treatment plants (PWTPs) to landfill sites and river bodies, without treatment, poses a great threat to the ecosystem and human health. In essence, the rising concern of managing residues, associated with the disposal cost, toxicity and stringent legislation, calls for more robust and effective technologies. In response, this study comes in handy owing to the green chemistry benefits of aluminium recovery from PWTPs for reuse.

Primary recovery methods include acid treatment and alkalization. Although these two recovery processes ensue a minimum of 60% recovery, organics and heavy metals solubilize during the process. Donnan dialysis as a separation, recovery and concentrating technology is investigated in this project. The aims and objectives were to optimize the recovery of aluminium using Donnan dialysis with respect to phase conditions, to evaluate the inhibition effect of selected metals on aluminium transport and finally, to establish the organic transport in Donnan dialysis.

Using a statistical approach, the feed phase conditions such as feed flowrate (0.64-2.21 mL/s), feed concentration (100-3300 mg/L), and pH (1.3-3.7) were considered against sweep phase conditions of acid concentration (0.25-1 N) and flowrate (0.64-2.21 mL/s). The response surface methodology's face-centered central composite design (FC-CCD) statistical method was adapted for the selection of influential factors and establishing the relationship between selected conditions. The FC-CCD used had three levels and six center points for analysis. The effect of Ca, Mg, Mn, Fe, Cu, Zn and Pb on Al permeation through the Nafion 117 membrane was studied at constant flow and concentration conditions. Once the effects in the binary inhibition study were completed, aluminium recovery from a residue obtained from a local PWTP was conducted. Simultaneously, the rejection of organics by the membrane was also assessed during the aluminium recovery process.

Preliminary experiment validation experiments showed a high deviation of ±6.4 mg/L at the feed phase, 7.33% deviation at the sweep phase and mass balance closure greater than 95%. Furthermore, study on the water transport across the membrane was directly proportional to the acid concentration. Comparing HCl and H_2SO_4, HCl had a lower Van't Hoff factor, hence, was used in proceeding experiments. A one factor at a time experiment to determine the final range of feed concentration to use showed that a maximum of 2000 mg/L was required to meet a 50% recovery target.

The FC-CCD experiment showed that the ascending order of the effects of factors was sweep flowrate < feed flowrate < sweep concentration < feed concentration. The sweep flowrate had a negative influence on aluminium permeation and was statistically insignificant ($p > 0.05$). Quadratic and predictive models developed at different time intervals were statistically significant at a 95% confidence level. Also, a high recovery of 94% and high concentrating effect at the sweep phase was 1.65 in the 2:1 feed to sweep phase volume experiment.

Analysis of FC-CCD combinative study of feed concentration, pH of feed phase and feed flowrate showed that a high feed concentration (> 1000 mg/L) at a high pH (> 2.5) will yield an Al-recovery > 60%. At a 95% confidence level, the statistical analysis showed that the pH was the most significant factor. The interacting factors for the statistically significant model was feed concentration-feed flowrate and feed concentration-pH.

The one-on-one inhibitive study at equal phase flowrates and feed concentration revealed that Fe gave the highest inhibition while the least transport across the Nafion 117 membrane was Mn^{2+}. In descending order, $Fe^{2+} > Ca^{2+} > Zn^{2+} > Mg^{2+} > Cu^{2+}$. The rejection of organics is limited to 24-32 hours where a maximum of 98% rejection was achieved under the synthetized solution and acid digested residue runs.

In conclusion, Donnan dialysis by RSM has proven to be feasible for the recovery of aluminium from potable water treatment residue. Also, the FC-CCD adapted from the RSM is seen to be very promising, economical and a reliable alternative statistical tool to determine the most influential factor and predict and obtain the optimal operation conditions for a system. Therefore, there are economic, sustainable and research prospects of DD coupled with RSM towards recovery of metal salts and heavy metals from PWTP residues in large scale implementation.

DECLARATION

I, **Dennis Asante-Sackey** with student number 21752262, declare that:

i. The research reported in this thesis, except where otherwise indicated, is my original work.

ii. This thesis has not been submitted for any degree or examination at any other university.

iii. This thesis does not contain other persons' data, pictures, graphs, or other information, unless specifically acknowledged as being sourced from other persons.

iv. This thesis does not contain other persons' writing, unless specifically acknowledged as being sourced from other researchers. Where other written sources have been quoted, then:

   a. their words have been re-written, but the general information attributed to them has been referenced;

   b. Where their exact words have been used, their writing has been placed inside quotation marks and referenced.

v. Where I have reproduced a publication of which I am an author, co-author, or editor, I have indicated in detail which part of the publication was actually written by myself alone and have fully referenced such publications.

vi. This thesis does not contain text, graphics or tables copied and pasted from the Internet, unless specifically acknowledged, and the source being detailed in the thesis and in the References sections.

Signature

Dennis Asante-Sackey (Student) Date: 27th February, 2020.

As the candidate supervisors, we do agree to the submission of this dissertation that has orally been defended.

Prof. Sudesh Rathilal — (Main supervisor)

Prof. V.L Pillay — (Co-supervisor)

Singature of supervisor

Date: 30 April 2021

DEDICATION

This thesis is dedicated to,

the all-caring sister, Gladys Boachie

the overcome your distractions Father, Bishop James K. Nkrumah

and

the supportive and passionate brother, Emmanuel K. Tetteh

[Proverbs 3:5-6]

ACKNOWLEDGEMENTS

With a deep heart of gratitude, I would thank the Lord Jesus Christ for granting me the Grace and understanding and inspiration to complete this project.

I owe my sincere thanks and appreciation to my main supervisor Prof. Sudesh Rathilal for his contribution in the form of critique, guidance, advice and presence though out the research work. I also wish to thank Prof. V.L Pillay for my co-supervisor for taking me up on this research work and for giving me the needed direction and encouragement.

To Mr. Krivishen Pillay (Institute of Water and Wastewater Treatment-IWWT, DUT) and Mr. Jimmy Sathianathan Ramsamy Chetty (Chemistry Department) for advising and assisting with the analytical techniques for this work. Ildephonse Habyalimana, Mr Christy Terrence and Mr. Jaafar cannot be forgotten as they readily assisted in the purchase orders and other relevant acquisitions.

Furthermore, I would like to thank the Water Research Commision and the National Research Fund for their financial support to undertake this project.

There are friends who stick closer than a brother. I say thank you to My Ghanaian brothers, Dr. Isaac Dennis Amoah (IWWT-DUT), Emmanuel K. Tetteh, Mr. Edward Kwaku Armah and Elorm Ezugbe for their contributions towards my experiments and for proof reading the thesis.

Additionally, I want to to thank Sabatha Lithuli (U.S alumni colleague), Sis Bandi and the Winners Chaple-Durban for making South Africa a home to me. Also, I appreciate the gains after meeting with Pastor Dr. Obed Obeng-Addae (Christ Cosmopolitan Incorporated, Ghana) and Prophet

Dominic Andoh Owusu. Lastly, to my parents and siblings, I say a big thank you for the love and travails. God bless you all. Amen!

TABLE OF CONTENT

LIST OF FIGURES

LIST OF TABLES

ABBREVIATIONS

AEM	Anion exchange membrane
CEM	Cation exchange membrane
CCD	Central composite design
DBPs	Disinfection by-products
DD	Donnan dialysis
DOC	Dissolved organic compounds
DOE	Design of Experiment
FC-CCD	Face centered central composite design
IEM	Ion exchange membrane
MF	Microfiltration
NF	Nanofiltration
NOM	Natural organic matter
OFAT	One factor at a time
PDM	Pressure driven membranes
PWTP	Potable water treatment plants
PWTR	Potable water treatment residue

RSM	Response surface methodology
TOC	Total organic carbon
UF	Ultrafiltration

RESEARCH OUTPUTS

LOCAL AND INTERNATIONAL CONFERENCES

1) **Asante-Sackey, D**., Rathilal, S., Tetteh, E.K , Pillay, V.L., 2019, A central composite design for permeation study of aluminium by Donnan membrane process, Book of Abstracts, *4th Interdisciplinary Research and Innovation Conference*, Durban-South Africa, September17-20, 2019.
2) **Asante-Sackey, D**., Rathilal, S., Tetteh, E.K , Pillay, V.L., 2019, Alum recovery using a statistical response surface methodology approach, *6th South African Young Water Professionals Biennial Conference*, Water Institute of Southern Africa (WISA), Durban-South Africa, October 20-23, 2019. [Poster]
3) **Asante-Sackey, D**., Rathilal, S., Tetteh, E.K , Pillay, V.L., 2018, Optimization of Donnan Dialysis for alum recovery using Box-behnken design, *In CBU International Conference* Proceedings, 1007-1012, Central Bohemia University. DOI: http://dx.doi.org/10.12955/cbup.v6.1286

PEER REVIEWED JOURNAL ARTICLES

1) **Asante-Sackey, D**., Rathilal,S, V.L Pillay, Tetteh E.K., 2021, Acidification route transport of aluminium in a Donnan Dialysis system, *Membrane-MDPI (In-preparation)*
2) **Asante-Sackey, D**., Rathilal,S, V.L Pillay, Tetteh E.K., 2021, Binary inhibition study in a Donnan recovery of aluminium, *(In-preparation)*.
3) **Asante-Sackey,D**., Rathilal, S, V.L Pillay, Tetteh E.K., 2021, Donnan Dialysis for Al^{3+} using the Box-behnken approach, *Cleaner Production, (In-preparation).*
4) **Asante-Sackey, D.,** Rathilal, S, Tetteh, E.K., Ezugbe, E.O., 2021, Donnan Membrane Process for the selective recovery and removal of target metal ions-A review, *Membrane (Basel)*,[Under peer review].
5) **Asante-Sackey, D**., Rathilal,S, V.L Pillay, Tetteh E.K., 2020, Ion exchange dialysis for aluminium transport through a Face Centered Central Composite Design

Approach. *Processes*. DOI: 10.3390/pr8020160

6) **Asante-Sackey, D**., Rathilal,S, V.L Pillay, Tetteh E.K., 2019, Effects of Ion exchange dialysis process variables on Aluminium permeation using response surface methodology. *Environmental Engineering Research (EER)*. DOI: 10.4491/eer.2019.297

BOOK CHAPTER AND TECHNICAL REPORT

1) Tetteh, E., Rathilal, S., Chetty, M., Armah, E.K., **Asante-Sackey, D**., 2019. Treatment of water and wastewater for reuse and energy generation-emerging technologies. *InTech Open* ISBN 978-1-78923-9300, DOI: 10.5772/intechopen.84474
2) Pillay, V.L, Mophethe, M., **Asante-Sackey, D**., 2018. The Development and Evaluation of a Donnan Dialysis Process for the Recovery and Reuse of Al from Potable Water Treatment Residual Streams. Water Research Commission-South Africa, WRC Report No. 2470/1/18, ISBN 978-1-4312-0999-6.

CHAPTER 1

INTRODUCTION

1.1 Background

Life and the functionality of ecosystems depends on water. Global risk associated with the impact of water crises in this era cannot be neglected and limited to arid areas. Whilst a projected 71% of the world's population is exposed to 1 month water scarcity annually, 1.8-2.9 billion people live under severe scarcity conditions for 4-6 months (Mekonnen and Hoekstra, 2016). As billions continue to live with insufficient or no supply of water, global demand and poor water quality is expected to escalate. This is due to withdrawal pressures from industries, households and agriculture relative to the increasing population growth and climate change. With respect to the current water demand situation, demand projections show that fresh water withdrawals will increase by 55% from its current estimated volume to 5500 km^3 by 2050 and an expected 130% increase in drinking water demand by households (Koleva et al., 2017).

Efforts to meet water demand requires treating source water to standards using acceptable practices. The efficiency of raw water treatment depends on the treatment technology applied after having considered the quality of the sourced water. Commonly adopted water treatment schemes are conventional systems and a few infused hybrid schemes which consists of pressure driven membrane (PDM) filtration, ion exchange systems and adsorption (Emelko et al., 2011). Conventional treatments are mostly applied to raw rather with high turbidity, color and total

organic constituents. The main treatment scheme includes screening, coagulation, flocculation, clarification or sedimentation, filtration and disinfection (Teh and Wu, 2014).

Coagulation is a reliable, energy friendly and easy to operate process that forms an integral part of most potable water treatment schemes (Teh and Wu, 2014). This physicochemical process involves dosing and mixing coagulant to coalesce organic and inorganic pollutants into flocs. Chemical choice and treatment dosage depends on the pH, chemical cost, required treatment efficiency and waste characteristics. Hydrolytic salts of aluminium and iron are widely used mineral coagulants with aluminium sulphate or alum dominating in primary usage. Other coagulants such as pre-hydrolyzed forms under organic coagulants are also used as coagulation aids or flocculants. Considering the overall tariff charges on distributed treated water, coagulants used by the treatment plants account for 5% of the tariff (Goldbold et al., 2003; Niquette et al., 2004).

Coagulation affects the treatment performance of the entire water treatment process as it increases filter lifetime, improves microbiological characteristics and reduces the final cost of treated water (Debora et al., 2013). The resulting flocs settle rapidly and are removed in subsequent stages in the treatment network as potable water treatment residue (PWTR). The type of primary coagulant used in the treatment plant is used to describe the PWTR. Generated PWTR is often dumped in landfills, hydric, deep wells, sanitary sewers and surface water. Parallel to treating potable water, PWTR increase is characterized by the increasing population demand on water coupled with meeting stringent quality standards. This PWTR management practice is unsustainable owing to the increasing disposal cost per volume, concerns of contaminant accumulation, surface water pollution and land competition for other economic development agendas (Babatunde and Zhao, 2007; Keeley et al., 2014a; Maiden et al., 2015). Due to the awareness of these adverse impacts

and conflicting interest, implementation of stringent legislation has commenced in different parts of the world.

While coagulation with alum continues as a result of its large commercial availability, low market price and are easy of storage, its usage involves high dosing and is associated with large PWTR generation. Aluminium in high concentration has shown acute, sub-lethal and chronic toxicity effects on aquatic species. Their increase potentially contributes to Alzheimer disease and has been linked to other neurodegenerative diseases such as dialysis encephalopathy, parkinsonism dementia and amyotrophic lateral sclerosis (Kawahara and Kato-Negishi, 2011; Mortula et al., 2009; Teh and Wu, 2014). Generally, the toxicity of alum PWTR in surface water has been a subject of debate and the general non-toxic notions exist. Although alum PWTR is a good adsorbent with heavy metal fractions of cadmium, copper, chromium and zinc leaching below regulatory levels, other literature have reported PWTR with high toxic levels of these metals (Ahmad et al., 2016a; Mortula et al., 2009). Ahmad et al. (2016) and Mortula et al. (2009) have indicated that alum PWTR may affect algal growth in receiving streams and cause chronic sub-lethal toxicity effects on trout species. Considering the high adsorption capacity of aluminium for phosphates, application of alum PWTR on soil inhibits the plants from utilizing phosphate and other anionic fractions of fertilizers (Okuda et al., 2014).

Seeing the increasing market share of coagulants, it is obvious that alum demand is high owing to its dominance in the water treatment industry. From the considerable cost incurred by water treatment plants on coagulants and the legislative pressure on PWTR management, the recovery and utilization process that provides environmental and economic benefits is much sort for. Recovering alum in the residue creates a new market value for coagulant recycling in order to sustain the chemical consumption and complete utilization cycle. Aside the expected disposal

volume reduction and subsequent reduction in the cost of alum PWTR disposal, recovery of coagulant and reuse can reduce the demand of fresh commercial coagulant by 70% (Keeley et al., 2012).

1.2 Recovery and Quality concerns

Regeneration of alum from PWTR is by the traditional acidification and alkalization processes (Keeley et al., 2012). Destruction of the amorphous structure of the alum PWTR by acid digestion has been studied using different acids such as nitric, sulfuric and hydrochloric acid. However, acid digestion with sulfuric has shown much Al yield as it is less rigorous and requires less dosing, lower temperature and shorter contact time (Miroslav, 2008; Okuda et al., 2014; Ulmert and Särner, 2005). Mostly, optimum recovery of aluminium with sulfuric acid is reported for a pH range of 1-3 and 11.2-11.4 for alkaline extraction using hydroxides of sodium and calcium (Ahmad et al., 2016a; Keeley et al., 2014a).

The problem with the acidification and alkaline recovery approach is the solubilization of heavy metals, natural organic matter (NOM) and other fractions of total organic compounds (TOC) adsorbed on the particulate structure of the residue. Heavy metal solubilization is excessive in acid recovery of alum while organic matter is present in alkaline supernatant (Keeley et al., 2014a). In order to achieve more recovery at lower pH values, more sulfuric acid is required and this results in the leaching of high organometallic fractions. The process, therefore, lacks specificity in terms of optimal process variables. Although most research continues to look at the sulfuric acid potential on recovery and its effects on various PWTR applications, the process of acid recovery was halted on a large scare implementation in the 1970's (Keeley et al., 2012).

The expectation of recovery is to provide treatment viability as commercial coagulants. As such, the presence of solubilized organic matter and heavy metals would affect the efficiency of the chemical treatment and quality of water. Natural organic matter affects the aesthetic parameters such as color, taste and odor. Their presence serves as precursors for bacterial growth in water distribution lines and the formation of disinfection by products (DBPs) (Powers and Gonsior, 2019). Through the reaction of NOM with water disinfectants, the formation of DBPs leads to several adverse health effects not limited to carcinogenicity, cytotoxicity and mutagenicity (Li and Mitch, 2018; Powers and Gonsior, 2019). The bonding of NOM and metals to form organometallic complexes remain in solution until their binding capacity have been saturated (Jeswani et al., 2015).

1.3 Selectivity Recovery of Residue

Organometallic build up in water during treatment with recovered coagulant is undesirable. Selectivity recovery therefore involves the recovery of alum in its target Al^{3+} form using the principle of molecular size and charge exclusion. Ordinarily, solid fractions of recovered coagulant can be achieved by solid filtration or gravitational settling. Options for secondary treatment or separation of recovered aluminium from the PWTR includes pressure driven membranes (PDMs), conventional ion exchange and Donnan dialysis (Evuti and Lawal, 2011; Keeley et al., 2014a).

The selectivity of PDMs are based on their molecular weight cut-off (MWCO), which is expressed in daltons (1 Da = 1 $gmol^{-1}$). Ultrafiltration has been used to achieve 52-90% aluminium recovery and 50-75% total organic compounds (TOC) retention using MWCO of 2-50 kDa (Keeley et al., 2014b; Ulmert and Särner, 2005). Similarly, the use of nanofiltration (150-300 MWCO) in recovery will result in the further concentration of aluminium in the retentate stream (Cheng et al., 2016b). However, the bane of PDMs is organic fouling, permeation of low molecular weight

hydrophobic dissolved organic carbon, its high energy requirement and high process cost (Keeley et al., 2014a).

Conventional ion exchange processes involves the use of resins to selectively adsorb positively charged coagulant metals or adsorb anionic components leaving behind the cationic fractions in solution. The use of Purolite C106 and Purolite C100x10 with a weak carboxylate and strong sulphonate functional groups respectively, achieved over 90% recovery of aluminium from alum PWTR (Petruzzelli et al., 2000b, 1998). Adsorption on the resin surface requires desorption and regeneration of resin. In addition to solvent entrainment, desorption and regeneration stages are chemicaly intensive and increases the process cost.

Another ion exchange membrane process is considered as an emerging technology for recovery selectivity. Also known as Donnan membrane process, Donnan dialysis is a concentration gradient driven process that utilizes ion exchange membranes to separate ions by the counter current transport of ions across the membrane. Depending on the charge of the ion of interest in the electrolytic solution, a cation exchange or anion exchange membrane is used. Cation exchange membranes are polymers embedded with negative charges and vice versa for anion exchange membranes. By their fixed charges, cation exchange membranes will permit the transport of cations (counter ion) and restrict the permeation of anions (co-ions). Similarly, anion exchange membranes will not restrict cations (co-ions) and permit the interaction of anions (counter ions) with the membrane (Davis, 2000; Tanaka, 2015).

1.4 Problem Statement

With the demand on a selective technology for the recovery of Al-coagulant from PWTRs as a sustainable intervention to traditional PWTR management, Donnan dialysis appears as a

technically feasible option. This is due to their simple to use and energy efficient characteristics. Additionally, as a highly selective and non-fouled process, the Donnan dialysis edges over the secondary treatment processes (Evuti and Lawal, 2011; Keeley et al., 2014a).

Different configurations have been used in studies involving Donnan dialysis. However, there is limited information on the effect of multiple process variables on the recovery of aluminium in a Donnan dialysis process. Optimum conditions and transport inhibition by PWTR constituents in the recovery process is not well reported. The limited information of simulating experimental sequence to develop a relationship between input variables and response provides a huge research gab to be filled.

1.5 Aims and Objective of study

The aim of this study is to investigate the optimum range of operation for geometric and engineering variables that affects the recovery of alum from potable water treatment residue in a laboratory scale counter flow Donnan dialysis cell.

Objectives are as follows:

1. To investigate the effect of flow rate and concentration of the feed phase and sweep phase on the recovery of aluminium.
2. To evaluate the combined effect of pH, optimal flow and concentration conditions on aluminium transport.
3. To investigate the inhibition of heavy metals in a binary transport with aluminium.
4. To evaluate the aluminium kinetics and recovery using real PWTR solution and investigate the efficiency of organic rejection by the Donnan process.

1.6 Thesis Organization

The dissertation consists of five chapters as follows:

Chapter 1:

Introduction of thesis, problem statement, objectives of the study and structure of the dissertation.

Chapter 2:

Comprehensive literature review on potable water treatment residue (composition, production and recovery advantages), Donnan dialysis (advantages and disadvantages, research trends and application areas, design schemes, process integration, and important equations) and the design of experiment.

Chapter 3:

Research methodology and techniques for data acquisition of the parameters of study, set-up design and operational reliability of DD cell is treated in this chapter. The experimental matrix and investigation using the statistical tool is expounded.

Chapter 4:

Interpretation of empirical results through a quantitative and qualitative data analysis approach. The first section of the results is a selective step to look into the significant factors that affect the process by using synthetic feeds. This is followed by presenting the results of aluminium recovery in an acid digestion range using synthetic feed and the significant factors. Furthermore, the inhibition of selected metal ions on Al^{3+} recovery is reported. Lastly, the performance of the membrane to reject or permeate organics and the simultaneous transport of aluminium is investigated for a real feed.

Chapter 5:

Conclusion of study with reports and declaration of new findings, recommendations and suggestions for further studies of alum recovery using the Donnan dialysis.

CHAPTER 2

LITERATURE REVIEW

2.1. Water Treatment

The interactions of components of the fresh water ecosystem, namely, producers, decomposers and consumers with light, water, suspended solids and dissolved nutrients affects the water quality in the ecosystem. Anthropogenic activities also increases undesirability and therefore serves as a driving tool for the spread of diseases (Akoto et al., 2017). The source water such as rivers, lakes, dams and ground water must, therefore, be treated to meet specific usage and demand using chemical and mechanical processes. High demand of water has also resulted in the treatment of sea water for the provision of clean water (Koleva et al., 2017).

Conventional water treatment is a three-stage process: primary, secondary and tertiary. Depending on the total solids and fragments in the source water, a screening process (barracks and bar screens) is added to the coagulation and flocculation process of the primary stage. The secondary stages involves clarification, media filtration and disinfection. Granular media filters are composed of a layered bed of anthracite coal (0.8-1.2 mm), sand (0.5-0.8 mm), finely rushed garnet (0.4-0.6 mm) and magnetite (0.3-0.4 mm) and other high density materials (Singh, 2015). Recent modification to conventional treatment chain includes, direct filtration and inline filtration prior to coagulation, dissolved air flotation for coagulation-clarification and sludge blanket clarification for sedimentation and slow sand and diatomaceous earth for filtration (David Kuo and Xagoraraki, 2016). Examples of disinfectants are chlorine, oxides of chlorine, chloramines and ozone (Powers

and Gonsior, 2019). Prior to distribution, the pH of the water is regulated and stored to conclude the tertiary stage.

2.1.1 Coagulation

Physical treatment processes for the removal of suspended and colloidal particles are ineffective in water processes. For example, silts and colloids settle in 3-hours and 3-years, respectively (Singh, 2015). The resistance of suspended solids and colloids to agglomeration is due to their mutually repellant forces created by their similar surface charges. Therefore, high valence cations are used to neutralize the surface charges by reducing the zeta potential to below the van der waal's attractive forces and aggregate the micelles to form clumps. The clumps then coalesce the colloidal particles (Singh, 2015).

Generally, coagulants are classified into mineral and organic. Mineral coagulants such as hydrolytic salts of aluminium (aluminum sulfate, aluminum chloride, aluminum chlorohydrate and sodium aluminate), salts of iron (ferric chloride, ferric sulphate, ferric alum and ferrous sulphate) and their pre-hydrolyzed forms of poly-aluminum chloride, poly-aluminum sulphate, poly-ferric chloride and poly-ferric sulphate are commonly used in commercial quantities as primary coagulants for water treatment (Bratby, 2016; Tetteh and Rathilal, 2019; Ooi et al., 2018). Organic coagulants are cationic, anionic or nonionic polyelectrolyte of polyamines, aluminum chlorohydrate, poly-diallyldimenthylammonium chloride and melamine-formaldehyde resins. They are primarily used as coagulation/flocculation aids and have comparatively superior treatment performance and lower insoluble metal residue at a lower dosing range compared to mineral coagulants that have a high market cost (Tetteh and Rathilal, 2019).

2.1.2 Alum in Water treatment

Commercially referred to as alum, aluminium sulfate [$Al_2 (SO_4)_3 . xH_2O$] is mostly used as coagulant by PWTPs. Alum is often purchased in solid (block, kibbled or ground) and liquid forms. The water of crystallization coefficient (*x*) of the solid-state ranges 14-21 and contains 7.5-9% Al or 18% w/w Al_2O_3. The aluminium content in the liquid is standardized at 4.2% or 8% w/w Al_2O_3 (Brandt et al., 2017).

Adsorption affinity of alum for metal ions and anions such as fluoride, phosphate and perchlorates are high (Brandt et al., 2017). The dissolution of aluminum salt in water disregarding the existence of other ions that may be present in water is represented below in Equations 2-1 to 2-3:

Equation:

$$Al_2(SO_4)_3.14H_2O + 6H_2O \rightleftharpoons 2Al(OH)_3 + 3H_2SO4 \qquad 2\text{-}1$$

$$3Ca(HCO_3)_2 + 3H_2SO_4 \rightleftharpoons 3CaSO_4 + 6CO_2 + 6H_2O \qquad 2\text{-}2$$

or

$$Al_2(SO_4)_3.14H_2O + 3Ca(HCO_3)_2 \rightleftarrows Al(OH)_3 \downarrow + 3CaSO_4 + 6CO_2 \qquad 2\text{-}3$$

By the dissolution of alum in water, different products of hydrolyses with different structures, charges and polymerization character such as Al^{3+}, $Al(OH)$, $Al(OH)^{2+}$, $Al_{13}(OH)_{34}{}^{5+}$, $Al(OH)_4{}^-$ and many more are formed and their nature can be controlled by pH (Bratby, 2016; He et al., 2016). Coagulation, therefore, occurs at an optimum pH range of 6.5-7.5 and 5.5-6.5 for lowland and upland water, respectively. The hydrolysis product for effective coagulation is a factor of the mixing efficiency, pH, and coagulant dosage. The dosage of the acidic salt and the natural alkalinity of water which is controlled usually with calcium bicarbonate leads to the formation of

the hydroxide of aluminium product as in Equation 2-3. The product, $Al(OH)_3$ has low solubility and hence precipitates out of the water during treatment (Brandt et al., 2017).

2.2 Potable water treatment residue

Potable water treatment residue (PWTR) are the total solid-water waste product formed during the water treatment process and is removed from the underflow pipes of clarifiers and filters during backwashing. The volume of residue and residual characteristics are dependent on the plant production conditions, amount of solids in the sourced water, chemical properties of the water impurities and type, purity and dosage of coagulant (Evuti and Lawal, 2011; U.S. EPA, 2011). Quantification of the water and solid fractions of PWTR indicate that the water fraction is 1-5% of the volume of untreated raw water and solids are equivalent to that of the raw water. An estimated 80-90% of the solids generated are removed from the clarifiers. The residue removed during the backwashing of filters are described as high volume and low solids with a suspended solids range of 30-300 mg/L (Cornwell et al., 2010; McTigue and Cornwell, 2009).

Until recently, PWTRs was associated with sewage sludge and this has accounted for limited literature on PWTR production per country. While the global estimation of PWTRs is at 10,000 tons (dry basis) per year, Ahmad et al. (2016b) puts a single PWTPs production at 100,000 ton per annum. The desparaties therefore indicates that not all countries have reported on PWTPs generation. According to Frías et al. (2014), a 1 m^3s^{-1} capacity PWTP generates 9.15 tons per day of residue. Figure 2-1 provides the available PWTR data on a dry and wet weight basis. On continental and national basis, the data establishes the data gap and puts the summation of PWTR contributions available by countries at over 3 million tons (dry weight) per annum. Data Available for residue generation is defined on a wet basis for South Africa and Portugal. Due to the number of treatment plants an organization holds in Australia, PWTR generation varies from 150-43,500

tons of PWTR per annum with the highest generation, 2000 tons (dry weight) per annum from a single site (Maiden et al., 2015).

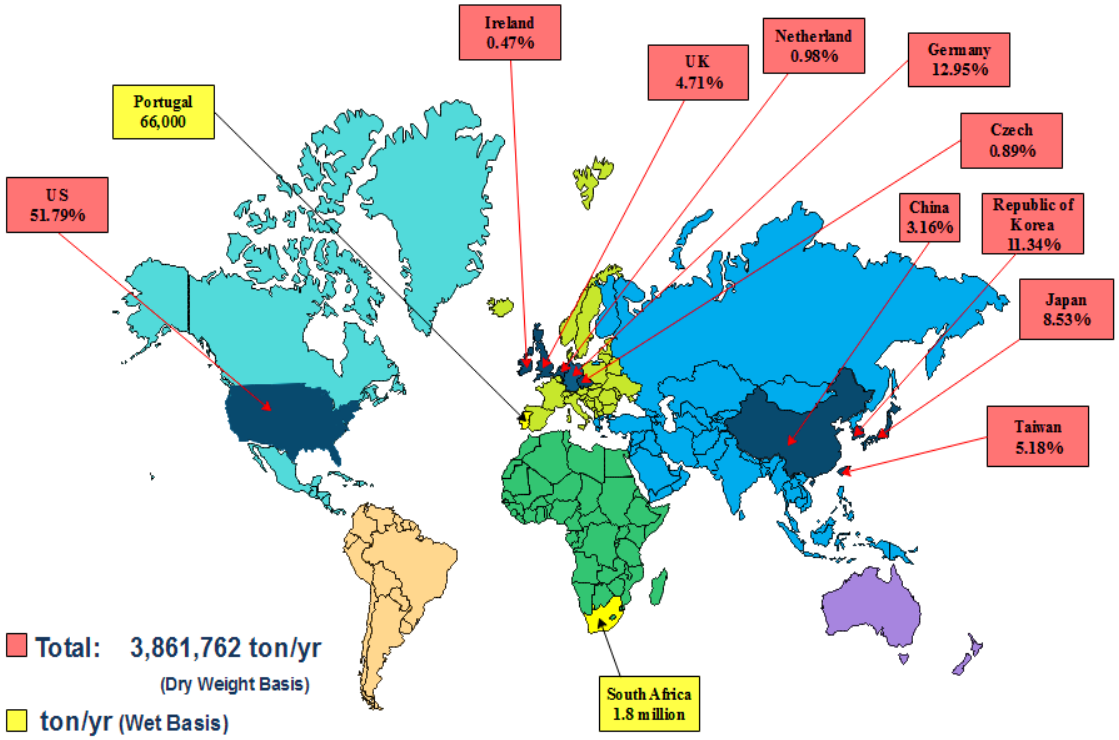

Figure 2-1: Geographic preview of PWTR generation (Adapted from Huang and Wang, 2013; Jung et al., 2016; Okuda et al., 2014; Wurzer et al., 1995 and Miroslav, 2008)

Fundamentally, PWTRs from PWTPs that uses alum as a primary coagulant are referred to as Alum-PWTRs (Al-PWTR). Similarly, Fe salts as primary coagulants will generate Fe-PWTRs. Ulmert and Särner (2005) assumed that a PWTR arising from 50% precipitated $Al(OH)_3$ and 50% raw water impurities would produce 1 million dry solids annually and 200 million for a dry solid content of 0.5%. During the precipitation of $Al(OH)_3$, organometallic pollutants of the raw water

adheres onto the glutinous structure. Physicochemical compilation of SiO_2 dominating alum PWTR shows traces of Zn, Ni, Cu, Cr, Cd and Hg. Also, first five metals found in high concentration relative to aluminium in ascending order are Mg-Mn-K, Ca-Fe (Ahmad et al., 2016a; Ippolito et al., 2011).

Like all other residue, alum PWTRs are made up of a heterogeneous mixture of natural organic compounds characterized as TOC and DOC. Natural organic compounds are grouped into hydrophobic, transphilic and hydrophilic fractions with hydrophobics comprising over 70% of DOC. This is due to their easy removal during water treatment as a result of their high colloidal anionic surface charge and more hydrophobic nature. Hydrophobic NOM is made up of humic (50-500 kD) and fulvic (0.5-2 kD) acid, while aliphatic carbohydrates, amino acids, nitrogenous compounds, and proteins constitute the low molecular hydrophilic ends. The physicochemical properties and amount of NOM depends on the source, age, biogeochemical fate cycles and climate (Keeley et al., 2014b; Liu et al., 2009; Matilainen et al., 2011; Weng et al., 2002).

2.3 Alum recovery

There are two primary processes for coagulant recovery which includes acidification and alkalization (Evuti and Lawal, 2011). Secondary treatments aimed at purification and concentrating of leachate from the primary stages include pressure driven membrane and conventional ion exchange processes. Under the acidification and alkalization treatment, reaction between acids and residue are shown in Equations (2-4 to 2-8). Aluminium as the target ion forms coagulant species with the acid or base used for the leaching process.

Acidic:

$$Al(OH)_3 + 3HNO_3 \rightarrow Al(NO_3)_3 + 3H_2O \qquad 2\text{-}4$$

$$Al(OH)_3 + 3HCl \rightarrow AlCl_3 + 3H_2O \quad 2\text{-}5$$

$$2Al(OH)_3 + 3H_2SO_4 \rightarrow Al(SO_4)_3 + 6H_2O \quad 2\text{-}6$$

Alkaline:

$$Al + 3H_2O + NaOH \rightarrow Na[Al(OH)_4] + \tfrac{3}{2}H_2 \quad 2\text{-}7$$

$$2Ca^{2+} + 2Al(OH)_4 + 8H_2O \rightleftarrows Ca_3Al_2(OH)_{12} + 6H_2 \quad 2\text{-}8$$

Five notable observations are made in acidification and alkalization for recovery of aluminium:

1) H_2SO_4 has higher Al-recovery over HCl and HNO_3 (Okuda et al., 2014; Ulmert and Särner, 2005).
2) Poly aluminium chloride PWTRs have higher Al-yields than alum PWTR (Chen et al., 2012; Nair and Ahammed, 2017, 2014).
3) Treatment of residue with NaOH has higher yields than lime leaching due to lower calcium solubility (Masschelein et al., 1985).
4) There is high metal and organic solubilization in both processes.
5) Recovered coagulant requires further purification using membrane processes and ion exchange. Microfiltration, ultrafiltration and nano filtration have pore size ranges of 0.1-10 µm, 0.05 µm-1 nm and 0.5-5 nm, respectively. The MWCO classification begins from ultrafiltration as 1-500 kDa, 0.1-0.5 kDa for nanofiltration and below 0.1 kDa for reverse osmosis (da Silva Biron et al., 2018; Mohammad et al., 2015; Warsinger et al., 2018). Amongst the pressure driven membranes, ultrafiltration has been addressed as the simplest. Thin polyamide supported with polysulfone ultrafilter of 2 kDa MWCO was used to recover 87% lowland alum residue with 58% dissolved organic compound (DOC) rejection (Keeley et al., 2014b). Similarly, a multi-process, recovery that included a 2kDa MWCO

ultrafilter achieved 52% Al and 80% DOC retention (Ulmert and Särner, 2005). However, key observation made by Keeley et al. (2014b) showed that only high end hydrophobic organic compounds were retained with the permeation of less abundant lower molecular weight compounds. Also, the known effect of fouling was found to reduce flux by 75% for thickened residue and 20% for unthicken residue, thus, affecting the continuous operation and causing energy inefficiency.

Until now, there is no specific usage of nanofiltration on alum PWTR. However, its application on poly aluminium chloride residue has been reported. The rejection rate of nanofiltration reveals its efficiency to concentrate aluminum ions to a peak concentration irrespective of the initial concentration. Nanofiltration recovery of Al concentrated the initial feed of 1017 ppm by a factor > 6 for an acidified poly aluminum PWTR (Cheng et al., 2016a) and 2610 ppm by about three times (Cheng et al., 2016b) in the retentate. Nano filtering of alkaline leached feed of 2520 ppm was enriched to 2022 ppm. However, the phenomenon of heavy metal and organic matter concentration occurred in both recoveries, impeding the recovery through membrane surface deposition. Also, despite relatively high Al-concentration in the retentate phase of both feeds with respect to initial concentration, the high values of organo-metallic fractions makes it impossible for re-use as a coagulant. During the concentrating of aluminum by nanofiltration for alkaline feeds, the permeate liquid contained more Al as low valence aluminate permeates more than the high valence in acidic mediums (Cheng et al., 2016b).

Related in technique to adsorption, conventional ion exchange involves the exchange of ions between insoluble exchange resins, which are cationic or anionic containing electrostatically bound ions and the solution of interest. The resins subdivided into strong acidic cation, weak acidic cation, strong basic cation, and weak basic exchange resins are used in fixed columns or mixed in

a suspended reactor such as magnetic ion exchange (MIEX) and suspended ion exchange (SIX) processes. Strong and weak acidic cations have sulfonic acid and carboxylic acid groups, respectively, whilst strong basic are mostly made of quaternary ammonium groups. Weak anion exchanges comprises of primary (1°), secondary (2°) and tertiary (3°) amine moieties. During the exchange process, electro neutrality is maintained as the solid releases replacement ions to the solution causing a non-physical altering of the gel-like structure of microspheres (Finkbeiner et al., 2018; Paull and Nesterenko, 2013; Watson, 2018). As earlier described in Section 1.2, the study by Petruzzelli et al. (1998) and Petruzzelli et al. (2000) using the strong acidic cation and weak acidic cations all achieved high recovery. However, of much concern on that limited study was the resin regeneration requirement and solvent entrainment. All these extra processes increases the cost of recovery.

2.4 Donnan dialysis

Donnan dialysis (DD) is a potentially useful green treatment membrane process. It is a concentration gradient driven process used to separate and concentrate ions from diluted solutions by the stoichiometric counter transport of these ions across an ion exchange membrane (IEM) (Strathmann, 2004). The ions diffuse from a donor or feed phase through either a cation exchange membrane or an anion exchange membrane to the acceptor or sweep phase. For the purpose of this study, the terms feed and sweep phase will be used.

Donnan dialysis has often been interchanged with Diffusion dialysis due to their indistinguishable principles of operation and application advantages. Whilst Diffusion dialysis is utilized in the recovery of mineral acids or alkalis from waste acid and alkaline solutions, Donnan dialysis is applied in the recovery of toxic or valuable heavy metal ions (Luo et al., 2011; Sata, 2007; Strathmann, 2004; Tanaka, 2015). The simple and easy to operate DD system exhibits functional

primacy over the conventional ion exchange process, electrodialysis, chemical precipitation and pressure driven membrane. The DD process is an energy efficient, low installation and operational cost, no risen regeneration and a non-fouling process that possess rural application benefits (Davis, 2000; Oehmen et al., 2011; Pyrzynska, 2006; Tanaka, 2015).

The key function to DD is the IEM which gives the negative and positive separation effect. Both cation exchange membranes (CEMs) and anion exchange membranes (AEMs) are available. The CEMs are embedded with fixed negative charges, thus permeates counter ions, and excludes co-ions. Anion exchange membranes have fixed positive charge groups (Davis, 2000; Luo et al., 2018). Co-ions are therefore ions of the same charge with the IEMs fixed charged groups and vice versa for counter ions. The CEMs and AEMs are composed of hydrophilic ionic groups and anchored by hydrophobic polymer chains. Notable amongst the hydrophilic functional moieties in CEMs are SO_3^-, PO_3H^-,–COO^-, PO_3^{2-}, $C_6H_4O^-$ and NH_3^+, NRH^{2+}, NR_2H^+, NR_3^+ and PR_3^+ for AEMs (Ran et al., 2017; Xu, 2005).

The fundamental principle of 1924's F.G Donnan study established a Donnan equilibrium from the electrostatic repulsion of co-ions by the IEM (Strathmann, 2004). Figure 2-2 illustrates the exchange of aluminium and hydrogen ions through a CEM and the exclusion of sulphate and chloride co-ions. The feed and sweep phase contain the electrolytic solutions of aluminium sulphate from a PWTR and hydrochloric acid, respectively. Since the ion transport is time dependent, the exchange continues until an electrochemical potential equilibrium and counter ion transport equilibrium is reached between the electrolytic solutions (Davis, 2000). Consequently, the aluminium in the feed solution decreases . The ion of interest is now recovered in concentrated form in the sweep solution. In Figure 2-2, the initial PWTR solution which contains aluminium sulphate would then be recovered as aluminium chloride.

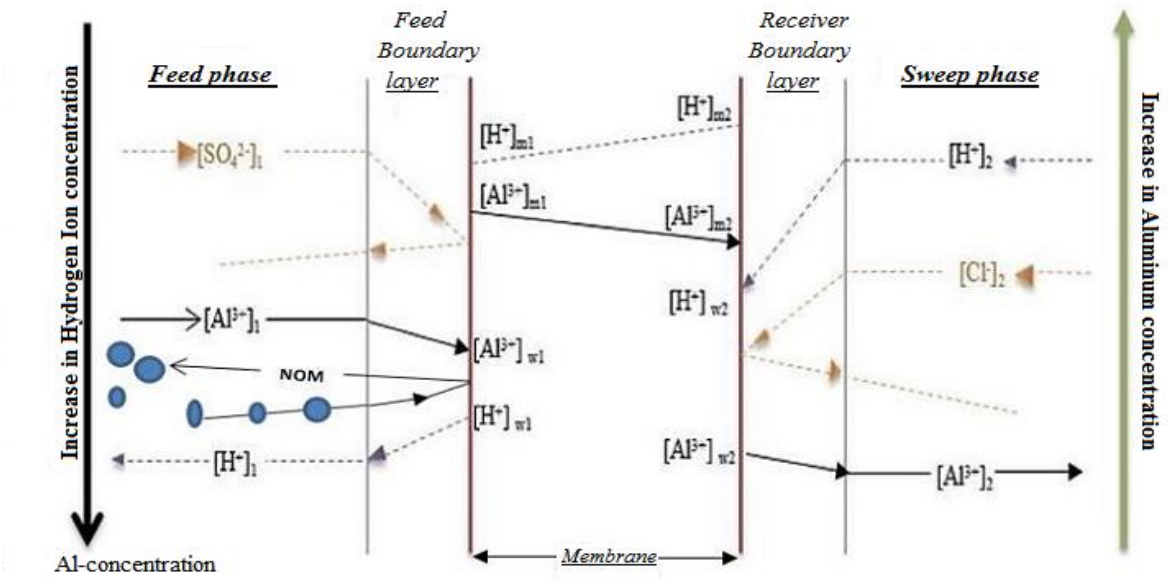

Figure 2-2: Al^{3+}-H^{+} transport through a cation exchange membrane (Adapted from Keeley et al., 2014a)

2.4.1 Thermodynamics of Donnan dialysis

The DD process is delineated with the second law of thermodynamics and two essential equations are crucial to the process. The first equation is the Nernst-Planck equation that describes the permeate amount produced per unit area of the membrane surface per unit time. It is a reformulation of the macroscale diffusion law by Ficks and can be used to determine ion transport through a membrane. The Ficks law (Equation 2-9) is only used to precisely describe the flux through a membrane for counter ions with a similar diffusion coefficient, hence the expansion to develop the Nernst and Planck's equation (Equation 2-10). Contribution to develop equation 2-10 included equation establishment and experimental reinforcement by Nernst while elaboration of the theory was performed by Planck.

$$J_m = \frac{D_m}{\partial l}(C_m - C'_M) \qquad 2\text{-}9$$

where J_m is the flux of the ion (mol m^{-2} s^{-1}); C_m and C'_M are the metal ion concentration in bulk solution and the interface on the feed side (mol m^{-3}); D_m is the diffusivity (m^2 s^{-1}) and l is the length of the membrane.

Five assumptions were made in deriving the Nernst-Planck equation (Ho et al., 1993) as follows:

- Transport of ions is a membrane diffusion controlled process
- Negligible number of co-ions in the membrane compared with the ion exchange capacity and no permeation of co-ions.
- Existence of thermodynamic equilibrium at membrane-solution interface.
- Osmotic water transport across the membrane can be neglected
- Preservation of overall electro neutrality in the system.

From these assumptions, Nernst-Planck equation is given as:

$$J_m = -D_m\left(\frac{dC_m}{dt} + Z_i C_m \frac{F}{RT}\frac{d\emptyset}{dl}\right) \qquad 2\text{-}10$$

where J_m is the flux; C_m is the metal ion concentration in the bulk solution (mol m^{-3}); D_m is the diffusivity (m^2 s^{-1}); l membrane thickness (m); R is the ideal law constant (J K^{-1} mol^{-1}); T is the absolute temperature (K); Z is the ionic charge; F is the Faradays constant (C mol^{-1}) and ϕ is the electric potential.

Davis (2000) provides the second important equation that expounds on the relationship between the initial concentration and final concentration of solutions at both feed and sweep phases as:

$$\left(\frac{[C_a]_f^+}{[C_a]_s^+}\right)^{\frac{1}{Z\alpha}} = \left(\frac{[C_b]_f^+}{[C_b]_s^+}\right)^{\frac{1}{Zb}} \qquad 2\text{-}11$$

The subscript f and s denotes the ions in the feed phase solution and sweep phase solution respectively. C_a is the concentration of the target metal, Z_a is the ionic charge of the target metal,

C_b and Z_b is the concentration and ionic charge of the ionic species substituting the target metal. It can be deduced that an increase in the concentration of the substituting ionic species (C_b), increases the final concentration of target metal (C_a) recovered. Also, a target metal ion with higher Z_a than Z_b (the substituting ionic species) would result in higher recovery and concentration of the target metal ion.

The equilibrium concentration can also be expressed as a function of the concentrations and volume of the feed and sweep phase solutions as:

$$\frac{\left(\frac{(C_f - x)}{V_f}\right)}{\left(\frac{x}{V_f}\right)} = \frac{\left(\frac{x}{V_s}\right)}{\left(\frac{(C_s - x)}{V_f}\right)} \qquad 2\text{-}12$$

where C_f and V_f are concentration and volume of feed phase, C_s and V_s are the concentration and volume of the sweep phase, x is the number of moles transported through the membrane.

2.4.2 Donnan dialysis system

This section deliberates on the main features of a DD system which includes the ion exchange membrane, the cell design and membrane modules which have been reported in literature.

2.4.2.1 Ion exchange membrane (IEM)

IEMs are also classified into five (5) categories by the distribution and pattern of the fixed ionic groups: monopolar, amphoteric IEMs, inorganic-organic (hybrid), bipolar membranes and mosaic membranes. Most IEMs on commercial application are identified as monopolar with a single-line pattern (Strathmann, 2004; Xu, 2005).

Depending on the charge group interconnection on the matrix phase of the membrane structure, IEMs are identified as homogenous and heterogeneous with varying properties and process advantages. In a homogeneous membrane, charged groups are bonded to a polymer backbone

while in an heterogeneous membrane, the ion exchange material is mixed with the polymeric matrix without chemical bonds in between them (Ariono and Khoiruddin, 2017; Wenten, 2016). Homogeneous IEMs exhibit high conductivity and permselectivity and have even distribution of functional sites over the heterogeneous IEMs, they have poor mechanical properties, high production cost and complex production stages. The low electrochemical properties of the heterogeneous IEMs are associated with ionic mobilization pathways, leakage of co-ions in the solution phase and the availability of inert fractions (Ariono and Khoiruddin, 2017).

IEMs are designed and produced to have desirable characteristics such as high permselectivity, high conductivity, good mechanical strength, structural stability and high chemical and thermal stability (Strathmann, 2004). The characteristics are also dependent on factors such as size of ion exchange resin, resin loading, resin distribution, polymer used, solvent and method. CEMs have proven high stability in strong alkaline solutions than AEMs. Until recently, most commercially available CEMs and AEMs are homogeneous: Aciplex, Selemion Femion, Nafion, Fumasep, FKS, Ralex and Neosepta are known IEMs (Hassanvand et al., 2017; Wenten, 2016). .

Non-commercial membranes are often developed for performance evaluation and comparison with commercial membranes. These membranes are either synthesized or result from structural modification of existing membranes. To develop the surface, permselectivity efficiency and ion exchange capacity (IEC) of any membrane, various preparation and modification techniques which includes phase inversion, irradiation and film etching, microfabrication, film stretching, sintering of powders, track-etching, electro-deposition, sol-gel process and coating (dip coating, in situ polymerization, plasma polymerisation, interfacial polymerization) are applied (Ladewig and Al-Shaeli, 2017; Sata, 2007; Strathmann, 2004; Wenten, 2016). However, surface engineering and modification is focused on the use of solvent-free technologies.

In summary, IEM characteristics which are ion conductivity, hydrophilicity and hydrophobicity, ionic properties, embedded ion exchange groups, charge density and membrane-ion-affinity are the foundation for application in various ion exchange processes which includes DD (Chandra et al., 2019; Luo et al., 2018; Ran et al., 2017; Sata, 2007). The selectivity transport functionality of the membrane (characterised by morphology and microstructural variation) for target ions in the mist of multivalent ions influence their choice to achieve various DD separation objectives.

2.4.2.2 Nafion membrane

Nafion by DuPont with history of commercial usage has shown satisfactory properties. After their first application in the late 1960's in chloro-alkali cells, it has been adopted in wide ion transport applications. The chemical structure of the CEM, as illustrated in Figure 2-3, is a co-polymer of hydrophobic tetrafluoroethylene (teflon) backbone and perfluorovinyl ether side chains terminated in strongly hydrophilic sulfonyl fluoride groups within the polymer (Duan et al., 2012; López Días et al., 2019). The sulfonyl fluoride, after polymerization, is hydrolysed and the ions are exchanged to produce the perfluorosulfonic acid. The rich hydrophilic sulfonic acid pendent groups which is made up of sorbed water is then surrounded by a hydrophobic matrix of tetrafluoroethylene and perfluorovinyl ethers. Water sorption swells and restructures the hydrophilic groups to form a proton conducting network for ionic and water transport. This accounts for the distinct properties as high cation and hydroxylated species permeation, good mechanical and thermal strength, high ionic conductivity and high chemical and oxidative stability (Andrada et al., 2018).

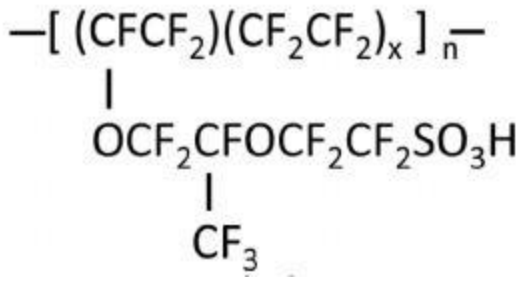

Figure 2-3: The chemical structure of Nafion

Nafion membranes are formed through extrusion or casting in solution of the precursor. Casting is followed by hydrolysis conversion to ionic Nafion. The type of Nafion with regards to properties and morphology are highly dependent on the concentration of the pendent group which is referred to as the equivalent weight (EW). Most types of Nafion have an equivalent weight of 1100 g eq^{-1}. The EW of the membranes can be identified from the first two numbers and thickness of the membrane from the last number. For example, Nafion 117 has an equivalent weight of 1100 g eq^{-1} and thickness of 0.007 inches. Table 2-1 presents a list of Nafion membranes and their respective EW and nominal thickness adapted from Duan et al. (2012) and Tang and Pan (2015).

Table 2-1: Commercially available Nafion membranes with their respective properties

Nafion	Formation	Equivalent weight (g eq^{-1})	Nominal thickness (µm)
115		1100	127
117		1100	178
1035	Extrusion	1000	89
212		1100	50-51
211	Solution casted	1100	25.4
XL	Reinforced	-	27.5
1110	Extrusion	1100	254

2.4.2.3 Membrane activation

The activation of membrane prior to its usage in a DD system is essential to achieve a high membrane hydration. It ensures the setting up of transport pathways for the permeation of ions. Crucial to the conditioning process is the removal of impurities and factory defects from the surface of the membrane. Immersion and conditioning in acid is commonly adopted by researchers (Napoli et al., 2013).

The sequence of conditions commences with immersion in H_2O_2, rinsing in distilled water or boiling water and proceeded with acid conditioning with HCl, H_2SO_4 and/or HNO_3 at elevated temperature $\leq 90^oC$ (Duan et al., 2012; Iben Nasser and Ahmed, 2015; Napoli et al., 2013). The treatment chain is then completed by final rinsing in either deionized water at high or normal temperature. However, most Nafion treatments do not opt for HNO_3 conditioning. Napoli et al. (2013) has shown that further treatment of the membrane with 1% dilute HCl for 3 hrs enhances ionic transport by increasing the inter-pore hydration of the membrane.

Neglecting the peroxide conditioning, other treatments introduce NaOH neutralization in-between two acid conditioning steps which uses HCl and H_2SO_4 interchangeably at different treatment times for the particular membrane (Çengeloğlu et al., 2001; Ersoz and Kara, 2000).

2.4.2.4 Donnan dialysis cells

Various compartments to contain the feed and sweep phase solutions and membrane have been developed over the years and reported in literature. These modules are designed to meet main design criteria cited by Davis (2000) for Donnan dialysis. The membrane and module criteria are:

1) High resistance to thermal and chemical attack
2) Should minimize fouling and boundary layers through the promotion of high cross flow

velocities at low flowrate

3) Should have a high filtration area to volume packing ratio.
4) Should not require extensive pre-treatment of the feed.
5) Should be easily scalable to take larger throughputs.

A simple two compartment cell has seen development with the attachment of external feed and sweep side vessels. Flow patterns are set-up with compressed air, magnetic stirrer, shaking blocks or baffles. Figure 2-4 illustrates the different DD compartment designs. These compartments are made from several materials such as borosilicate glass, periplex glass, methyl methacrylate and Teflon. Also cell arrangement vary and hybrid structures have included a 20 cell pair mounted with CEMs, 11 cells consisting of 5 feed and 6 sweep cells and a 3-4 membrane cell (Garmes et al., 2002; Vanoppen et al., 2015; Wiśniewski and Rózańska, 2007).

Four modules, notably, flat sheet, spiral wound, hollow fiber and the tubular type are known in the membrane industry. However, two modules are applicable in the DD system as there is the requirement of separate solutions flowing on either side of the membrane for counter exchange of the ions. The plate and frame module, one of the earliest designs for packing flat sheet membranes consists of the membrane and a mesh spacer sandwiched between two blocks and plates. Also, smaller tubular compartments housing membranes are fitted into a large tube to form the tubular module (Baker, 2012). With respect to the promotion of high cross flow velocity, high filtering area to volume packing ratio and pre-treatment requirement, flat sheet modules show low performance whilst tubular modules have medium performance characteristics.

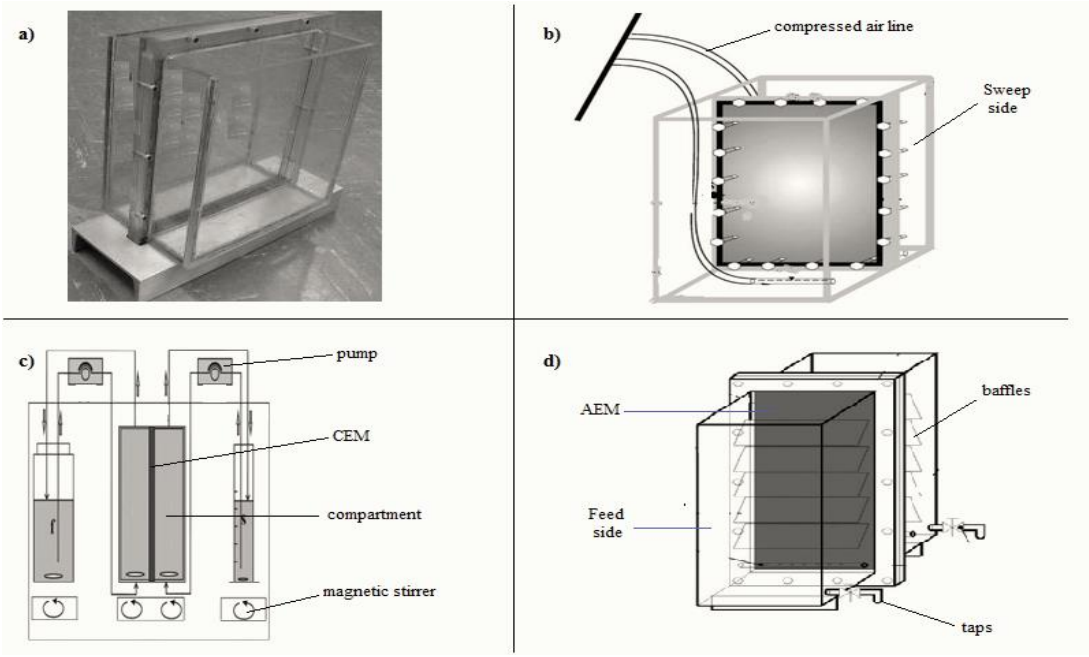

Figure 2-4: Donnan Designs: a) simple compartment; b) simple compartment with compressed air agitation by Prakash and SenGupta (2003); c) Compartment with external vessels (Marzouk et al., 2013b; Szczepański and Szczepańska, 2017); d) Point of Use system by Zhao et al. (2012)

2.5 Operating variables of Donnan dialysis

Depending on the DD configuration, operating variables that affect recovery, separation and concentration of target ions of concern are the concentration and flowrates of feed and sweep phases, electrolytic sweep solution, valence of counter ion, pH, experimental duration, membrane type and morphology. Out of these factors, some have been partially or theoretically investigated and others extensively experimentally investigated. Other factors have limited or no information in literature. Studies of Donnan dialysis for the recovery for cations and anions have been presented in Table 2-2 in section 2.6.1 The table includes factors of study and their outcomes. However, this section presents a synopsis of some factors.

2.5.1 Extensively Investigated variables

Valence of counter ion, membrane type and morphology has been extensively investigated. The information on these factors enable proper selection of operating conditions and their effect on transport in single or binary or multi-ionic solutions.

2.5.2 Valence of Ions in Solution

Four key fundamental principles have established from works by Miyoshi (1998, 1997), Ring et al. (2015) and Xue et al. (1990) on mono and divalent alkali and alkaline earth metal transport in donnan dialysis. These are:

1) The ions in the feed phase must always be of equal or higher ionic charge than the sweep phase.
2) A higher valence difference greater than 1 provides a larger driving force
3) Monovalent ions have higher flux than divalent ions.
4) Easier migration of monovalent ions to form pairs than divalent ions.
5) Transport of metals at low and high concentrations are controlled by boundary layer diffusion and membrane diffusion. The Reynolds number does not pose a major effect.
6) Flux of ions in DD is not affected by co-ions.

The high flux of monovalent ions over divalent ions was hypothesized by Miyoshi (1997). In the hypothesis, monovalent ions were free to transport from one fixed ion to another fixed ion while bivalent/trivalent ions needed to transport from two or three fixed ions to another of similar ion group which is complex to achieve. The transport of trivalent Al by Prakash et al. (2004) categorized the concentrating into three zones: the kinetically driven zone, the Donnan equilibrium zone and the osmotically driven one. The kinetically driven zone is governed by a high

concentration gradient between the two electrolytic solutions. With time, the gradient decreases as aluminium concentration at the feed side decreases bringing the transport to the Donnan equilibrium zone. The recovery of aluminium reaches a maximum and reduces again by the hydrodynamic transport of water. This is attributed to osmosis, hence, the osmosis driven zone.

2.5.3 Membrane type and morphology

The effect of membrane type and morphology has it that, homogeneous sulfonated membranes demonstrate high diffusion rates, about 5-10 times higher than heterogeneous membranes. Flux for Al and Fe through homogenous Nafion was found to be 8.27-8.40 x 10^{-4} eq.$m^{-2}s^{-1}$ and 2.13 x 10^{-4} eq.$m^{-2}s^{-1}$ respectively, whilst heterogeneous Ionac MC 3470 had a flux of 7.34 x 10^{-5} eq.$m^{-2}s^{-1}$ (Keeley et al., 2014a). The coagulant recovery study by Prakash et al. (2004) attributed the low Al-H inter-diffusion coefficient value in Ionac MC 3470 to the absence of ionogenic groups in the membrane phase. As such, Nafion has 30 times higher selectivity for Al than the heterogeneous CEM. Also, in two homogenous membranes with similar thickness, high transport of the target metal ion would be attributed to the membrane with high ion exchange capacity and water content value (Keeley et al., 2014a; Prakash et al., 2004).

Various synthesized membranes and modified commercial membranes have been used to study the recovery of different metal ions. These membranes have improved in morphology and stability to ensure efficient removal and recovery of metal ions. Table 2-2 in section 2.6.1 provides information about the modified membranes.

Homogenous AEMs with thin membrane functional layers and less cross-linked polymeric structure provides sufficient intra-molecular void spaces for high transport of arsenate. Pessoa-Lopes et al. (2016) attributed low permeation of big divalent anions to the denser highly

crosslinked polymeric structure. The tortuosity factor of homogenous gel is greater than that of heterogeneous gel for a given volume of solid fraction. However, against the recovery advantage of thin homogenous AEMs, high recovery in thick AEMs could be attributed to the effective tortuosity value of two. Furthermore, thick membranes would show high recovery as a result of high anion exchange capacity and less dense polymeric structure (Pessoa-Lopes et al., 2016; Velizarov, 2013).

2.5.4 Partially and mathematically investigated variables

Concentration and volume of feed phase and sweep phase has been investigated theoretically using the Nernst-Planck equation to relate the feed phase variables to the final concentration of volume of both phases (Davis, 2000; Ho et al., 1993; Prakash and SenGupta, 2005). Similarly, the usage of simplified models from Equation 2-10 by Agarwal et al., (2012) for mono-monovalent and mono-bivalent cations showed that reducing the salt concentration at the sweep side reduced the selectivity of the membrane. Agarwal and Goswami (2016) hypothesized that Equation 2-10 was applicable for pseudo-steady state approximation only for pure ionic solution at salt concentrations greater than 1 M while Szczepański and Szczepańska (2017) continued that non-steady state approximation of DD models should be applied when feed solution salt concentration is less than 0.01 M.

Prakash and SenGupta (2003) and Prakash et al. (2004) for the recovery of aluminium from PWTR, achieved over 70% recovery. The effect of an increasing sweep concentration showed that recovery uptake increased with an increasing sweep concentration from 1 M to 2 M. However, the final Al concentration at the sweep side in the 2M H_2SO_4 experimental run decreased when compared to recovery at 1 M (Prakash et al., 2004). The reduction in recovery was attributed to

osmosis water transport. Szczepański and Szczepańska (2017) on the non-steady state transport indicated that, observable osmotic transport of water occurs at high sweep concentration up 1 M.

The effect of pH has been studied only on AEMs for the transport of arsenate. Using NaCl as sweep salt, it was observed that the membrane self-diffusion coefficient increased with increasing pH from 4.5-9.2 (Zhao et al., 2010). However, although heterogeneous Yam membrane had a higher self-diffusion coefficient, the ion-membrane affinity, intermembrane ionic transport and membrane thickness aided homogeneous Jam to have effective performance with over 90% As(v) removal from a feed solution of pH 7-9.2. Zhao et al. (2010) then hypothesized the As species present in bulk solution and membrane pore solution at different pH values during the modelling studies with the Nernst-Plancks equation.

2.6 Current Trends in Donnan dialysis

Donnan dialysis applications cover various industries spanning from the mineral process to the water and wastewater treatment industry. Laboratory scale experiments for the recovery and removal of metal species are reviewed in single processes for target metal ions and multi-stage processes.

2.6.1 Donnan dialysis only

This section focused on recoveries of target metal ions with Donnan dialysis only as cited in Table 2-2.

Table 2-2 Donnan Dialysis for the recovery of target metal species

Cation	Stream	Phase Conditions: Volume (Feed:Sweep] ratio	Phase Conditions: Feed pH	Phase Conditions: Sweep condition	Membrane	Time (hrs)	Highlights	Reference
Al^{3+}	Al-PWTR	4:1	3-3.5	1-2 M H_2SO_4	Nafion 117 (HM) Ionac 3470 (HT)	24	Ionac recovery of Al^{3+} was 55% lower than Nafion 117 Trace permeation of Fe^{3+}, Zn^{2+}, Cu^{2+} and As	(Prakash et al., 2004; Prakash and SenGupta, 2003)
Ti^{4+}, Fe^{3+}, Al^{3+}, Na^{+}	Bauxite waste	-	0.7-0.1	0.05- 1 M HCl	Neosepta CMB (HM) Neosepta CMX (HM) ICE 450- SA_3T (HT) ICE 450- SA_3S (HT)	2-3	Fluxes for all membranes follow the order $Fe^{3+} > Al^{3+} > Na^{+} > Ti^{4+}$. Recovery in all membranes mostly follows the order of $Na^{+} > Fe^{3+} > Al^{3+} > Ti^{4+}$ Recovery High in ICE 450- SA_3T and lowest in CMB Chelating agents either increases or decreases transport of metal ion.	(Çengeloğlu et al., 2003, 2001)
Au	Circuit board scrap	1:1	0.84	0.1-4 M NaCl	Micro-pore grafted CEM	8-10	89% Au recovered and trace transport of Cu and Ni despite being in high mass ratio in feed after 4 cycles of treatment.	(Agarwal et al., 2016)
Fe^{3+}	Fe-PWTR	2:1 4:1	3-3.5	1 M H_2SO_4	Nafion 117 (HM) Nafion 115 (HM)	24	82% Fe recovered in lower feed: sweep volume against 76% for high feed to sweep p volume ratio	(Keeley et al., 2016; Prakash and SenGupta, 2003)
Ca^{2+} and Mg^{2+}	Lime PWTR	1:1	-	0.02 HCl	Nafion 117 (HM)	13	20% Ca^{2+} recovered and 50% Mg^{2+}.	(Wang et al., 2010)
Ca^{2+} and Mg^{2+}	Tap water	-	6.8-7	0.1 M HCl	Four Modified PVDF membrane	2.5	80% recovery of Mg^{2+} and 70-72% recovery of Ca^{2+}. Modification improved membrane properties, hence better performance than synthesized and unmodified PVDF membrane.	(Şahin et al., 2009)
Cu^{2+} and Ag^{3+}	Synthetic solution	2- 10:1	-	1- 3 M HNO_3	Selemion CMV (HT)	24	Fluxes are $Cu^{2+} > Ag^{3+}$. Selectivity of both cations improve with the insertion of cation exchange textile between the CMV membranes. Cu^{2+} enrichment in sweep solution was 1.5-3.9 while Ag^{3+} was 1.2-7.9.	(Berdous and Akretche, 2002)

Cr^{6+}	Synthetic solution	-	4	0.1 -1 M NaCl	Selemion AMV (HM) Neosepta AFN (HM)	24	AFN removal ranged from 12-23% and AMW was 1.4- 9.1%. Statistical model was generated using 24-full factorial approach	(Marzouk et al., 2013a, 2013b)
Cu^{2+}, Co^{2+} and Ni^{2+}	Synthetic solution	2:1	-	0.01 M H_2SO_4 (pH 1-4)	ICE 450- SA_3T (HT) ICE 450- SA_3S (HM) Spectrapor Dialysis membrane	3.3	Flux of metal ions decreases with increasing pH of sweep solution for ICE membranes and vice versa for spectrapor. Recovery of metal ions by membrane is SA_3S> SA_3T > Spectrapor	(Ersöz et al., 2001)
$Cr^{3+}$and Cu^{2+}	Synthetic solution	-	3	0.1 HCl	Four different PVDF/P2FAn composite membrane synthesized with dopants	2.5	Flux and recovery of Cu is higher than Cr due to smaller hydration volume. Dopant effect on Cr recovery were similar for NSA and PTS. Dopant effect on Cu recovery was SDS> ABS > PTS > NSA.	(Koseoglu et al., 2010)

HM = Homogenous membrane; HT = Heterogeneous membrane; PVDF= Polyvinylidene fluoride ; PTS= p-toluenesulfonate, NSA =1,3 (6 or 7)-naphthalene trisulfonic acid; ABS= o-aminobenzen sulfonic acid, SDS=sodium dodecyl sulphate; P2Fan= poly2-fluoroaniline

2.6.2 Multi-recovery process

Process integration and combination is key to optimal ion recovery and concentration as means to achieve synergic advantage with individual process limitation and economic disadvantages addressed. The DD process has been used as a possible pre-treatment for the removal of ion inhibitors, fouling, and scaling sediments and as a post-treatment to further remove target ions. Table 2-3 consist of two stage combinative processes for the recovery. Donnan dialysis has been integrated in three or more multi-stage processes such as the recycling of lithium ion battery (Sonoc et al., 2018) and recovery of Fe from Fe-PWTR (Keeley et al., 2016).

DD processes in reverse osmosis (RO) and ion exchange (IEX) application studies looked into regeneration of resins using RO brines as the sweep phase for DD regeneration step and direct DD treatment of water and wastewater (Bryjak et al., 2007; Vanoppen et al., 2015). Vanoppen et al. (2015) expounded that DD as pretreatment for RO was affected by the monovalent to multivalent

cation ratio in the feed stream. In other studies, a Donnan enhancement factor was included into the existing Spiegler–kadem model for salt removal in a nanofiltration of binary, ternary and quaternary system (Levenstein et al., 1996). The donnan effect was established to enhance removal using polyacrylic acid sodium salt with molecular weight of 60 000 dalton.

In electrodialysis (ED), DD as a pretreatment increases the limiting current density of the feed solution for the desalination stage due to a change in the ionic composition of the solution (Wiśniewski and Rózańska, 2007). Whilst most DD-ED research have used either AEMs or CEMs, Rózańska and Wiśniewski's (2009) modifications used an integrated system made up of Selemion-CMV and Neosepta AFN which are CEM's and AEM's, respectively. Neosepta ACS has been admitted as very useful in the DD removal of bromide and bromate ions in a DD-ED treatment (Wiśniewski et al., 2014).

Also, focus has been channeled to microbial desalination (MDS) as it has demonstrated potential to treat wastewater and simultaneously generate electricity when microorganisms convert biochemical energy in organic matter into electricity, creating the needed potential gradient for desalination to occur (Santoro et al., 2017). Also, the adoption of MDS into DD is due to the abundance of hydroxide ions that can serve as an alkaline solution which may be used to produce dissociated ions for removal (Ping et al., 2015; Santoro et al., 2017).

onventional treatment of water and wastewater involves the use of coagulants to remove contaminants as flocs. High chemical demand, direct application, pH fluctuations and residual ion contamination is associated with coagulations. Oehmen et al. (2011) established that coagulant application at the sweep side provided extra driving ions for counter transport of target ions.

Table 2-3: Donnan dialysis and other treatment processes

Combined Process	Target Metal/ ion	Feed Phase for DD	Comments	Reference
Coagulation	As	Spiked natural water	$AlCl_3$ had higher flux than $FeCl_3$ at the receiver side due to adsorption of Fe^{3+} precipitates on AEM that are positively charged at lower pH thereby creating additional boundary layer for permeation.	(Oehmen et al., 2011)
Selective resin regeneration step	B	Boron selective resin (BSR) slurry and boric acid	Brine from First RO desalination can be used for regeneration of BSR. Donnan separation is controlled by desorption of boron from BSR particles.	(Bryjak et al., 2007)
Electrodialysis	Ca^{2+} ,Mg^{2+} and HCO_3^-,NO_3^-, SO_4^{2-}	Brackish solution	Desalination increased by 21% with observed reduction in energy consumption after 79-89% Ca^{2+}, 75-90% Mg^{2+} and [83-85% NO_3^-, 40-78% HCO_3^- and 84-95% SO_4^{2-}] DD recovery of membrane scalers in multi component system for different feed/sweep ratio of (1:1, 2:1 and 4:1) and membranes.	(Rozanska et al., 2006; Rózańska and Wiśniewski, 2009; Wiśniewski and Rózańska, 2007; Wiśniewski and Różańska, 2006)
	Br^- and BrO_3^-	Enriched natural water	Whilst DD achieved 86-91% recovery for Br and 93-97% for BrO_3. Recirculation of salt from electrodialytic treatment of DD receiver waste stream into DD achieved 61-78% and 79-86% for Br^- and BrO_3^- respectively.	(Wiśniewski et al., 2014)
Defluoridation by Adsorption	F^-,	Flouride contaminated Ground water	Al_2O_3 has better adsorptivity at sweep phase of DD system than ZrO_2 for all ions. Flouride concentration decreased from 3.8-4.1 mgL^{-1} by 73.20%, 68.90%, 30.90 % for DD+ Al_2O_3, DD+ ZrO_2 and DD only respectively in the continuous flow system.	(Garmes et al., 2002)
Microbial desalination	Br^-	Saline solution	Enhanced boron (20-42%) removal by DD process increased microbial desalination by about 15-35%. However, an MDS + DD process results in 50-70% removal than 38-60% in DD+MDS treatment.	(Ping et al., 2015)

Reverse Osmosis	Ca^{2+} and Mg^{2+}	Potato Processing waste water and Tap water	DD pretreatment before RO achieved 77% Ca^{2+} and 70% Mg^{2+} for wastewater, 79% Ca^{2+} and 71% Mg^{2+} for tap water. Modelling results indicates that DD can increase RO treatment 16% and 47% more for wastewater and tap water	(Vanoppen et al., 2015)
Struvite	Zn^{2+}, K^{+}, Na^{+}, Mg^{2+}, Fe^{3+}	Hydrolyzed sludge liquid	Statistical approach in hydrolyzing sludge liquid. Struvite composition met regulatory requirement as DD recovery of metal composition high.	(Uysal et al., 2017)

2.7 Process Limitation of Donnan dialysis

Donnan dialysis, unlike the pressure driven membrane process, is an concentration gradient driven process. As such, it is not affected by cake forming on membrane, rather, by concentration and the driving force.

2.7.1 Concentration Polarization

The concentration polarization is an inevitable phenomenon in Donnan dialysis as it affects the flux when the concentration of specific ions increase or decrease at the solution-membrane layer as a result of selective permeation through the membrane. The occurrence of a significant boundary layer on the surface of the membrane causes polarization. Due to the transport of some species more readily than others with subjection to the membrane's selectivity, the retained species concentrates at the upstream of the membrane surface (Baker, 2012). Parallel to that, the selected transported species which is higher in the bulk phase decreases in concentration as it approaches the membrane interface and enters the boundary layer formed. An ideal situation is presented in Figure 2-5 where Figure 2-5a presents a situation of no concentration polarization since no concentration gradient has been formed yet. As such, the flux of the permeable species is higher

in the membrane (J_1^m) than in solution (J_1^s). The concentration of the target species is constant up to the membrane surface. When significant layer sets in, as indicated in Figure 2-5b, concentration of target species decreases before it reaches the membrane surface. The concentration at the solution membrane surface facing the feed phase is different from the concentration of the target species in the bulk solution.

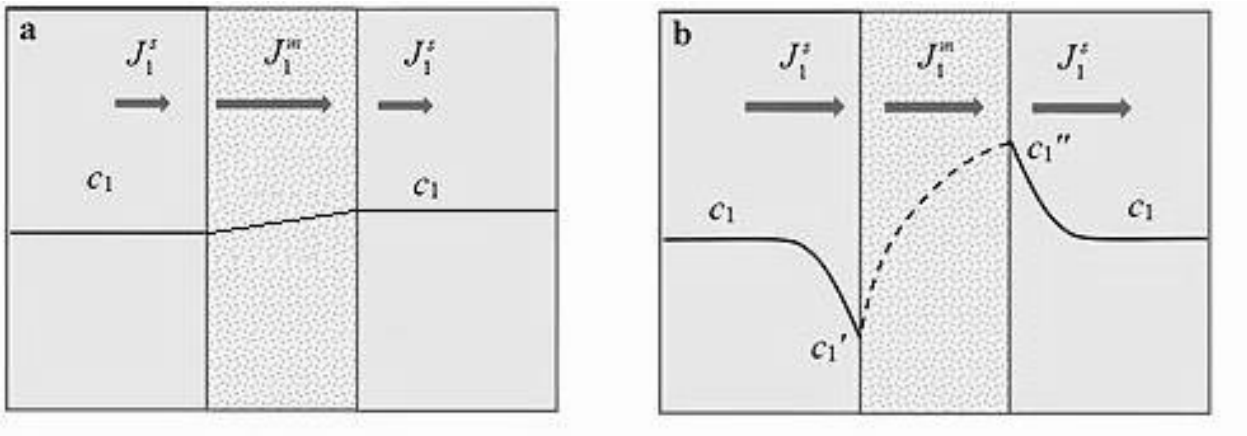

Figure 2-5: Fluxes and concentration profiles of membranes in operation; a) no concentration polarization b) with concentration polarization (Adapted from Pal, 2017)

Baker (2012) postulates a solution with two sub routes to controlling concentration polarization in membrane systems. By ensuring turbulent flow in the system, the boundary layer thickness reduces through the promotion of uniform species concentration in the phases. Turbulent flow can be achieved by increasing the flowrate over the membrane or by using baffles to manipulate the flow patterns of the solution to generate a turbulent regime.

2.7.2 Osmosis effect

Osmosis is the transport of water molecules across a semipermeable membrane necessitated by the difference in concentration at two sides of the membrane. The transport from the low region to the high region is for solvents while the semipermeable membrane rejects solutes.

Various studies on water transport have been conducted on Nafion cation exchange membranes. In Xie and Okada's (1995) and Okada et al.'s (1998) studies, the number of moles of water transporting across a Nafion 117 membrane was attributed to electrostatic interactions between ions in solutions and water dipoles. Additionally, the size of cations in solution contributes to water transport. When dipole charges between cations and water molecules are dominant, charges hold adjoining water molecules and move in unison across the membrane with the aid of electrostatic interactions. Okada et al. (1998) observed that, transport of water across the membrane increased with a decrease in ionic radius of hydrophilic cations and an increase in water transport for decreasing ionic radius in hydrophobic cations. Large cations in solution, by reason of volume exclusion, tended to push water molecules through to aid water transport.

Duan et al. (2012) expanded the studies on water transport through Nafion 115, Nafion 1110, Nafion 1035 and Nafion 212 membranes using the studies by Eikerling (1998) on Nafion membranes as a basis. Eikerling (1998) hypothesized that water transport across the Nafion 117 was as a result of driving forces, notably capillary pressure, external pressure gradient and osmotic pressure. Increasing the temperature decreased the viscosity of water and increased the hydrophilic volume fraction thereby increasing water transport across the membrane (Duan et al., 2012). Other outcomes included the increase in water transport at decreasing weight of Nafion and an increase in membrane thickness resulted in increased water permeation. Finally, an increase in the hydrostatic water pressure also increased the water transport across the membrane.

2.8 Limited literature and limitations towards full scale operation

After almost 95 years of the inception of DD, the technology is yet to be fully researched and have its full potential understood. As an extremely slow kinetic process for ion transport that takes a longer period to achieve equilibrium, concentration and separation of metals species, many approaches have not geared towards industrial applications (Ben Hamouda et al., 2017; Turki and Amor, 2017). Akretche (2000), therefore proposed the integration of Donnan dialysis to other separation processes rather than the single DD system. Table 2-3 of section 2.6.2 cites the research improvements when DD is incorporated with other process.

Another potential deterring factor to the application of Donnan dialysis is the higher purchasing cost of the membrane and the variable membrane selectivity (Keeley et al., 2012). However, this is the situation for every emerging technology as initial purchase affects the total expenditure cost. Research and development is therefore geared towards addressing such problems. The cost will decline when global demand soars with progress in research and development towards cheaper membrane production costs.

Factors such as feed flowrate, electrolytic sweep solution flowrate and experimental duration have limited information in literature and therefore drives the need for future investigation. As seen in Table 2-2, the various documented research does not make variations to these process conditions. Also, the few comparative studies with respect to pH, sweep solution for the species of interest has been performed using one factor at time. A more advanced approach has been the usage of the Nernst-Planck's equation in determining the flux of target ions through the membrane of choice,

with the exception of Marzouk et al. (2013b, 2013a). Furthermore, experimental duration varies depending on feed concentration, DD module and objective for the set research.

2.9 Design of Experiment

Design of Experiment (DOE) is a logical approach of evaluating and comprehending the relationship that exists between process and product variables affecting targeted response factors such as product performance, quality and physical properties. In a quest to improve on the quality of systems, obtaining enough suitable data and having an appropriate analytical tool to make important decisions and optimize performance is essential. This therefore tends to avoid making tentative decisions of variables on parametric impact based on assumptions. However, in experimental design, assumptions are tested. Design of Experiment has design advantages over quality management, mechanical and other process evaluation tools (Montgomery, 2017; Wagner et al., 2014).

Design of experiments follows experimental limits, specific experimental conditions and applies statistical techniques at any point within the limits to generate required information with minimum experimental runs. The selected DOE assists in achieving goals such as accommodation of noise and other random errors, estimation to be made of the magnitude of the noise, declare statistical significance of factors and evaluation of the practical importance of variations (Mark and Workman, 2018). During experimental matrix design and data processing by the experimental tool used, techniques such randomization, replication and blocking is adopted. Randomization is used to avoid systematic error and biased conclusion by setting experiments in an irregular structure. In order to estimate the error, replication by repetition of selected points is done. Finally, the blocking

technique is used to handle the influence of nuisance factors that is known and controllable. Experiments are, therefore, grouped according to their likeness in order to maintain internal and external validity (Antony, 2014; Barton, 2013).

2.9.1 Response surface methodology

One of the appropriate tools used to determine optimum conditions and provide information required for process design is the response surface methodology (RSM). The response surface methodology is a compilation of mathematical and statistical techniques helpful for developing models and analyzing the problems in which independent multi-controlling variables influence the dependent variable or response. The relation between the input controlling variables and the dependent response is then represented graphically. Response surface methodology has been applied in different areas which includes modelling and optimization in electronics, biotechnology, water, and wastewater treatment processes, automotive, agriculture, food processing and other process industries. Notable processes in the water and wastewater treatments are coagulation-flocculation, adsorption, electro-chemical processes, advanced oxidation processes (AOP) and disinfection (Bashir et al., 2012; Nair et al., 2014).

In RSM, for an assumption that all independent controlling variables are measurable, the relationship viewed as a surface can be expressed as Equation 2-13

$$Y = \phi\ (x_1, x_2, x_3, \dots\dots, x_{i,} \dots\dots, x_k) \qquad 2\text{-}13$$

where Y is the characteristic response of the system; ϕ is the response function; x_i is the independent variable; i and k are the number of variables. The powers of x_1, x_2 to x_k is up to a certain degree (d) where $d \geq 1$.

Furthermore, two relevant polynomial models are used in RSM. The first model, as seen in Equation 2-14, is for special cases and this includes first-degree models (d=1). The second degree model (d=2) is also expressed in Equation 2-14 (Kleijnen, 2015).

$$Y = \beta_o + \sum_{i=1}^{k} \beta_i x_i + \epsilon \qquad 2\text{-}14$$

$$Y = \beta_0 + \sum_{i=1}^{k} \beta_i x_i + \sum_{i<j} \sum \beta_{ij} x_i x_j + \sum_{i=1}^{k} \beta_{ii} x_i^2 + \epsilon \qquad 2\text{-}15$$

where Y, β_0, β_i, x_i, and ϵ are the characteristic response, constant term, coefficient, independent variable and random experimental error at a zero mean, respectively.

In RSM, the designs that fit the first – degree order designs and the second-degree order are referred to as first-order designs and second-order designs, respectively. Common first-order designs include 2^k factorial, simplex design and the Plackett-Burman design. Also, the designs under the second-order are 3^k factorial, Box-Behnken design (BBD), Doehlert matrices and the central composite design (CCD). In all these designs, experimental limits (low and high) are set to define the study space. The highs and lows are coded as +1 and -1, respectively. In second order designs, as the levels are equally spaced, independent center points coded as '0' and their interactions with coded +1 and -1 are used for optimization (Kleijnen, 2015).

The conventional way of optimization involves experimenting using a one-factor-at-a–time (OFAT) or one-variable-at-a-time (OVAT). As such, one factor is varied while the other variables are kept constant. Limitation associated with this process includes (Nair et al., 2014):

1) Inability to run multiple experiments
2) Time and resource intensive
3) High number of experiments which affects experiment cost.
4) Lack of interactive effect evaluation amongst independent variables

5) High risk of failing to identify the exact optimum form of the experimental limits.

The RSM uses fewer experimental runs to optimize a process under multivariable control. Additionally, under their five step loop process; (i) selection of independent variables and the limits, (ii) selection of experimental design and undertaking experiments using a design matrix, (iii) linear regression model generation based on recorded response, (iv) model verification of adequacy and fit and (v) two-dimensional and three dimensional graphical representation of the model and acquisition of optimal conditions (Nair et al., 2014), independent and interactional effects and statistical significance of variables are evaluated.

2.9.2 Central composite design

The central composite (CCD) design originally introduced by Box-Wilson is widely used in response surface applications for constructing a second-order polynomial without using a complete full factorial (2^k) or fractional factorial designs. The levels of the factorial points which comes from the full or factorial design coded as -1 and +1 are augmented with an axial portion consisting of 2*k* points and a number of center point replications shown in Figure 2.6, to allow for efficiently evaluating of the first and second order terms and the estimation of curvature. The axial points are symmetrical with the center points on the coordinate system at a distance $\boldsymbol{\alpha}$ from the design center. (Kleijnen, 2015; Sahoo and Barman, 2012).

Although the Box-Behnken design has fewer runs and avoids extreme points, the CCD has high efficiency to handle up to a maximum of 6 independent variables. Instead of a sequential approach for experiments with a lot of variables, optimization at such situations can be carried out on a parallel sequence in CCD (Nair et al., 2014). Furthermore, desired properties for the CCD is dependent on the number of center points and the distance, $\boldsymbol{\alpha}$, from the center points.

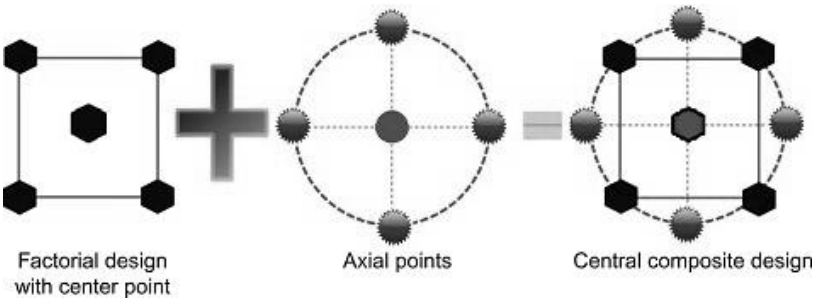

Figure 2-6: Generation of central composite design for two factors

The CCD consists of the face centered, central composite circumscribed and central composite inscribed. The original CCD is in the form of the central composite circumscribed. The axial points in the CCD are created by an extension of the high and low values of each variable to set up design space extremes. The circular or spherical symmetrical design has five levels. ($-\alpha$, -1, 0, +1, $+\alpha$) (Cevheroğlu Çira et al., 2016). In the inscribed CCD, the limits set for the variables are also the axial points and the system further computes appropriate factorial points inside the boundaries of the limits. Finally, face-centered CCD has the axial points located in the center of each face of the cube, hence $\alpha = \pm 1$ (Sahoo and Barman, 2012). Figure 2.7 is a set of examples on three varieties and their structure for two factors ($k = 2$) and three factors ($k = 3$).

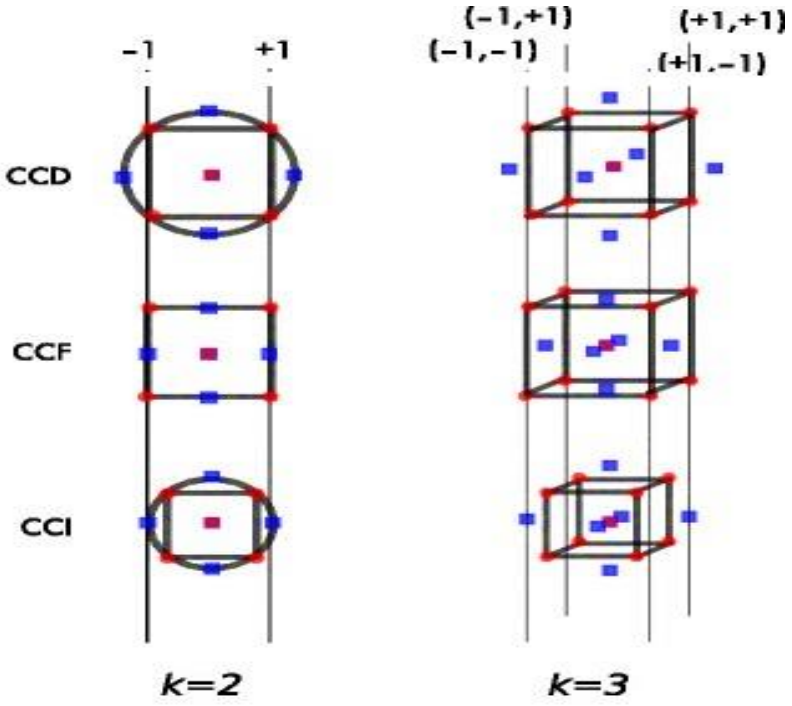

Figure 2-7: Experimental design for two and three factors for Central composite design types (Adapted from Toms et al., 2017)

3.0 Summary of literature review

Primary recovery of aluminium PWTR involves acidification and alkaline treatment to solubilize the ion of interest. However, other metal ions and organics are leached into solution. As such, secondary treatment such as pressure driven membrane processes and conventional resin-based ion exchange processes have been used. However, ion exchange by Donnan dialysis is a relatively new green process for the removal, recovery, separation, and concentration of ions. It is a simple to use, energy effective and non-fouling process.

Donnan dialysis has been applied on a laboratory scale to various production and waste streams in the mineral and water treatment processes. In the recovery of aluminium from potable water treatment residue, the process has shown performance efficiency in the rejection of organics.

However, a general disadvantage of DD is their slow kinetics and high cost of ion exchange membranes. These have derailed progress in industrial applications of DD.

The conventional investigation process in DD takes the one factor a time approach. However, statistical modelling provides an avenue to model DD for the recovery of aluminium under varied operational variables. Statistical modelling allows designing of experiment matrices which provides assessment of independent and interactional effects of factors for a given range of values. Models are then generated and response surface plots generated for effective decision making. This process allows significant reduction in cost and time of experiments for scale up. The approach is also a better option for optimization and prediction of responses from the experimental data.

CHAPTER 3

MATERIALS AND EXPERIMENTAL METHODOLOGY

3.1 Introduction

This chapter presents the processes for the Al-recovery studies using the Donnan dialysis (DD) system. This includes the mounted experimental set-up and a detailed drawing of the DD test rig. Furthermore, the chemicals used, membrane treatment process, experimental procedure and analytical techniques used, are discussed.

The design of the experimental matrix for high and low levels of the feed and sweep concentrations and their flowrates using the Face centered central composite design (FC-CCD) is highlighted. Also, the FC-CCD design was combined with significant variables to further optimize the process by simulating the acidification process at low and high feed concentration which is performed in the second stage. The third range of experiments were to investigate the transport flow inhibition of other metals to Al-recovery. Lastly, PWTR is fed to the DD system to evaluate the simultaneous recovery of Al and permeation of organics through the membrane.

3.2 Donnan dialysis set-up

In this experiment, a flat sheet membrane module was used. The rig block to house the membrane is made from PVC. Each block has a total volume of 2144 m^3. Leaks were prevented by the use of an acid resistant rubber gasket of thickness 3 mm to seal the block set on each side of the membrane. Tubes connecting the membrane rig to the peristaltic pumps of the feed and sweep vessels are from PTFE with an internal ID of 12 mm. The conceptual design of the rig encasing a

Nafion membrane is shown in Figure 3-1, experimental set-up illustrated in Figure 3-2, summary of experimental process flow diagram in Figure 3-3 and actual experimental set-up in Figure 3-4.

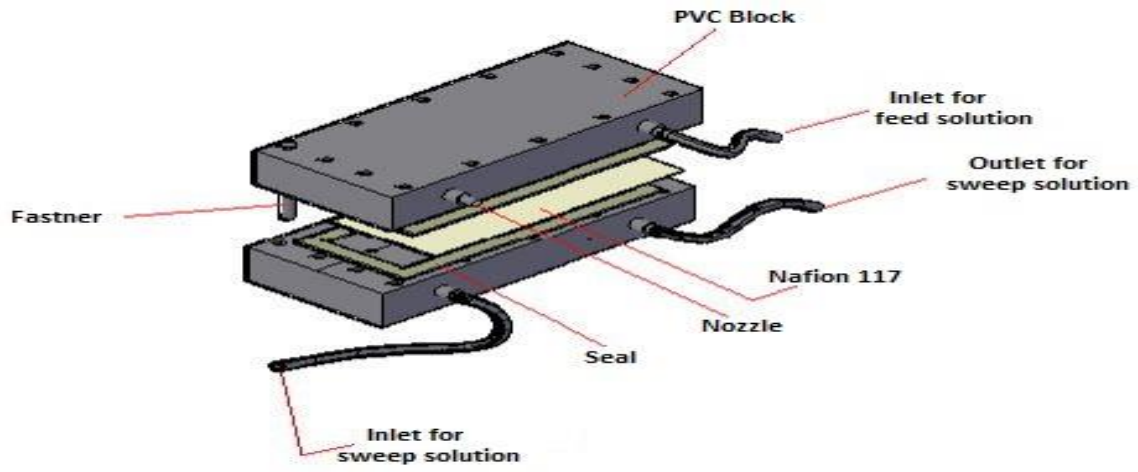

Figure 3-1: Conceptual diagram of PVC made rig with a Nafion membrane (Adapted from Asante-Sackey et al., 2020)

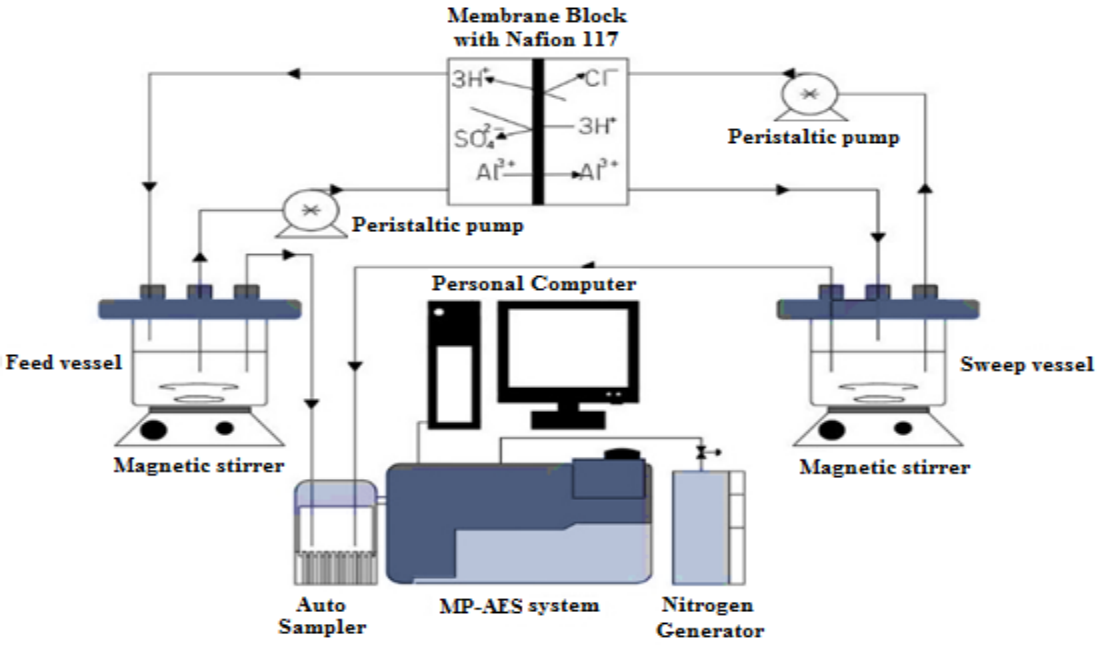

Figure 3-2: Schematic diagram of Donnan dialysis Experimental set-up. (Adapted from Asante-Sackey et al., 2019)

3.3 Experimental Procedure:

3.3.1 Materials

- The reagents used in this process are analytical or higher grade chemicals. Bulk aluminum octadecahydrate [$Al_2(SO_4)_3.18H_2O$; ≥ 97%)], hydrochloric acid [HCl; 38% w/w; density = 1.2 g/mL], sulfuric acid [H_2SO_4; 95% w/w; density = 1.84 g/mL)], copper sulfate pentahydrate [$CuSO_4.5H_2O$; 98- >100%], zinc sulphate pentahydrate [$ZnSO_4.7H_2O$; 99.5- >100%], ferrous sulfate heptahydrate [$FeH_{14}O_{11}S$; ≥ 99.0%], magnesium sulfate heptahydrate [$MgSO_4.7H_2O$, ≥ 98%], calcium sulphate dehydrate [$CaO_4S.2H_2O$; 99- >100%], manganese (II) sulfate monohydrate [$MnSO_4.H_2O$; ≥ 99%] and sodium hydrogen carbonate [$CHNaO_3$; 99.0- > 100%] were supplied by Lichro Chemicals - South Africa.
- Nafion 117 cation exchange membrane manufactured by DuPoint Industries was purchased from Merck, South Africa. The equivalent weight, thickness, working area and ion exchange capacity are 1100 $gmol^{-1}$, 177.8 µm, 205 cm^2 and 0.94 meq/g respectively.
- Potable water treatment residue was obtained from a local treatment plant in Durban - South Africa that uses alum in their conventional water treatment scheme.
- Deionized water was generated by using Purite-HP+BOOST 030773 at the Water Laboratory of the Department of Chemical Engineering-Durban University of Technology.
- Prolab PL 010 Oven is used for drying the real PWTR samples.

3.3.2 Pump Calibration

The pumps (maximum flowrate = 2.6 mL/s) were calibrated before commencing the experimentation and the rig was commissioned. A randomization approach was used where different levels of the pump speed was investigated in a random manner. The randomized levels were put into similar blocks to have a randomized complete block design (RCBD). Using a stop

watch, beaker and measuring cylinder, the RCBD is followed to achieve pump calibration. The flowrate at each pump setting under each single RCBD is shown in Table 3-1.

Table 3-1: Randomized calibration method

Blocks	1	2	3	4	5
	25	50	100	25	75
Pump Speed	75	25	50	100	50
(%)	100	100	75	50	25
	50	75	25	75	100

After following and completing the RCBD, the pumps were commissioned and leak tests on the rig was performed. The leak testing indicators and procedures are provided in Appendix B.

3.3.3 Membrane Treatment

Membrane treatment or activation is an important step in ensuring the membrane efficiency. The hydration method has often been used to increase the number of water molecules bound with hydrophilic sulfonic groups. Activation of the Nafion 117 was commenced by soaking the membrane in deionized water for 15 min and then removed and treated with 3 wt. % H_2O_2 at 60^oC for an hour. The membrane was then neutralized with deionized water before 3 wt. % HCl conditioning at 90^oC for an hour. The membrane was rinsed again with deionized water for another 15 mins and acid treated in 1 wt. % HCL solution for 3 hours at room temperature. Final rinsing with the deionized water for about 15 min is performed for the full activation of the membrane.

3.3.4 Feed and Sweep solutions

Synthetic and real feed from PWTR were prepared and used for this study.

3.3.4.1 Synthetic solution

The concentration of aluminium used in this experiment ranged between 100-3300 mg/L. The concentrations of Al were prepared such that the mass of alum 3 g < Alum < 112 g. The concentration of hydrochloric acid used in the sweep tank ranged between 0.25 - 1 M. The weighed mass of alum and measured volume of acid were dissolved and diluted respectively into the desired volume of 3 L and 1.5 L for feed and sweep phases, respectively.

Also, the pH range (1.3-3.7) requirement for specific feed concentration (FC) was achieved using pre-determined concentration of H_2SO_4, $CHNaO_3$ or HCl. Feed metal inhibition on transport was done on a 1:1 Al: metal basis. The optimized conditions for significant and insignificant factors are used as base settings for studies involving pH simulation and inhibition in binary feed solutions.

3.3.4.2 Raw sludge

Raw sludge, rich with alum residue was obtained from a local South Africa potable water treatment plant from the first stage of the dewatering process, stored in a plastic bag and then transported in an ice storage to the laboratory. The sludge was stored in a refrigerator at 4^{o}C under dark conditions to prevent physicochemical changes. Samples were dried in the Prolab PL 010 oven for 24 hrs and crushed using a mortar and pestle to increase the surface area. Digestion of 20 g of the sludge was done using 1 L of 0.05-0.5 M HCl for 24 hrs to obtain different Al concentrations. The sample was filtered off to obtain leachate to be used for the feed phase.

3.3.5 Donnan dialysis Process

3.3.5.1 Start Up and Operation

The treated membrane was encased in the PVC block and fastened together. Synthetic solution or PWTR fed into the feed tank was pumped using a peristaltic pump (A1N31F-7T) with maximum flowrate of 2.6 m/s to the Nafion 117 cation exchange membrane using the experimental matrices shown in section 3.3.2. The recirculating counter flow process between the acidic salt solution and the specified sweep solution was conducted for a maximum of 32 hrs. In the experiment, electrolytic solutions in feed and sweep vessels were was agitated with magnetic stirrers as illustrated in the experiment flow diagram (Figure 3-3) and the real set up for the DD process (Figure 3-4). Samples were taken every four hours for analysis.

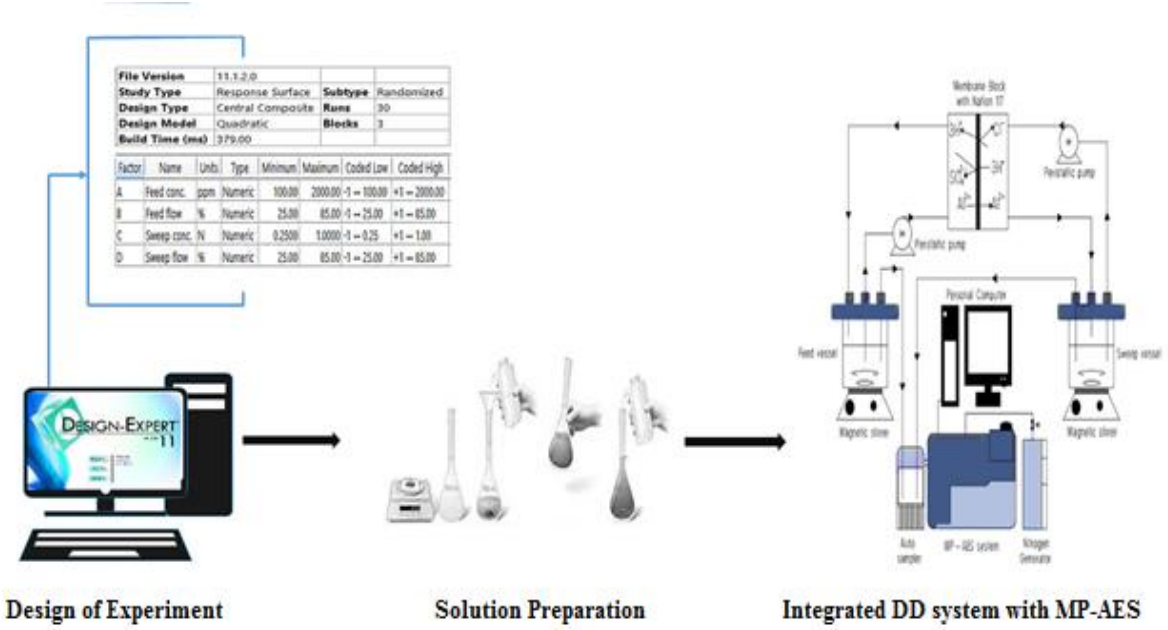

Figure 3-3: Experimental flow diagram for Donnan dialysis process (Adapted from Asante-Sackey et al., 2020)

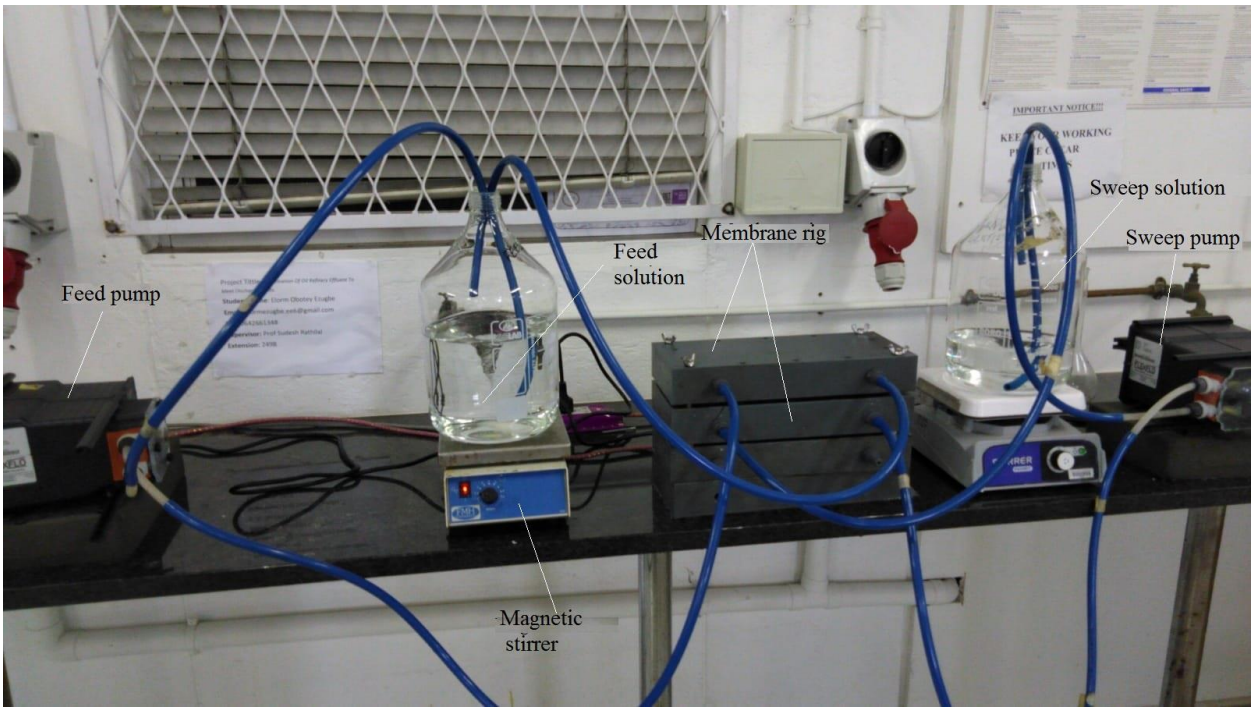

Figure 3-4: Actual Experimental set-up

3.3.5.2 Shutdown and Storage

The peristaltic pumps for feed and sweep phases were shut down after every complete run and the contents emptied. The feed and sweep tanks were then filled with deionized water. The pumps were operated at mid flow rates to circulate the deionized water to clean the rig. The recirculation and cleaning process was done for an hour before the pumps were switched off and tanks emptied. The Nafion membrane was then removed from the PVC housing and saturated in 1 wt. % HCl and rinsed for 15 min in demineralized water before was is replaced back on the block.

After shut down, the Nafion 117 is rinsed in deionized water for an hour and further conditioned in 1 wt.% HCl for 3 hrs. This step was to aid in the removal of adsorbed ions on the membrane surface and re-saturate the membrane with hydrogen ions. Lastly, the conditioned membrane was rinsed off with deionized water before set to dry and stored in an airtight bag.

3.3.6 Analytical Instruments

The analytical instruments used for this project are the Agilents's Micro plasma atomic emission spectrophotometer (MP-AES; MY 18379001) and the Varian's Ultra violet-visible (UV-Vis) spectrophotometer (model 3E). The MP-AES was for the quantitative analysis of aluminium in the feed and sweep phase samples taken periodically. On the other hand, the UV-Vis spectrophotometer was used to analyze the amount of organics present in the feed solution and amount permeated to the sweep solution for recovery using the PWTR. The operating procedure of the MP-AES and the UV-Vis are provided in Appendix B-2 and Appendix B-3 respectively.

3.7 Experimental Matrix

The experimental matrix followed the one-factor at a time (OFAT) to set up the high and low range for the experiments. The lower range was 100 ppm and the higher range was 2000-3300 ppm for the alum. The feed concentration (FC) are selected based on the concentrations in acid leachate and filtrate reported by Prakash et al. (2004), Petruzzelli et al. (1998), Petruzzelli et al. (2000a) and Petruzzelli et al. (2000b). Furthermore, the acid concentration chosen was from investigations made by Prakash et al. (2004). The feed and sweep flowrates used for specified concentration of the acidic salts was 0.65 mL/s and 2.21 mL/s for low and high flowrate, respectively. Table 3-2 below provides the OFAT matrix used.

Table 3-2: OFAT experimental ranges

Al concentration (mg/L)	**HCl (M)**	**Flow rate**		
		mL/s	Percentage	Rating
-	-	0.65	25	Low
2000- 3300	1	2.21	85	High

To investigate the full independent and interactional effects within the boundary set after the OFAT studies, the face centered central composite design (FC-CCD) approach was used. For objective 1, the significant effects of the chosen process variables at extreme low and high conditions on recovery of aluminium were investigated. Design Expert software-Version 11 by Stat-Ease Incorporation – Minneapolis (MN, USA) was used for the design of the experimental matrix, evaluation of the experimental data, empirical modelling, response surface plots and optimization of the experimental conditions. The total number of experiments was 30 and comprised of 16 factorial, 8 axial and 6 center points. Tables 3-3 and 3-4 provides the coded forms, while Tables 3-5 and 3-6 show the actual values for objectives 1 and 2.

Table 3-3: Actual values for FC-CCD for Objective 1

Symbol	**Variable**	**Coded levels of variables**		
		-1	**0**	**1**
X_1	Feed concentration (mg/L)	100	1050	2000
X_2	Feed flowrate (%)	25	55	85
X_3	Sweep flowrate (%)	25	55	85
X_4	Sweep concentration (M)	0.25	0.625	1

Table 3-4: Coded values for FC-CCD for objective 1

Run	Feed conc. (mg/L)	Feed flow (mL/s)	HCl sweep conc. (M)	Sweep flow (mL/s)
1	1	-1	-1	-1
2	-1	1	-1	-1
3	-1	-1	1	-1
4	1	1	1	-1
5	-1	-1	-1	1
6	1	1	-1	1
7	1	-1	1	1
8	-1	1	1	1
9	0	0	0	0
10	0	0	0	0
11	-1	-1	-1	-1
12	1	1	-1	-1
13	1	-1	1	-1
14	-1	1	1	-1
15	1	-1	-1	1
16	-1	1	-1	1
17	-1	-1	1	1
18	1	1	1	1
19	0	0	0	0
20	0	0	0	0
21	-1	0	0	0
22	1	0	0	0
23	0	0	0	0
24	0	1	0	0
25	0	0	-1	0
26	0	0	1	0
27	0	0	0	-1
28	0	0	0	1
29	0	0	0	0
30	0	0	0	0

The acid or alkaline (in excess) digestion of PWTR, solubilizes the $Al(H_2O)_3(OH)_3$ or simply $Al(OH)_3$ into aluminium sulphate complex (if sulphuric acid is used) or aluminium hydroxide complex (for alkaline medium). The final pH of the recovered coagulant is within the pH range of the acids (pH =1 to pH = 3) (Ahmad et al., 2016a) or alkalines (pH = 11.2 to pH = 11.8) (Masschelein et al., 1985). However, the acidification route has proven to have high primary Al-recovery. For this purpose, Objective 2 focuses on the effect of pH (≤ 3.7) and its interaction with significant factors according to the matrix in Tables 3.5 and 3.6. The optimum conditions for any of the insignificant factors from Objective 1 were used. Their selection is for efficient process economic reasons.

Table 3-5: Actual values for FC-CCD for Objective 2

Symbol	**Variable**	**Coded levels of variables**		
		-1	**0**	**1**
X_1	Feed conc. (mg/L)	100	1050	2000
X_2	Feed flowrate (%)	25	55	85
X_3	pH	1.3	2.50	3.70

Table 3-6: Coded values for FC-CCD for objective 2

Run	Feed conc. (X_1; mg/L)	Feed flow (X_2; %)	pH (X_3)
1	1	1	1
2	1	-1	-1
3	0	-1	0
4	1	-1	1
5	1	1	-1
6	-1	1	-1
7	0	1	0
8	0	0	-1
9	-1	-1	-1
10	0	0	-1
11	0	0	0
12	0	0	0
13	0	0	1
14	0	0	0
15	0	0	0
16	-1	0	-1
17	0	1	1
18	0	-1	1
19	1	1	0
20	0	0	0

Furthermore, the metals of concern in the inhibition study with respect to aluminium transport were calcium, magnesium, manganese, copper, zinc and iron (II). A randomly selected concentration from a range of medium to high recovery observed in Objectives 1 and 2 were used for the 1:1 inhibitive Al-transport study in the binary trivalent-divalent solution as shown in Table 3-7.

Table 3-7: Trivalent-Divalent binary runs for Objective 3

Standard	Binary Runs
Al^{3+}	Al^{3+}/Ca^{2+}
	Al^{3+}/Mg^{2+}
	Al^{3+}/Mn^{2+}
	Al^{3+}/Zn^{2+}
	Al^{3+}/Cu^{2+}
	Al^{3+}/Fe^{2+}

Lastly, the leachate from the acidification of the PWTR was characterized and permeation study for Al and organics conducted. This followed the process in section 3.3.6 to obtain two concentration points to conduct the studies for objective 4.

CHAPTER 4

RESULTS AND DISCUSSIONS

4.1 Introduction

The main focus of this chapter is to discuss the experimental results obtained using the designed counter-flow Donnan dialysis system used for Al-recovery. The section is divided into four sections. In the first section, the experimental runs are validated using the concentration and repeatability process, with Al-transport accounted for using the mass balance and hydrodynamic transport of water. The section then follows with discussion on the investigated performance under multivariable conditions to maximize the Al-recoveries. The optimized conditions and models obtained are then highlighted. The outcome of the investigation from inhibition of metals and transport of organics across the membrane with the simultaneous recovery of aluminum is then presented.

4.2 Validation and error analysis

The RSM approach provided repeatable center points for validation of the result. It was imperative to validate results with pre-experimental runs by using the concentration balance and repeatability analysis. The essence of the repeatability approach is to ensure that there is no mass loss due to experimental leakage in the rig. As such, under the same experimental conditions, the experiment was repeated twice. Samples were taken at equal time intervals, diluted and analyzed using the MP-AES. The performance was evaluated with a feed concentration of 200 ppm of aluminium, 0.5 M HCl as the sweep concentration and a feed/sweep flowrate of 0.625 m/s. Reliability of analytical instruments was performed in-between the sample analysis with a quality control of 25

mg/L. The overall analysis calculation included the experimental error. The error in the quality control is presented in Appendix C. The repeatability experiment and analysis was performed three days apart. To minimize position and vibrational disturbances, the pumps were firmly cushioned to the bench.

Figures 4-1 illustrates the aluminium transport from the feed phase and its acceptance in the sweep phase at equal flow rates. Both conditions consist of the original run and two repeated results (rep 1 and rep 2) to obtain profiles for feed and sweep at the different conditions set for the DD process. Data for the entire 28 hr study was collected every 4 hrs. The percentage deviation process was used in evaluating the error. Percentage deviation in statistics measures the extent to which individual data points deviate from the average measurement. To determine the percentage deviation, the mean of the data points was statistically determined and followed by establishing the average deviation of the data points from the mean. The average deviation from the mean was then divided by the mean and then converted into a percentage. Table 4.1 shows the percentage deviation at each time interval for different experimental conditions.

Observing the three feed lines in Figure 4-1, the largest error occurred at 4 hrs, followed by 24 hrs. The large ±6.44 Al concentration error at the initial time period between 0 – 4 hrs can be due to disturbance associated with the starting up of the pump. Also, during initial starting up, concentration gradient is extremely steep, resulting in a sporadic exchange. Evidently, the varied flowrates establishes the fact that unequal flowrates affect the exchange behavior at the solution-membrane interface and the membrane-membrane internal transport scheme. After the initial 4 hr deviation, a more than 60% drop in deviation was observed between 8-20 hrs of flow. A similar effect occurred at 4 hrs and 24 hrs in the sweep phase as shown in Table 4-1. The difference between the high deviation reported at 4 hrs and 24 hrs was ±0.16. Although the sweeping strength

is high at the sweep phase, thereby causing the Al^{3+}-H^{+} exchange, the flow position of the acid could also affect the membrane-solution contact. The feed solution is gravity aided as it flows over the membrane surface, however, the sweep solution is not due to the acid flow beneath the membrane.

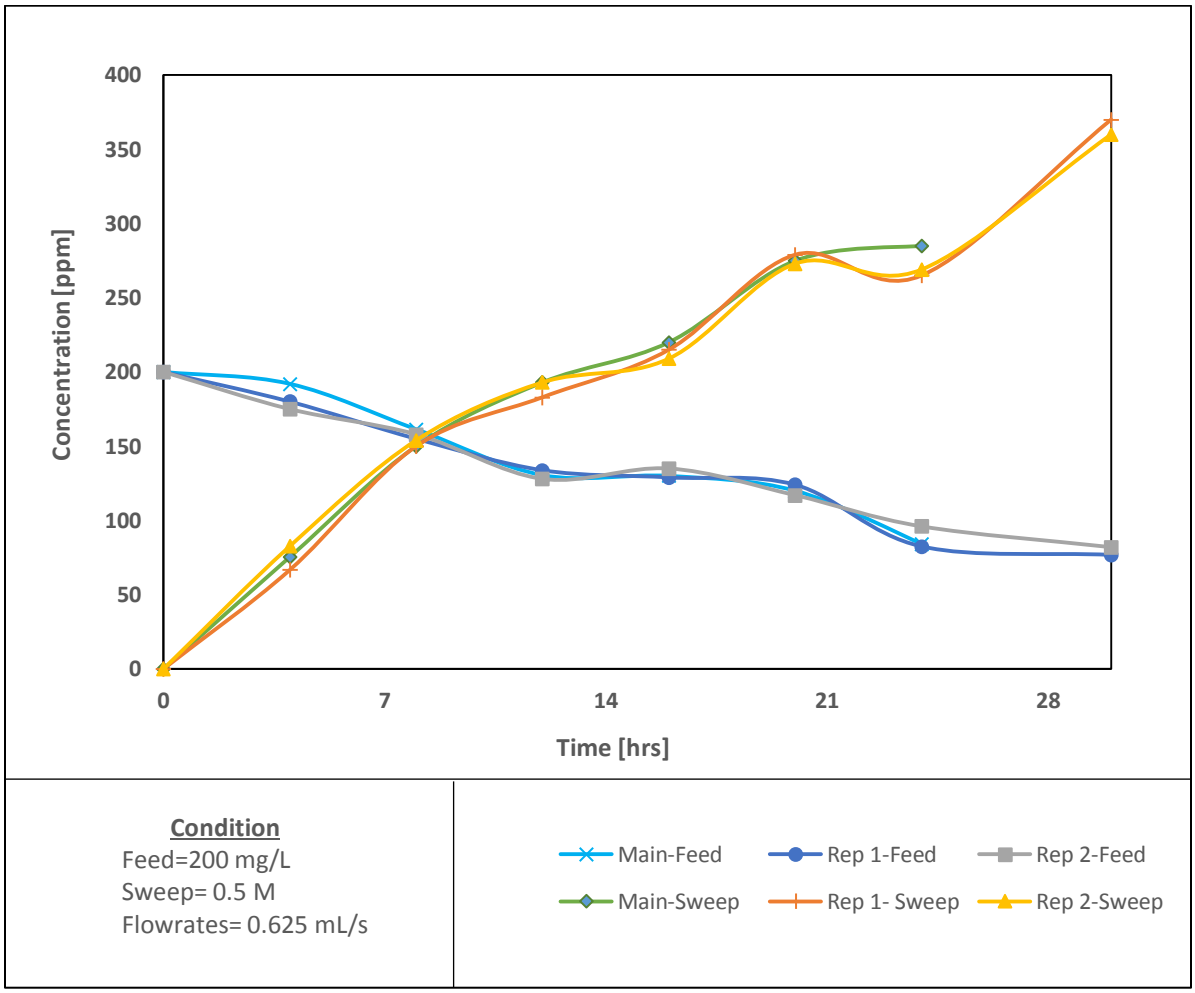

Figure 4-1: Repeatability runs for error analysis at 0.625 mL/s phase flowrates, 0.5 M HCl and 200 mg/L Al^{3+}

Table 4-1: Error analysis for feed and sweep phases at equal flowrates

Feed phase				Sweep phase		
Time (hrs)	Mean (ppm)	Average deviation (ppm)	Deviation (%)	Mean (ppm)	Average deviation (ppm)	Deviation (%)
0	200	0.00	0.00	0.00	0.00	0.00
4	182.33	±6.44	3.53	74.93	±5.49	7.33
8	158.13	±2.18	1.38	151.33	±0.89	0.59
12	130.77	±2.02	1.55	189.67	±4.44	2.32
16	131.33	±2.44	1.86	214.67	±3.78	1.76
20	120.33	±2.44	2.03	275.63	±2.24	0.81
24	100.25	±5.61	5.58	266.33	±5.33	1.95
28	88.70	±3.13	3.53	332.00	±4.67	1.41

4.2.1 Mass balance and verification

In order to keep track of the ionic or elemental Al in the designed single component DD system where stoichiometric counter mass transport occurs, a mass balance must be performed. Starting with an Al-concentration of 3300 mg/L at the feed phase, 2 M H_2SO_4 at the sweep phase, a feed to sweep volume ratio of 2:1 and phases' flowrate kept constant at 2.39 mL/s, the transport profile was determined. A 10 mL sample at each phase was taken at regular time intervals.

Analytical results for samples analyzed with the MP-AES and the corrected volume was used for the mass balance verification as shown in Table 4-2. A 4.24% mass difference was unaccounted for but is within the acceptable accuracy of analysis. The unaccounted Al remained in solution at the feed phase, while others were at the membrane-solution interface on the DD system.

Table 4-2: Mass Balance for High feed verification run

Phases	Initial mass of Al^{3+} (mg)	Final mass of Al^{3+} (mg)
Feed	9768	2655.74
Sweep	0	6698.50
Total	9768	9354.24
Percentage difference	4.24%	

bserving from the transport profile Figure 4-2, an increasing Al^{3+} in the sweep phase from its decrease in the feed phase resulted in highest Al concentration of about 6500 mg in the sweep and the lowest Al of almost 890 mg in the feed phase. By a direct transport sequence, about 2400 mg of the aluminium ion is expected to be at the sweep phase. However, observing from the figure, the initial 3300 mg concentration of Al used in the verification run was concentrated 2.0 times at the sweep phase after 48 hours. The polynomial trend lines were fitted to the data to give a clear relationship between the appreciating and depreciating profiles in both phases.

The trend lines demonstrate the kinetic driven zone, the Donnan equilibrium zone and the osmotic driven zone reported by Prakash et al. (2004). In the sweep profile, the kinetic driven zone occurs between 0 - 10 hrs where almost a half of the Al in the feed was transported. The reduction in the concentration of aluminium after the 36 hr run could be due to the dilution as a result of the osmotic zone effect. The time zone between the kinetic driven zone and the osmotic zone is the Donnan equilibrium zone. Observingly, not much reduction in aluminium transport occurs after 32 hrs and a similar can be reported for the concentration of Al at the sweep phase.

After 48 hrs, the volume in the feed phase decreased by 580 mL while the sweep phase volume increased from 1500 mL to 2080 mL. The increase in volume at the sweep phase, therefore, decreased the concentration effect by about 8% after the peak zone of 6700 mg/L at 36 hrs.

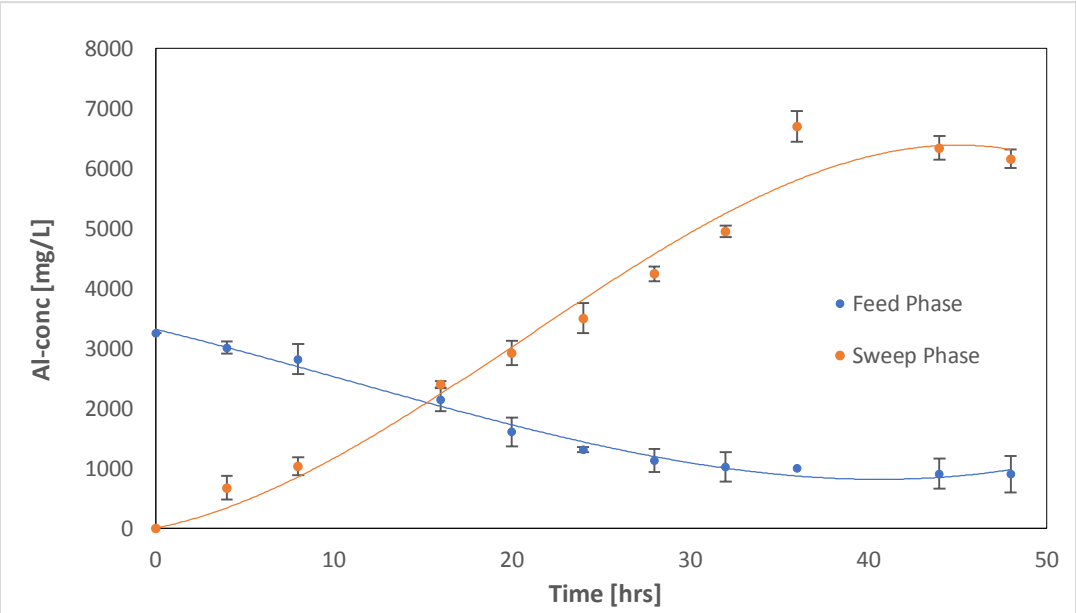

Figure 4-2: Feed and Sweep phase Al-transport profile for mass balance verification

4.2.2 Hydrodynamic transport

The transport of water across the Donnan system is inevitable as it is a limitation revealed by literature (Davis, 2000). The verification section in 4.2.1 shows that water flux reduces the concentrating effect of the DD by diluting the Al in the sweep solution. The osmotic effect across the membrane is, therefore, investigated with water and electrolytic solutions.

4.2.3 Water Transport

The experiments were conducted using water only for both phases, Al solution for the feed phase and water for the sweep phase, water and acid sweep solution, and lastly, an aluminium feed

solution against HCL and H_2SO_4 as the sweep solution. The water-water transport in a 2:1 volume ratio was conducted for 40 hrs. At the end of the experimental run time, the 2:1 volume ratio was maintained signifying no change in volume. Therefore, the water transport across the membrane from the feed phase to the sweep phase cannot be a function of pressure variations.

Dismissing the first claim with respect to the water-water transport experiment, the Al-solution of concentration 3300 mg/L was used. Maintaining the feed and sweep phase volume ratio, the sweep side water volume did not change after 50 hrs. However, in the investigation between the water as feed solution and 1 - 2 M acid solution, a 360 – 470 mL and 500 - 650 mL volume increase was measured for HCl and H_2SO_4, respectively. This showed that change in volume is proportional to the change in concentration of each acid.

The final water flux experiment was conducted using 3300 mg/L Al against 2 M acid solutions. At the end of the 40 hr run, the volume at the feed phase decreased by 720 mL for HCl sweep solution and 890 mL for H_2SO_4. The transport of water through the membrane in this run is higher compared to the water and acid solution runs. This is so as during ion exchange, water molecules are pushed through the membrane channels by volume exclusion (Okada et al., 1998). From Equation 4-1, the typical water generative transport within the DD system is seen and the resultant effect is the reduction in the recovery and concentration of transported aluminium across the membrane.

$$Al_2SO_4 + 6HCl \rightarrow 2AlCl_3 + 2H_2O + H_2SO_4 \qquad 4\text{-}1$$

Every chemical specie used in the experiment exerts an osmotic pressure during complete dissociation in water. Since the transport is hypothesized to be a secondary factor that causes water

transport, it is prudent to evaluate the osmotic pressure exerted by change in concentration. This osmotic pressure of a chemical in solution can be calculated from the Van't Hoff expression given by:

$$\pi = iMRT \qquad 4\text{-}2$$

where π is the osmotic pressure; i = Van't Hoff factor; M = molarity of species; R is the ideal gas constant and T is the temperature at 298.15 K.

The graph of osmotic pressure against concentration was evaluated using Equation 4-2 and plotted as shown in Figure 4-3. Tracing the osmotic pressure at 2 M on Figure 4-3, the aluminium sulphate exerts a higher osmotic effect than sulfuric acid. However, this was not so in the Al^{3+} effect on water transport as no water transport was recorded. The Al concentration (3300 mg/L) is equivalent to 0.031 M $Al_2(SO_4)_3.18H_2O$. From the graph, such a concentration will correspond to 3.7 atm and it is significantly lower than that of the acids. This, therefore, explains why no water transport was recorded.

Figure 4-3 points out that, at constant temperature, acids of the same concentration but with different Van't Hoff factors will not draw the same water through the membrane. Acids with high Van't Hoff factors would draw more water. As the concentration increases, the drawing effect of water through the membrane also increases. Hence the water increase across the DD system from the feed phase to the sweep phase is proportional to the osmotic pressure. The high osmotic pressure of sulfuric acid is the reason for the higher water transport than hydrochloric acid. The high water transport at 2 M sulfuric acid in Prakash et al. (2004) confirms this observation.

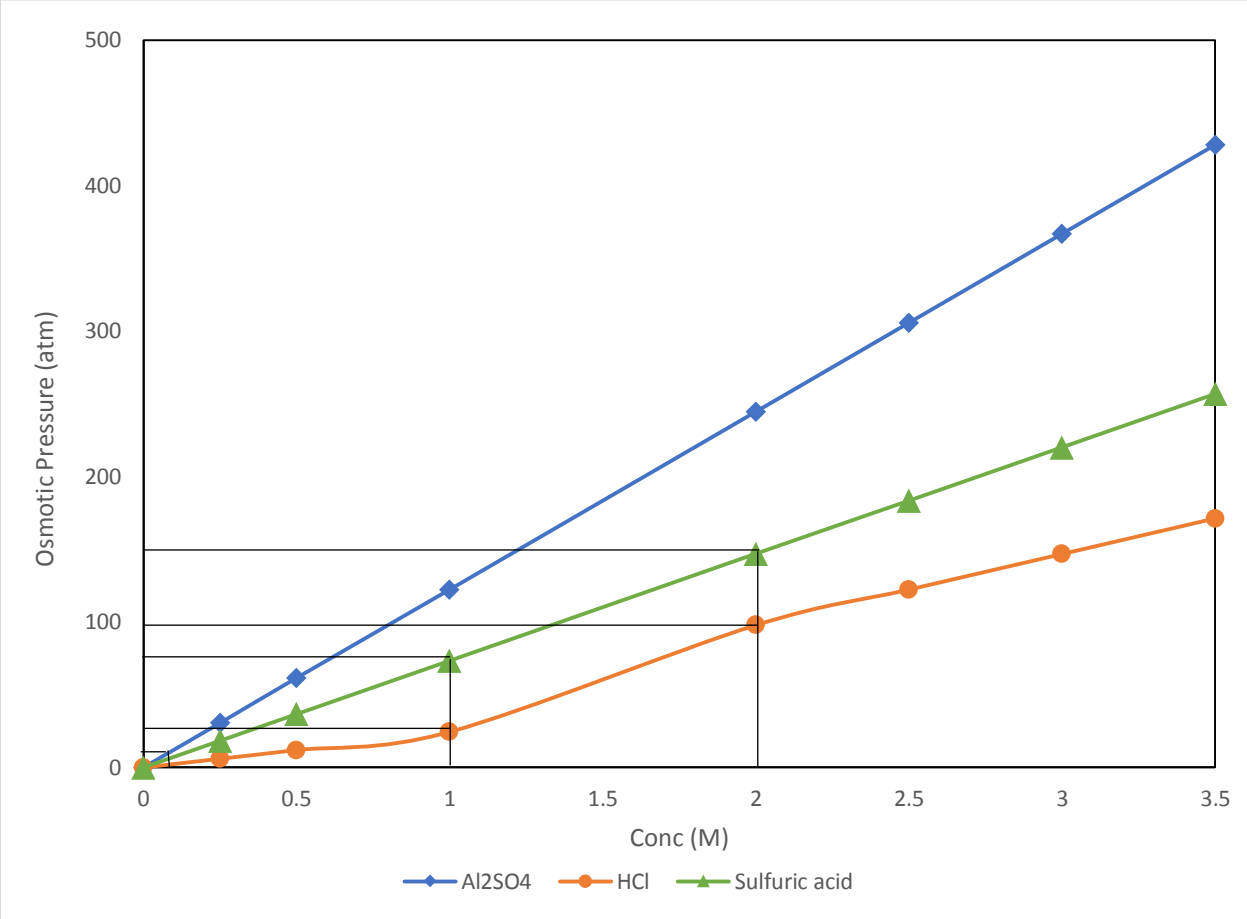

Figure 4-3: Effect of varying concentration of HCl, Al_2SO_4 and H_2SO_4 on Osmotic pressure

The water transport across the membrane can be minimized by operating at a low sweep concentration of the acids. However, the electrochemical potential gradient will also be reduced. Therefore, hydrochloric acid becomes the best acid to use as it corresponds to a lower osmotic pressure. Conclusively, HCl was then used for the remaining experiments. Also, a final sweep phase solution of $AlCl_3$ is a coagulant option used by PTWPs.

4.2.4 Operating Range for aluminium.

The objective of this section is to set the right operating condition for factors in the next studies. From section 4.3.1, HCl has been selected as the sweep solution. The maximum concentration is set to 1 M. Davis (2000) indicated that a sweep solution concentration higher than 1 M was not beneficial.

The one-factor at a time approach was then used to set the maximum concentration for aluminium specific to the DD system designed. Using a low (25%) and high (85%) feed and sweep flowrates and 1 M HCl, the aluminium concentration (2000 - 3300 mg/L) was set to meet a 50% recovery target. By this 50% recovery target, the operational functionality and limit of the DD system is achieved. Also, the economic advantage of recovery, recycling and reuse of coagulant is fully harnessed. Figure 4-4 shows the effect of low and high feed and sweep flowrates on aluminium recovery. After 24 hrs, the Al recovery was less than 50% with a starting feed concentration of 3000-3300 mg/L. The lowest Al recovery of 51.70% was found at 2000 mg/L under a high feed flowrate and high sweep flowrate condition. Hence, the concentration range for further experiments were set between 100-2000 mg/L.

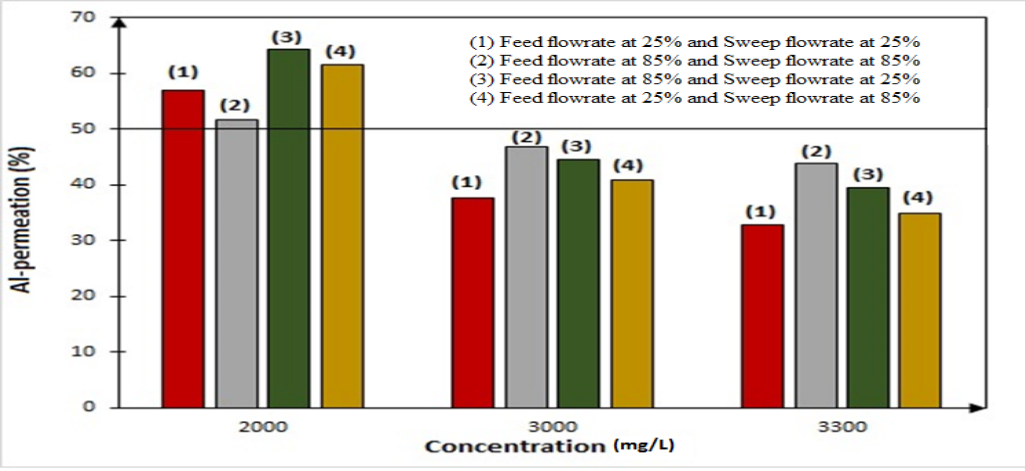

Figure 4-4: Al-recovery limit using OFAT approach

4.2.5 Summary of Preliminary studies

Four key investigations were performed for this objective. These were, the validation and error analysis, Al mass balance and hydrodynamic transport. The validation and error analysis showed that a high average deviation of ±6.44 for the feed phase and ±5.49 at the sweep phase was observed. Also, the mass balance indicated a 4.24% percentage difference. All deviations and differences are within an acceptable limit.

In determining the hydrodynamic effect, it was found that, water transported from the feed phase to the sweep phase. The volume of water that transported increased with increasing concentration. Also, the concentration was increased, affecting the osmotic pressure exerted by complete dissociation of chemical species. Unlike the hydrochloric acid and sulfuric acid, the high Van't Hoff factor of aluminium did not translate into a high water transport due to its low osmotic pressure. Hydrochloric acid was selected for subsequent Al-recovery experimentation due to its low water transport over sulfuric acid.

From literature, 1 M was accepted as the maximum operating range for HCl. Furthermore, the OFAT experiments on aluminium recovery at a 50% cut-off showed that the maximum aluminium concentration to be used for further runs should not exceed 2000 mg/L. The low range of 100 mg/L was selected with the aid of literature (Petruzzelli et al., 2000).

4.3 Significant effect

This section's objective is to investigate the significant effect of process variables that affect the amount of aluminium which can be recovered and concentrated through the counter flow Donnan dialysis process. The process variables are feed concentration, feed flowrate, sweep concentration and sweep flowrate. Process variables to consider varies with respective to the DD system used

for any target ion recovery. The basis and conditions for the process variables were chosen after references to supportive DD system literature by Prakash (2004), Zhao et al. (2012), Szczepański and Szczepańska (2017) and Marzouk et al. (2013b). With support from literature and the trend analysis in Figure 4-2 under section 4.2, the total experimental run was set to 32 hours.

Instead of using a screening design, the face-centered central composite design was selected for this investigation. The face-centered gives much experimental runs and boxes the investigation within the selected conditions. Extreme conditions for the process variables were considered to give a good and noticeable account of their impact on the aluminium transport from the feed phase to the sweep phase. As presented in Table 3-4 of section 3.4 and Table 4-3 of this section, the response for the design matrix was the percentage recovery of aluminium. The choice of the percentage recovery as response is appropriate as it will help to avoid flat graph lines at low concentrations due to the resultant effect of exponential increase in experimental conditions at the feed phase. For this purpose, a trend line approach was once again employed to give a clear indication of the transport zones. In order to avoid the concentration effect of the membrane on the aluminium at the sweep phase, the feed phase transport profile at regular time interval was used for the recovery study as transport is from the feed phase into the sweep phase.

In order to evaluate the effects of the process variables on the response, the matrix was analyzed and categorized. From the categorization, ten pairs of runs can be used for the evaluation of each effect. However, seven to eight possible profiles were used for the comparative study. The remaining data is presented in Apendix C .The experimental matrix for the FC-CCD runs presented in Table 4-3 is used to show the variable effect on the response.

Table 4-3: FC-CCD Design matrix in actual conditions

Run	Aluminum feed conc (mg/L)	Feed flow (mL/s)	HCl sweep conc (M)	Sweep flow (mL/s)
1	2000	0.65	0.25	0.65
2	100	2.21	0.25	0.65
3	100	0.65	1	0.65
4	2000	2.21	1	0.65
5	100	0.65	0.25	2.21
6	2000	2.21	0.25	2.21
7	2000	0.65	1	2.21
8	100	2.21	1	2.21
9	1050	1.43	0.625	1.43
10	1050	1.43	0.625	1.43
11	100	0.65	0.25	0.65
12	2000	2.21	0.25	0.65
13	2000	0.65	1	0.65
14	100	2.21	1	0.65
15	2000	0.65	0.25	2.21
16	100	2.21	0.25	2.21
17	100	0.65	1	2.21
18	2000	2.21	1	2.21
19	1050	1.43	0.625	1.43
20	1050	1.43	0.625	1.43
21	100	1.43	0.625	1.43
22	2000	1.43	0.625	1.43
23	1050	0.65	0.625	1.43
24	1050	2.21	0.625	1.43
25	1050	1.43	0.25	1.43
26	1050	1.43	1	1.43
27	1050	1.43	0.625	0.65
28	1050	1.43	0.625	2.21
29	1050	1.43	0.625	1.43
30	1050	1.43	0.625	1.43

4.3.1 Effect of Feed concentration

The effect of feed concentration on the percentage aluminium recovery was assessed using Runs 2 and 12, 4 and 14, 22 and 9, 21 and 30, 7 and 17, and 1 and 11. Looking at Runs 2 and 12, the feed flow, sweep concentration and sweep flowrate was operated at 2.25 mL/s, 0.25 M, and 0.65 mL/s, respectively. The feed concentrations were varied from 100 mg/L to 2000 mg/L. The study

at 4 and 14 was performed at a high sweep concentration of 1 M. Runs 9 and 30 on the experimental matrix are repetitive runs with feed concentration, sweep concentration and phase flowrates of 1050 mg/L, 0.625 M and 1.43 mL/s, respectively. For this purpose, Run 30 was used to represent the repetitive runs. In Run 22 and Run 21, a concentration of 2000 mg/L and 100 mg/L was compared with Run 30 at the same sweep concentration and phase flowrates. While the concentrations at Runs 1 and 7 reduces from 2000 mg/L to 100 mg/L in Runs 7 and 11, the conditions for Runs 1 and 11 occurred at low sweep concentration and phase flowrates. Runs 7 and 17 was performed at low feed flowrate and high sweep concentration and sweep flowrates as shown in Table 4-3. Figure 4-5a contains plotted values for Runs 7, 17, 30 and 21. The remaining comparative runs of 2, 12, 14 and 4 are shown in Figure 4-5b.

Increasing a low feed concentration of 100 mg/L by almost 10-20 times must invariably result in a high transport to the sweep phase. However, ion transport shows a trend of decreasing crossover from the feed to the sweep phase as feed concentration was increased. From Figure 4-5a, commencing at medium flowrates and sweep concentration, a 950 mg/L increase in Run 30 to make up 2000 mg/L in Run 22, reduced the recovery by 24.76% after 8-hrs and 27.73% for a day. A recovery of 58.75% at Run 22 after 32 hrs was about 27% less than that in Run 30. Comparing Run 30 and Run 21 (Figure 4-5a), a reduction in feed concentration increased the recovery by 1.4% more at 4 hrs to 1.7% more after 12 hrs. Evidently, for period 0-24 hrs, the recovery difference was between 1.4-3.45%. While the recovery at Run 22 was 27% less than Run 30, Run 30 was about 6.77% less than Run 21 after 32 hrs.

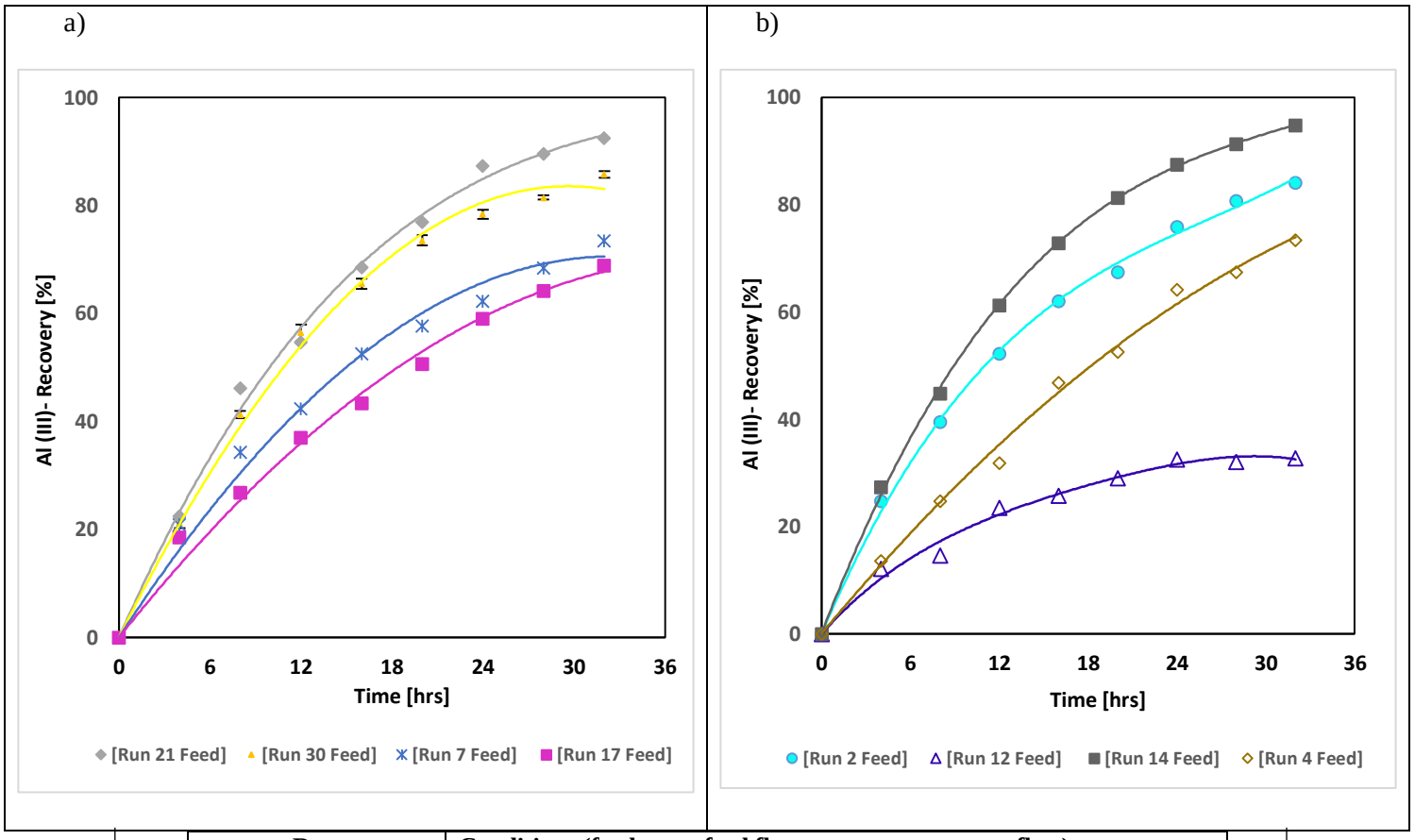

Run	Conditions (feed conc, feed flow, sweep conc, sweep flow)
2	100 mg/L, 2.21 mL/s, 0.25 M, 0.65 mL/s
12	2000 mg/L, 2.21 mL/s, 0.25 M, 0.65 mL/s
4	2000 mg/L, 2.21 mL/s, 1 M, 0.65 mL/s
14	100 mg/L, 2.21 mL/s, 1 M, 0.65 mL/s
7	2000 mg/L, 0.65 mL/s, 1 M, 2.21 mL/s
17	100 mg/L, 0.65 mL/s, 1 M, 2.21 mL/s
21	100 mg/L, 1.43 mL/s, 0.625 M, 1.43 mL/s
30	1050 mg/L, 1.43 mL/s, 0.625 M, 1.43 mL/s

Figure 4-5: Effect of feed concentration at constant flowrates and sweep concentration

Figure 4-5b compares Runs 2 and 12. The profile supported the trend of a reduction in recovery when the feed concentration is increased. In Run 2, the final recovery (> 83%) at the high feed flowrate and low sweep phase condition was 51.95% more than that observed in Run 12. No significant aluminium transport occurred between 24-32 hrs as 0.10-0.85 % difference was noticed in the 32% recovery at Run 12. Similarly, the pair of Run 14 and Run 4 resulted in a recovery of over 90% and 70 %, respectively. However, the results from Run 17 and 7 (Figure 4-5a) contradicted the trend. While aluminium is transported across the membrane, more water is received at the sweep phase at high sweep phase conditions. As such, the final aluminium concentration at the sweep phase was diluted at low feed concentration. The transport of Al^{3+} tends to increase at the high feed concentration (2000 mg/L) in order to observe the 73.35% recovery.

4.3.2 Effects of Feed flowrate

The pairs of Run 13 and Run 4, Run 23 and Run 24, Run 8 and 17 as well as Run 11 and Run 2 were used to expound on the effect of feed flowrate of the Al-recovery. Categorizing the conditions in Table 4-3 and Figure 4-6, Runs 8 and 17 were operated under low feed concentration and high sweep phase conditions while Runs 11 and 2 were under low feed concentration and low sweep phase settings (Figure 4-6a). Furthermore, Run 13 and Run 4 was under a high feed concentration and low sweep flowrate. The pair of Run 24 and 23 was carried out in medium feed concentration, and medium sweep phase conditions. The recovery kinetics of Runs 4, 13, 23 and 24 is presented in Figure 4-6b.

Commencing with low feed concentration range with respect to Run 11 and Run 2 (Figure 4-6a), a 21% and 27% recovery was recorded after 4 hrs for Runs 11 and 2, respectively. After 16 hrs, there was about 28% increase in recovery for Run 11 and 36% for Run 2. After 32 hrs of operation, increasing the feed flowrate increased the recovery to 84.40% in Run 2 from the 66.25% observed

in Run 11. While the change in recovery from 16 - 32 hrs was around 18.20% in Run 11, 22.6% change in recovery was observed in Run 2 for the same period. Also, in the same low feed concentration but a high sweep phase conditions , reducing the feed flowrate from a high 2.21 mL/ s in Run 8, to a low 0.65 mL/s in Run 17 reduced ion deposition on the active site of the membrane. As such, a 51% recovery from period 0- 8 hrs was reduced to about 27%. Using the 8 hrs recovery as a base point, the recoveries then increased between 32-36% at 24-hrs to have a greater than 85% Al-recovery in Run 11 and a less than 60% recovery in Run 2. After the DD run time, Al-recovery in Run 17 was 24.7% less than 93.65% in Run 8.

Considering Runs 23 and 24, the Al-transport was slow after 4 hrs for a high feed flowrate, than in Run 23's low feed flowrate. The recovery points in Run 23 showed that after a steady increase between 0-20 hrs, the transport tappers off to the end to have a recovery of about 60.54% after 32 hrs. On the contrary, a steady increase in transport kinetics was observed despite the slow kinetics in the first 4 hrs to have an over 75% recovery in Run 24.

Increasing the feed flowrate (low to high) in a high feed concentration, high sweep concentration and low sweep flowrate condition showed a similar trend. However, the high flowrate recovery in this condition was the lowest among the other conditions. A quick glance revealed a 73.45% recovery in Run 4 as compared to 81% in Run 24, 84.90% in Run 2 and 93.65% in Run 8 in an increasing order. Decreasing the flowrate from 2.21 mL/s to 0.65 mL/s resulted in a 67.33% Al-recovery after 32 hrs.

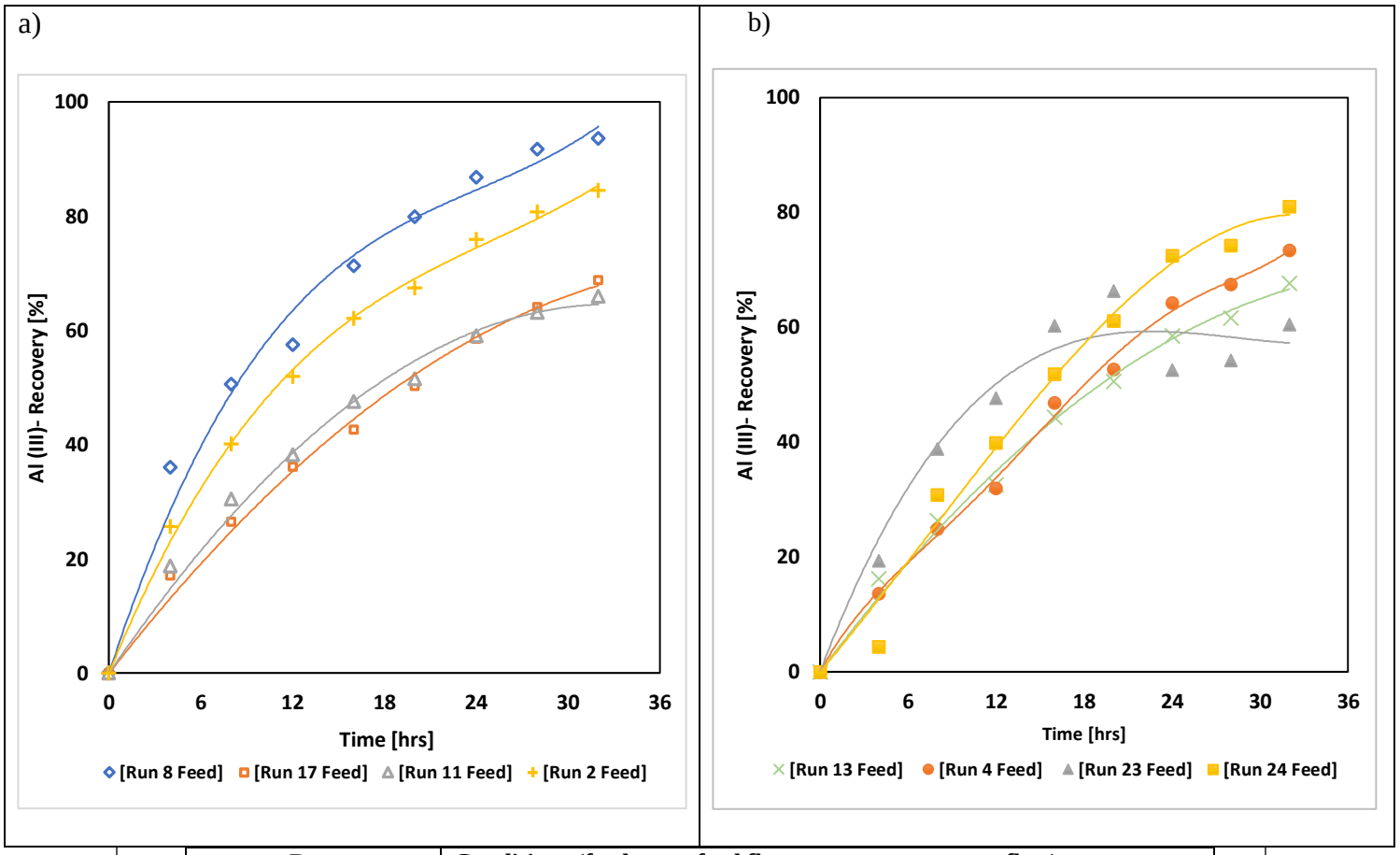

Run	Conditions (feed conc, feed flow, sweep conc, sweep flow)
13	2000 mg/L, 0.65 mL/s, 1 M, 0.65 mL/s
23	1050 mg/L, 0.65 mL/s, 0.625 M, 1.43 mL/s
4	2000 mg/L, 2.21 mL/s, 1 M, 0.65 mL/s
24	2000 mg/L, 2.21 mL/s, 0.625 M, 1.43 mL/s
8	100 mg/L, 2.21 mL/s, 1 M, 2.21 mL/s
11	100 mg/L, 0.65 mL/s, 0.25 M, 0.65 mL/s
17	100 mg/L, 0.65 mL/s, 1 M, 2.21 mL/s
2	100 mg/L, 2.21 mL/s, 0.25 M, 0.65 mL/s

Figure 4-6: Effect of feed flowrate at constant concentrations and sweep flowrate

4.3.3 Effects of Sweep Concentration

The principle of Donnan dialysis revolves on the concentration gradient between the feed phase and the sweep phase. By this, a higher acid concentration results in a higher gradient. This increases the kinetics and transport of aluminium across the Nafion 117 Membrane. However, having a sweep concentration ($\geq$ 1 M) leads to osmotic dehydration of membrane structure, reverse transport of ions, reduced Donnan exclusion and high water transport (Asante-Sackey et al., 2019; Davis, 2000). From the hydrodynamic transport, linear increasing order of water transport across the membrane with respect to high acid concentration dilutes the final concentration of target ion in the sweep phase.

Figure 4-7a shows the analysis of run pairing of 2 and 14 for a low feed concentration, high feed flowrate and low sweep flowrate condition. In the same figure, Run 5 and Run 17 compared the effect of sweep concentration at low feed phase settings and high sweep flowrate. Furthermore, Run 6 and Run 18 was chosen to demonstrate the sweep concentration effect at high feed phase conditions and sweep flowrate (Figure 4-7b). On the other hand, a medium acid concentration (0.625 M) and high acid concentration (1 M) was compared at a constant medium condition of 1050 mg/L feed concentration and 1.43 mL/s flowrates.

Considering Run 2 and Run 14, the difference in percentage recovery between period 0 - 4 hrs, was 1.38%. The effect after 4 hrs resulted in a recovery increase of between 1.08-1.20 times between 8-24 hrs. The final recovery of over 90% at 32 hrs in Run 14 was about 1.11 times that obtained in Run 2. On the contrary, increasing the sweep concentration reduced the kinetics of Al^{3+}-H^{+} counter transport between 1.09-1.47 times in Run 17 for period 4-20 hrs. Observing the sweep flowrate, more hydrogen present at the membrane-sweep solution interface induced any of the effects with regards to operating a membrane at 1 M or more. Due to Al sampling done at the

feed phase, the most possible reason would be reduced permeability. However, a gradual increase in recovery took place from 24 - 32 hrs to obtain a 59-69% recovery as compared to 59-62% (Run 5). By principle, the osmotic net force ensured rehydration of membrane gel structure in Run 17 which ensued the positive effect of increasing sweep concentration.

From the medium to high sweep concentration variation in Run 9 and Run 26, the recoveries differed by 0.43%, 0.05% and 0.24% for 4 hrs, 8 hrs and 12 hrs, respectively. The recovery continued to rise for the next 12 hrs to obtain an 84.95% recovery for Run 9 and 90.25% for Run 26.

Finally, the results displayed in Figure 4-7b for Run 6 and Run 18, indicated a 1.29 factor increase for the first 4 hrs. The highest factor increase of 1.98 was recorded on the 16 hr mark. This was due to a reduction in recovery in Run 6. At the end, 1 M increase resulted in a change in kinetics by a factor of 1.3-2.00.

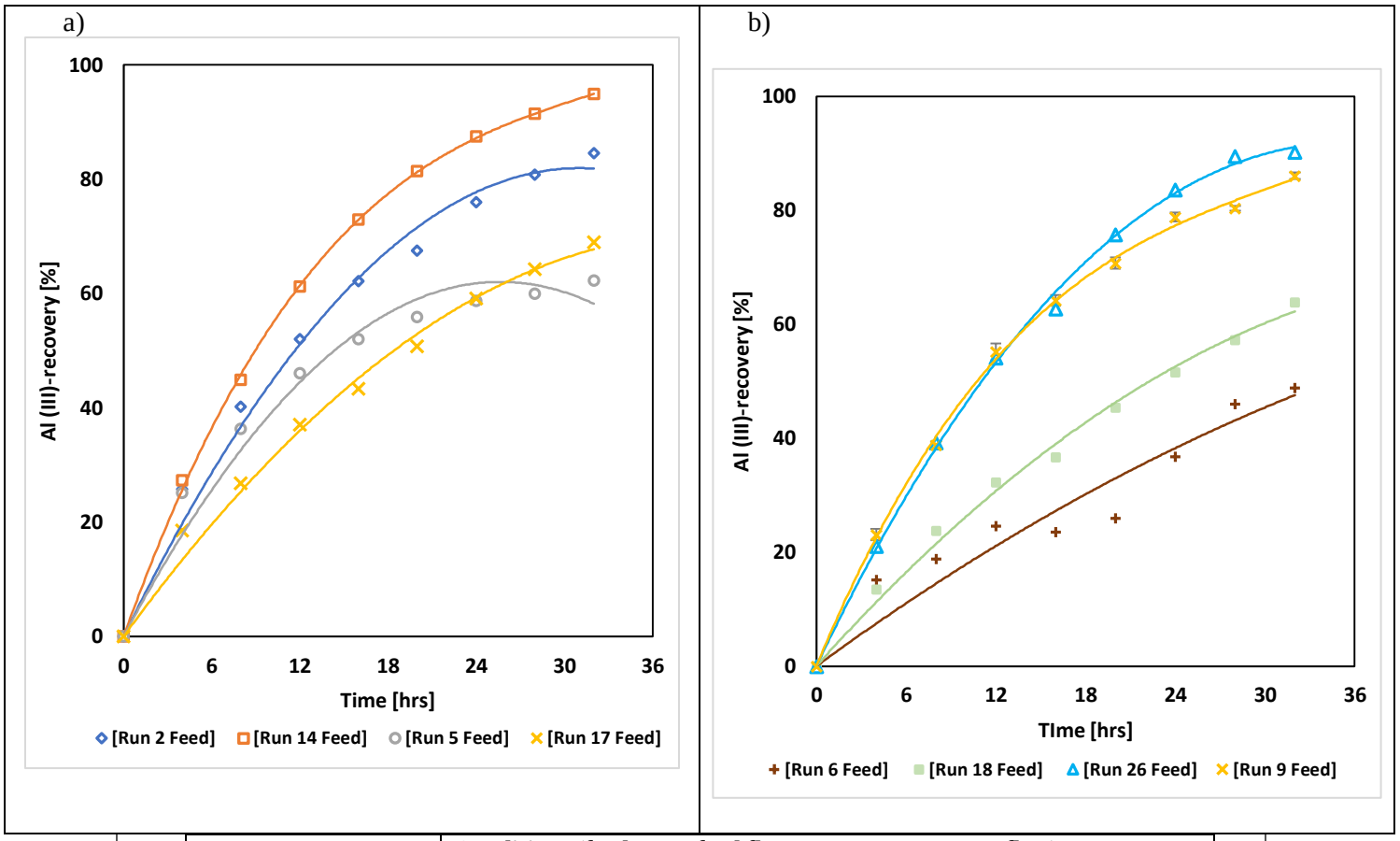

Run	Conditions (feed conc, feed flow, sweep conc, sweep flow)
2	100 mg/L, 2.21 mL/s, 0.25 M, 0.65 mL/s
14	100 mg/L, 2.21 mL/s, 1 M, 0.65 mL/s
5	100 mg/L, 0.65 mL/s, 0.25 M, 2.21 mL/s
17	100 mg/L, 0.65 mL/s, 1 M, 2.21 mL/s
6	2000 mg/L, 2.21 mL/s, 0.25 M, 2.21 mL/s
18	2000 mg/L, 2.21 mL/s,1 M, 2.21 mL/s
9	1050 mg/L, 1.43 mL/s, 0.625 M, 1.43 mL/s
26	1050 mg/L, 1.43 mL/s, 1 M, 1.43 mL/s

Figure 4-7: Effect of sweep concentration at constant flowrates and feed concentration

4.3.4 Effects of Sweep Flowrate

The sweeping ability from the deposition of H^+ on the membrane surface for Al^{3+} counter exchange is characterized by the sweep flowrate. More notably is the membrane-sweep solution and intramembrane behavior. The investigation was done using the run pairs of 27 and 28, 28 and 29, 13 and 7 as well as 12 and 6. Conditions for study are expounded below and results displayed in Figure 4-8:

1) Run 27 and Run 28: Varied from a low sweep flowrate to high sweep flowrate under medium feed phase conditions and medium sweep concentration.
2) Run 28 and Run 29: Varied from a low sweep flowrate to medium flowrate under medium feed phase conditions and medium sweep concentration.
3) Run 13 and Run 7: Varied from a low sweep flowrate to high sweep flowrate under high feed concentration, low feed flowrate and high sweep concentration.
4) Run 12 and Run 6: Varied from low sweep flowrate to high sweep flowrate under high feed phase conditions and low sweep concentration.

Commencing with Runs 27 and 28 in Figure 4.8a, the Al-recovery reduced with an increasing sweep flowrate for the entire period. While recovery at 4 hrs in Run 27 was about 21.24%, 19.25% was observed from Run 28. After 20 hrs of operation, 74% recovery was reached in Run 27 and 59% for Run 28. The investigation ended with an Al recovery of 77.40% for Run 28 which was 8.5% less than Run 27.

Looking at the same Figure 4.6a in sub section 4.3.2, an interchanging effect was observed in Runs 27 and 29. For period 0- 8 hrs, increasing the sweep flowrate implied a reduction in recovery. A similar occurrence was observed in period 24-28 hrs and vice versa for 12-16 hrs and 32 hrs. The same recovery, 73.57% was observed in both runs at 20 hrs. However, it is very evident that aside

period 4-8 hrs, with a difference in recovery between 2-3.2%, the difference was less than a percent. It would therefore not be misplaced to compare from a medium sweep flowrate (Run 29) to a high sweep flowrate (Run 28). After 32 hrs, Runs 29 and 28 differ by 8.59% while Runs 27 and 29 differ by 8.52 %. The difference of 0.04% suggests that the same impact occurs between Runs 27 and 29 as well as Runs 29 and 28.

The pair of Runs 13 and 7 was investigated at high feed concentration similar to Runs 12 and 6, however, these combinative runs showed different trends. In Figure 4-8b, increasing the sweep flowrate from 0.65 mL/s to 2.21 mL/s in their respective constant conditions indicated a resultant increase in recovery. The effect of the sweep flowrate in Runs 13 and 7 yielded a 2.8% and 4.9% difference in recovery in 4 hrs and 32 hrs, respectively. The order of increase took effect from 4 hrs, but in the same high feed concentration of 2000 mg/L, the recovery suggests that increasing the sweep flowrate decreased recovery from 0 to 20 hrs. The step up in recovery in Run 6 over Run 12 occurred from 24 hrs to 32 hrs to reach a final recovery of 45.65%. Clearly, recovery also reduced from 36.45% for 24 hrs to a final value of 36.20% for 32 hrs in Run 12. However, the dynamics of the effect of sweep flowrate in high feed concentration analysis would not be consistent with the order observed. Glancing back to compare Run 4 (Figure 4-6b) and Run 18 (Figure 4-7b), increasing the sweep flowrate from 0.65 mL/s to 2.21 mL/s in a high feed phase and high sweep concentration condition reduced the recovery. The final recovery after 32 hrs differed by 9.6%. The effect of the sweep flowrate in all conditions was highly dependent on the influence of the other three factors, namely, feed concentration, feed flowrate and sweep flowrate. The sweep flowrate effect was the least significant factor and sub section 4.4.1 would be used confirm this.

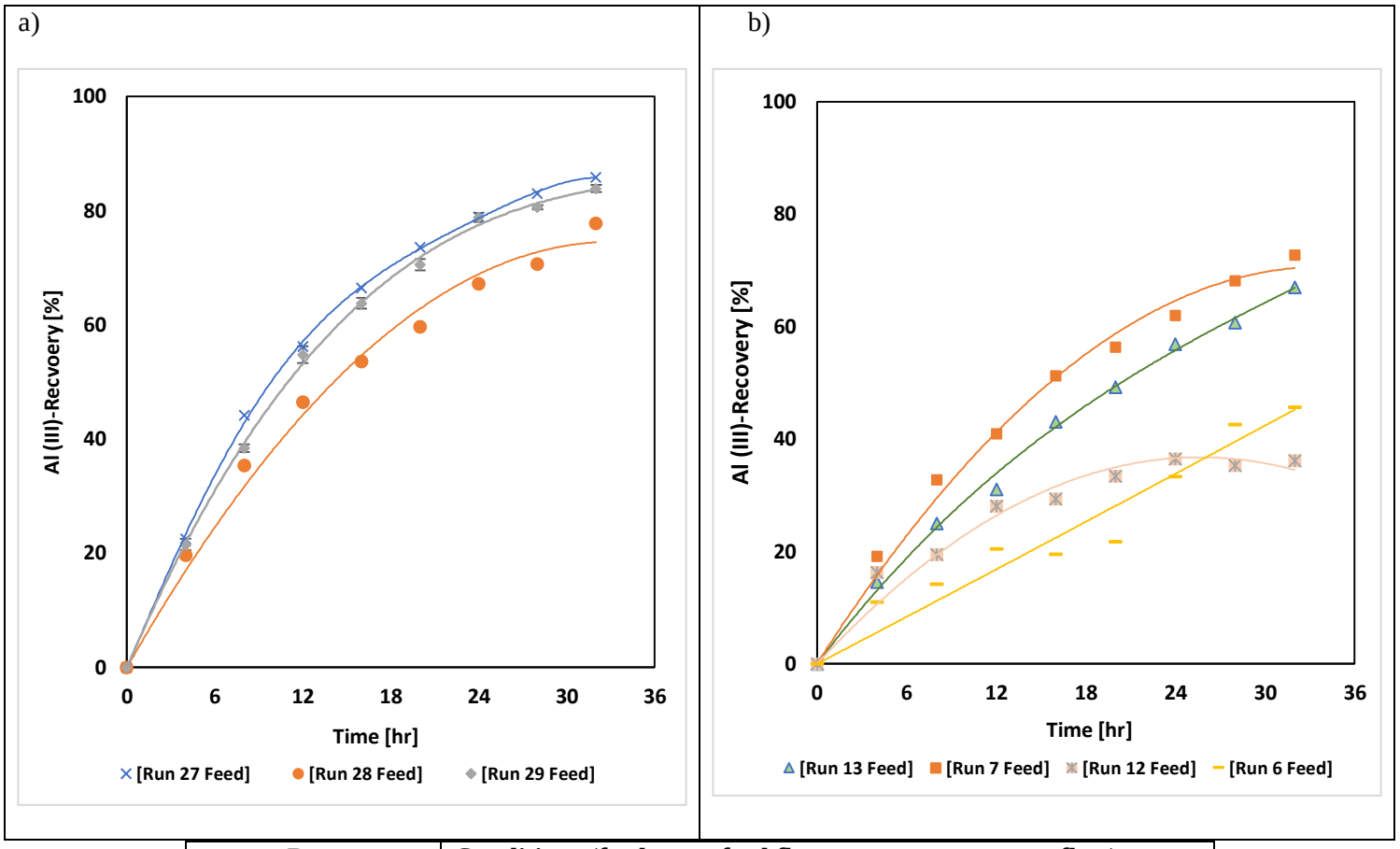

Run	Conditions (feed conc, feed flow, sweep conc, sweep flow)
27	1050 mg/L, 1.43 mL/s, 0.625 M, 0.65 mL/s
28	1050 mg/L, 1.43 mL/s, 0.625 M, 2.21 mL/s
29	1050 mg/L, 1.43 mL/s, 0.625 M, 1.43 mL/s
13	2000 mg/L, 0.65 mL/s, 1 M, 0.65 mL/s
7	2000 mg/L, 0.65 mL/s, 1 M, 2.21 mL/s
12	2000 mg/L, 2.21 mL/s, 0.25 M, 0.65 mL/s
6	2000 mg/L, 2.21 mL/s, 0.25 M, 2.21 mL/s

Figure 4-8: Effect of sweep concentration at constant flowrates and feed concentration

4.4 Models for Al-recovery

4.4.1 ANOVA Analysis

From the FC-CCD of experiments, the 24 hr zone was selected to conduct the analysis of variance (ANOVA). The second-order polynomial equation (2-15) was used to assess the impact of each factor on Al recovery. The Fisher test (F-test; F-value) and the probability value (*p*-value; $\alpha = 0.05$) was used to evaluate the degree of influence and significance of feed concentration, feed flowrate, sweep concentration and sweep flowrate. A statistically significant relationship between the response (Al-recovery) and the factors is denoted by *p*-value $\leq \alpha$. The total variability of the data is attributed to either specific causes in order to simulate the model. The data and ANOVA analysis is presented in Table 4-4.

Table 4-4: ANOVA for reduced quadratic model for four factor analysis

Source	Coefficient	Sum of Squares	Degree of Freedom	Mean of Square	F-value	P-value
Block	-	1.48	2	0.7395		
Model (Quadratic)		36.56	8	4.57	43.21	<0.001
X_1 Feed con.	-0.9181	15.17	1	15.17	143.48	<0.0001
X_2 Feed flow	0.3786	2.58	1	2.58	24.40	<0.0001
X_3 Sweep con	0.6746	8.19	1	8.19	77.45	<0.0001
X_4 Sweep flow	-0.0756	0.1030	1	0.1030	0.9737	0.3362 insignificant
$X_1 X_2$	-0.2930	1.37	1	1.37	12.99	0.0011
$X_1 X_3$	0.4143	2.75	1	2.75	25.97	<0.0001
X_1^2	-0.4590	1.10	1	1.10	10.41	0.0044

X_2^2	-0.5733	1.58	1	1.58	14.92	0.0010
Residuals	-	2.01	19	0.1058		
Pure Error	-	0.0002	3	0.0001		

Standard deviation = 0.3252; Mean: 7.96; CV% = 4.09; R^2 = 0.948; Adjusted R^2 = 0.926; Predicted R^2 = 0.882; Adeq precision = 20.790

The coefficient in terms of coded factors (-1, 0, +1) can be transformed into Equation 4-3 which predicts the Al-recovery using the matrix of the coded levels provided in Table 3-4. The highest negative impact from an independent term from Equation 4-3 was the feed concentration. As analyzed in sub section 4.3.1, increasing the feed concentration decreases the recovery. Also, the dynamics of the sweep flowrate is simplified from the single model to have the least independent negative impact on the recovery. However, due to the sweep flowrate serving as an integral run factor, it is kept in the model in Equation 4-3. Comparing the positive linear effects, sweep concentration impacted more than the feed flowrate.

$$Al - recovery\ (\%)_{24\ hrs} = (8.79 - 0.9181X_1 + 0.3786\,X_2 + 0.6746\,X_3 - 0.0756X_4 - 0.2930\,X_1X_2 + 0.4143\,X_1X_3 - 0.4590\,X_1^2 - 0.5753\,X_2^2 - 0.3546\,X_3^2)^2 \qquad 4\text{-}3$$

where X_1 is the feed concentration; X_2 is the feed flowrate; X_3 is the sweep concentration and X_4 is the sweep flowrate.

Furthermore, Equation 4-3 reveals that a positive effect exists with a feed concentration and sweep concentration interaction (X_1X_3). Asante-Sackey et al. (2019) also confirmed that a positive interactional effect also showed that the combinations of feed concentration-sweep concentration (X_1X_3) have a positive effect on the Al-recovery. The feed concentration-feed flowrate (X_1X_2) in

Equation 4-4 has an antagonistic effect on recovery due to their negative sign. Finally, three quadratic factors in descending negative influential order $X_2^2 > X_1^2 > X_3^2$ is shown in the coded equation.

The final reduced quadratic model generated by the Design Expert software is shown in Equation 4-4. The model predicts Al^{3+} recovery at 24 hrs using the actual values in their specific units. From the ANOVA analysis (Table 4-4), the linear sweep flowrate is insignificant ($p > 0.05$). The impact of the factors by the F-test shows that the feed concentration has the highest impact with an F-value of 143.48, followed by sweep concentration's 77.45 and feed flowrate's 24.40.

$$Al - recovery\,(\%)_{24\ hrs} = (4.67621 - 6.0 \times 10^{-5}X_1 + 9.3732 \times 10^{-2}X_2 + 3.72957X_3 - 1.0 \times 10^{-5}X_1X_2 + 1.163 \times 10^{-3}X_1X_3 - 5.08538E - 07\ X_1^2 - 6.39 \times 10^{-4}\ X_2^2 - 2.52141\ X_3^2) \qquad 4\text{-}4$$

The accuracy of prediction of the model is indicated by the coefficient of determination (R^2). The difference between the actual R^2 (0.948) and the predicted R^2 (0.882), the adjusted R^2 (0.926) and the predicted R^2 are in reasonable agreement as the differences are less than 0.2. The inclusion of the insignificant sweep flowrate does not affect the difference. Furthermore, the intensity of background interference on the desired signal from the model is shown by the adeq precision value (> 4). From the ANOVA analysis, the adeq precision of 20.790 is greater than 4 hence more desired signals. Finally, the model is reproducible since the coefficient of variation CV = 4.09 is less than 10%.

4.4.2 Interactional Effect

Evaluation of the correlative impact of significant interacting factors on the response is illustrated in three dimensional (3D) plots of the regression model in Figure 4-9 and Figure 4-10. The significant combinations were feed concentration and feed flowrate; sweep concentration and feed

concentration. From Figure 4-9a, increasing the feed concentration and increasing the feed flow increases the recovery process. However, this is to a degree on the feed concentration axis. Operating in a feed concentration region of 100-900 mg/L and feed flowrate between 45-85% would achieve a 77-90% recovery. Reducing the feed concentration from 2000 mg/L to 1100 mg/L under a 25-60% feed flowrate would yield a 47-70% Al-recovery after 24 hours of operation. Similarly, operating in the same feed region of 1100 mg/L to 2000 mg/L but under a feed flowrate of 50% to 85%, an aluminium recovery of 77-50% is reported. From the 3D and contour plots in Figure 4-9, the best interaction for a > 70% Al-recovery would be a feed flowrate between 44-74% and an increasing feed concentration at maximum of 1380 mg/L.

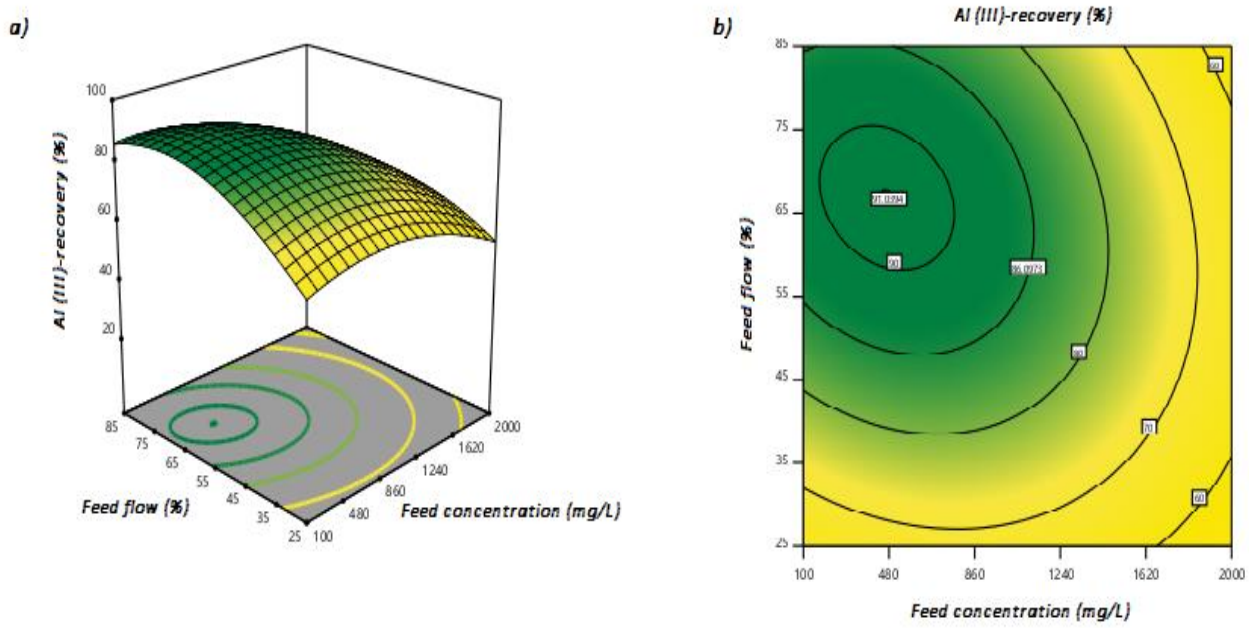

Figure 4-9: Effect of feed flow and feed concentration on Al-recovery; a) 3D plot b) contour plot

The interaction of sweep concentration and feed concentration (Figure 4-10) looked at how increasing potential difference affects Al-recovery in increasing Al-presence on the feed solution-membrane interface. Obtaining a > 55 % recovery would be possible in a decreasing feed concentration of 1200 mg/L to 100 mg/L and an increasing sweep concentration from 0.25 M to 0.7 M. In the same feed concentration region, increasing the sweep concentration from 0.5 M to 1 M would result in a 70% to 86% recovery. With a sweep concentration of 0.45-0.85 M, a 50-79% recovery is achieved under a feed concentration of 1200 mg/L to maximum. In order to avoid the effect of high sweep concentration on membrane performance, water transport and accompanying cost of chemical usage, the best settings to achieve high recoveries should be between 0.6–0.8 M.

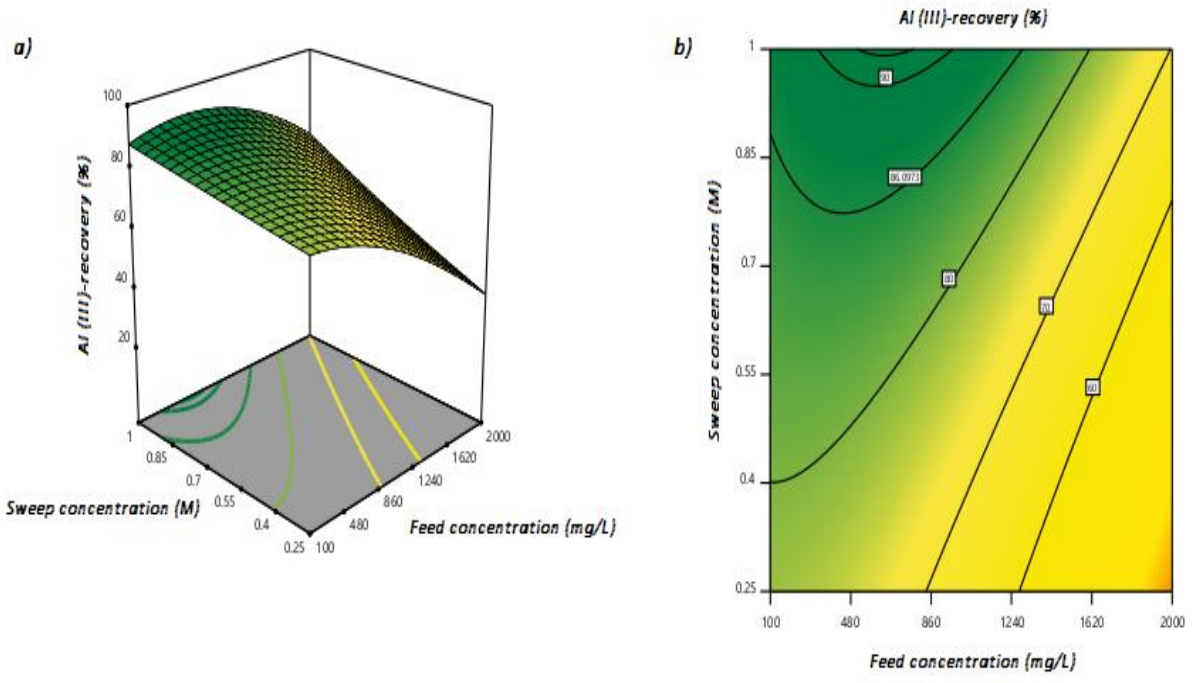

Figure 4-10: Effect of sweep concentration and feed concentration on Al-recovery; a) 3D plot b) contour plot

4.4.3 Optimization

The Design Expert software uses the numerical and graphical optimization to identify the desired settings to maximize and minimize output. Other three inherent optimization goals are, within range, target and none. A desirability (d_i) value is assigned to the settings whose response meets the optimization target (Mohapatra et al., 2019). The highest desirability of 100% is often required. Table 4-5 presents a list of the first six solutions by the predicted model for the target goal of 70% and the statistical software recommended the first solution as optimized conditions.

The first recommendation enables the usage of low sweep concentration to achieve an industrially feasible process and reduces the water transport from the feed phase to the sweep phase. Furthermore, since high energy consumption affects the recovery cost, minimum phase flowrates are required, most especially, for an insignificant sweep flowrate. The highest feed concentration at 1540.70 mg/L can be considered as the highest feed concentration to operate with. This, therefore, takes into account feed variations that comes from the water treatment residue. Using specific settings for any feed concentration less than 1540.70 mg/L could achieve recovery of ≥70% as it can be analyzed from the 3D and contour plots in the previous section and as shown by Asante-Sackey et al. (2019). Figure 4-11 shows the number of experiments conducted at a three day interval to validate the optimum conditions predicted by the model. Results from the conformational experiments using the selected conditions were in agreement with the predicted results with a 1.23% variation.

Table 4-5: Optimized solution results for Al-recovery

Number	Feed concentration (mg/L)	Feed flowrate (%)	Sweep concentration (M)	Sweep flowrate (%)	Al-recovery (%)	Desirability (%)
1	1540.70	63.5	0.695	47.60	70	100
2	1265.73	66.67	0.560	59.12	70	100
3	562.84	49.86	0.388	42.74	70	100
4	941.61	58.18	0.319	50.19	70	100
5	1395.91	74.35	0.687	44.06	70	100
6	159.377	40.76	0.215	26.31	70	100

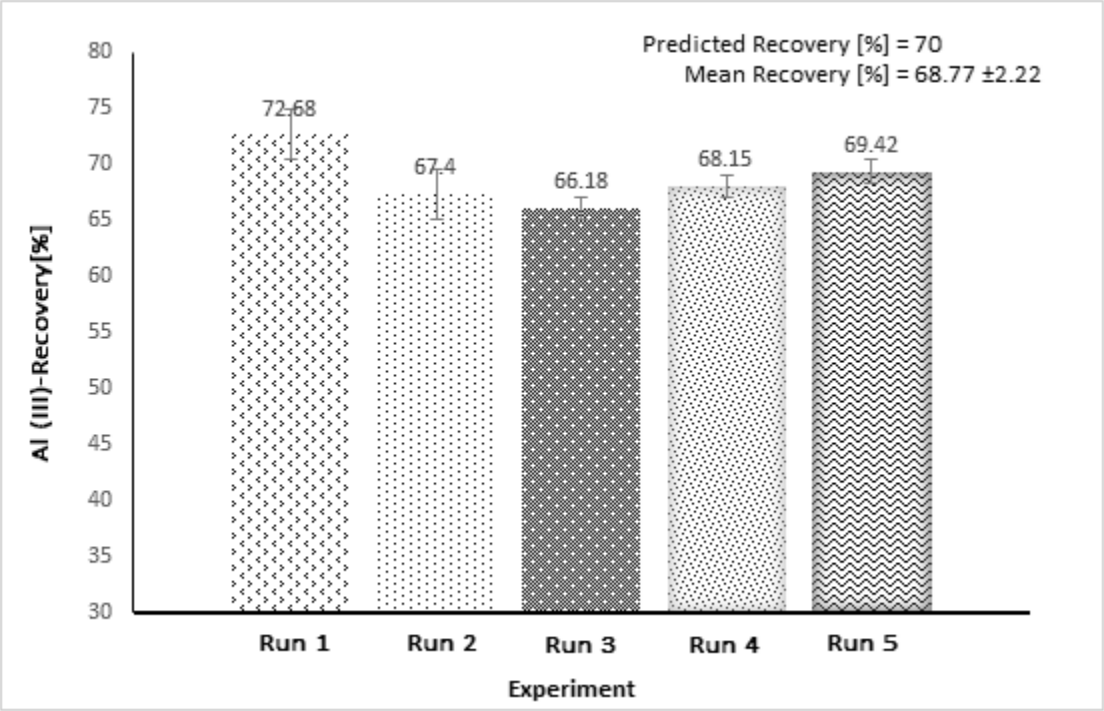

Figure 4-11: Validation Runs for Predicted recovery

4.4.4 Summary of impact of phase variables

Investigation on the kinetics of aluminium through Nafion 117 using Donnan dialysis was performed to determine the effects of feed concentration, feed flowrate, sweep concentration and sweep flowrate. From the face centered central composite design experimental runs and analysis, the feed concentration, sweep concentration and feed flowrate in descending order were the most significant process variables. Although the sweep flowrate is an insignificant factor with p-value greater than 0.05, due to the configuration of the DD system, it was included to a final model to predict aluminium recovery at 24 hrs. Statistical results of high adequacy ratio (20.79), actual R^2 (0.948), adjusted R^2 (0.926) and predicted R^2 (0.882) values showed that the experimental data was well fitted on the model. As such the model can route through the design space.

The significant interactions were the feed flowrate-feed concentration and sweep concentration-feed concentration. In the feed flowrate-feed concentration combination, increasing the feed flowrate increases the recovery while increasing the concentration increases the recovery up to a medium concentration and then a decline is observed. This effect is intertwined with the sweep concentration. Increasing the sweep concentration increases the recovery. Although high feed concentration results in reduced recovery, increasing the sweep concentration at high feed concentration also increases the recovery. Recovery is high for a low to medium feed concentration.

The optimum conditions to achieve a 70% recovery was found to be 1540 mg/L for the feed concentration, 63.5% for feed flowrate, 0.7 M for sweep concentration and 47.60% for sweep flowrate and this was obtained at a desirability of 100%. The conformational runs showed that a 69% recovery can be obtained using optimum settings assigned by the statistical tool.

4.5 Acidification Transport

Prior to DD for the recovery of aluminium is an acid digestion or alkaline treatment of PWTR. Acid digestion, reported in concentration or pH is widely used in primary Al recovery due to high solubilization of $Al(H_2O)_3(OH)_3$. With a focus on acid pH, different Al concentrations can be recovered from PWTR sourced from different locations at the same optimum pH. The same can be said for recovery of similar Al concentrations for equal quantity of PWTR recovered at a different optimum acid pH. For this purpose, the effect of feed concentration, feed pH, and feed flowrate at a fixed sweep flowrate and sweep concentration is studied. The sweep concentration (0.75 M) and sweep flowrate (55%) were kept at a constant to study how feed phase conditions can influence recovery. Selection of conditions for the sweep concentration and sweep flowrate was based on findings in the previous section.

The actual conditions set for the FC-CCD approach in this study may be seen in Table 4-6. The high and low points of feed concentration was maintained at 100 mg/L and 2000 mg/L, respectively while maintaining the high and low feed flowrate at 25% and 85%, respectively. Also, the initial pH range (1.3 – 3.7) for the feed solution was adjusted by adding dropwise, 1 M H_2SO_4 and 3 M $NaHCO_3$. Aside the choice of pH range being supported by Ahmad et al. (2016b), possible precipitation of aluminium hydroxide which occurs during the reaction of biocarbonate and aluminium sulphate would not occur within that range.

4.5.1 Modelling

In this section, the RSM was used to investigate the independent and interactional relationship that exists between the input factors and the Al-recovery. The experimental data from the FC-CCD matrix was inputted and simulated. Table 4-6 contains the actual and predicted results for the range of input variables at different levels of each run. The actual response was fitted on a second order

polynomial equation. The quadratic model was suggested by the Design Expert software and expressed as a function of the feed concentration (X_1), feed flowrate (X_2) and pH (X_3), together with their quadratic effects (X_1^2, X_2^2, X_3^2) and three interaction effects (X_1X_2, X_1X_3, X_2X_3).

Table 4-6: Design matrix in actual conditions with respective response for FC-CCD approach

Run	Feed conc. (X_1; mg/L)	Feed flow (X_2; %)	pH (X_3)	Al-recovery (%)- 28hrs	
				Actual	Predicted
1	2000	85	3.7	69.84	69.86
2	2000	25	1.3	32.4	31.60
3	1050	25	2.5	72.79	77.22
4	2000	25	3.7	75.9	74.25
5	2000	85	1.3	30.72	30.73
6	100	85	1.3	69.50	68.85
7	1050	85	2.5	79.49	80.06
8	1050	55	2.5	84.10	81.39
9	100	25	1.3	60	58.74
10	1050	55	1.3	52.74	53.70
11	1050	55	2.5	83.77	81.39
12	1050	55	2.5	80.60	81.39
13	1050	55	3.7	88.2	92.42
14	1050	55	2.5	79.30	81.39
15	1050	55	2.5	81.24	81.39
16	100	55	2.5	87.20	90.86
17	100	85	3.7	98.72	97.46
18	100	25	3.7	92.35	89.76
19	2000	55	2.5	58.25	59.69
20	1050	55	2.5	80.32	81.39

As shown in the coded Equation 4-5, the coefficient of first order terms indicates the impact of the single terms $X_2 < X_1 < X_3$. Furthermore, the interactive terms affects the Al-recovery in a decreasing order of $X_2X_3 > X_1X_3 > X_1X_2$. The model with respect to actual values is presented below as Equation 4-6.

Coded:

$$Al\ (III)_{\ 28hrs}(\%) = (9.02 - 0.9030X_1 + 0.0796X_2 + 1.14X_3 - 0.1776X_1X_2 + 0.2964X_1X_3 - 0.0588X_2X_3 - 0.3926X_1^2 - 0.1540X_2^2 - 0.5509X_3^2)^2 \qquad 4\text{-}5$$

Actual:

$$Al\ (III)_{28hrs}(\%) = (4.20225 - 0.00034X_1 + 0.032107X_2 + 2.68182X_3 - 6.23319 \times 10^{-6}X_1X_2 + 0.000260X_1X_3 - 0.001633X_2X_3 - 4.3502810^{-7}X_1^2 - 0.000171X_2^2 - 0.382560X_3^2)^2 \quad \textit{4-6}$$

4.5.2 ANOVA Analysis and Diagnostic Plots

The ANOVA analysis to evaluate the response model is presented in Table 4-7. The analysis shows the inclusion and elimination of conditions for the model in order to help heighten the relationship between the single, interactional and quadratic terms on the response. The model was found with a 95% confidence level and a degree of freedom of 9. The sum of squares value of 0.3332, F-test of 259.46, P-value of <0.0001 and an adequate precision of 53.1391 which is greater than 4 were all found to be in the limits used to accept a model as significant. Relative to pure error, a 1.21 F-value for the lack of fit (LOF) indicates that the LOF is not significant. However, the LOF's p-value of 0.04657 implies that the insignificant terms are included in the model due to pure noise. The interactional feed flow-pH is partially significant with a P-value greater than 0.1. Nonetheless, the term does not make the model insignificant and also it was kept to satisfy the parent term.

Table 4-7: ANOVA for reduced quadratic model for three factor analysis

Source	Sum of Squares	Degree of freedom	Mean Square	F-value	P-value	Decision
Block	0.3332	2	0.1666			
Model	25.83	9	2.87	259.46	< 0.0001	Significant
X_1-Feed conc.	8.15	1	8.15	737.22	< 0.0001	
X_2- Feed flow	0.0634	1	0.0634	5.73	0.0436	
X_3- pH	13.06	1	13.06	1180.37	< 0.0001	
$X_1 X_2$	0.2525	1	0.2525	22.83	0.0014	
$X_1 X_3$	0.7029	1	0.7029	63.55	< 0.0001	
$X_2 X_3$	0.0276	1	0.026	2.50	0.1526	Insignificant
X_1^2	0.4138	1	0.4138	37.40	0.0003	
X_2^2	0.0637	1	0.0637	5.76	0.0432	
X_3^2	0.8146	1	0.8146	73.64	< 0.0001	
Residual	0.0885	0.0885	0.0111			
Lack of Fit	0.0592	0.0592	0.0118	1.21	0.4657	Insignificant
Pure Error	0.0293	3	0.0098			
Cor Total	26.25	19				
Standard deviation = 0.1052; Mean = 8.46; CV = 1.24; Adeq Precision = 53.1391						

The overall performance was interrogated based on the actual R^2, adjusted R^2 and predicted R^2 provided in Figure 4-12a. The actual R^2, which is 0.0034 less than 1 established how well the experimental data correlated and fitted the model. Validation of the significance of the model was further looked into with the difference between the adjusted R^2 and predicted R^2. Since the difference was greater than 0.2, the model is significant. Furthermore, the less than 0.2 difference between the actual R^2 and predicted showed how closed the experimental and predicted data points are to the diagonal line. The reliability, reproducibility, precision and repeatability of the model is shown with the 1.24% CV that is less than 10%. In addition, the normal probability plot in Figure 4-12b showed a normal distribution as maximum plots did not egress from the straight line. The

linearity of the plots support the condition of a normal distribution of the error term (Babu et al., 2019). Lastly, Figure 4-12c indicated that the non-linearity trend of the data points with random scattering around the regression line at 0.00. In the presence of no time-related-error at the background, the negative residual implies over prediction, an under prediction for a positive residual and data plots close to the regression line for the exactness of prediction (Asante-Sackey et al., 2020). In all, there were no outliers as responses were within the ± 4.59464.

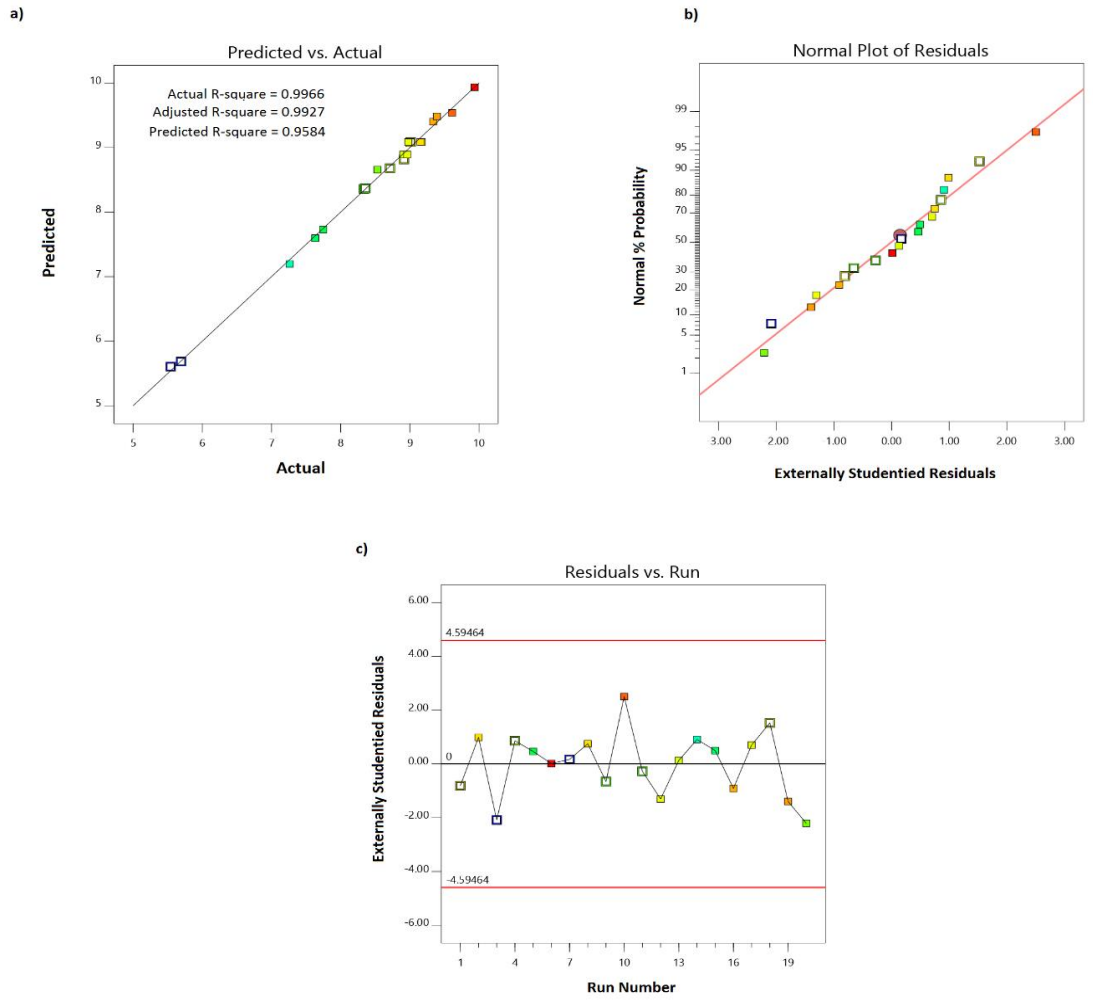

Figure 4-12: a) Predicted vs Actual plot for Equation 4-5; b) Normal probability plot; c) Residual vs run plot

4.5.3 Interactional Effect

The combinative impact of interacting single factors on the response can be well demonstrated using 3D-plots. Figure 4-13 and Figure 4-14 shows the terms of an interacting feed concentration and feed flowrate; feed concentration and pH. The effect of feed flowrate and pH was not illustrated in terms of insignificance as shown in the Table 4-7 on the ANOVA analysis. Increasing the feed concentration (Figure 4-13) increased the bulk distribution over the membrane surface. This inturn increased the concentration polarization effect. Hence, it reduced the selectivity and ion transport across the membrane (Luis, 2018).

The Feed concentration-feed flowrate interaction showed a high recovery of 80% to a greater than 90% when the feed flowrate is increased for a feed concentration range $100 \leq X_1 \leq 1140$ mg/L at 28 hrs. However, the increasing selectivity due to increasing flowrate at low to medium feed concentration declines after 1240 mg/L in Figure 4-13a. An estimated Al recovery within 55-70% would be achieved for a feed concentration greater than 1600 mg/L with a linearly increased flowrate.

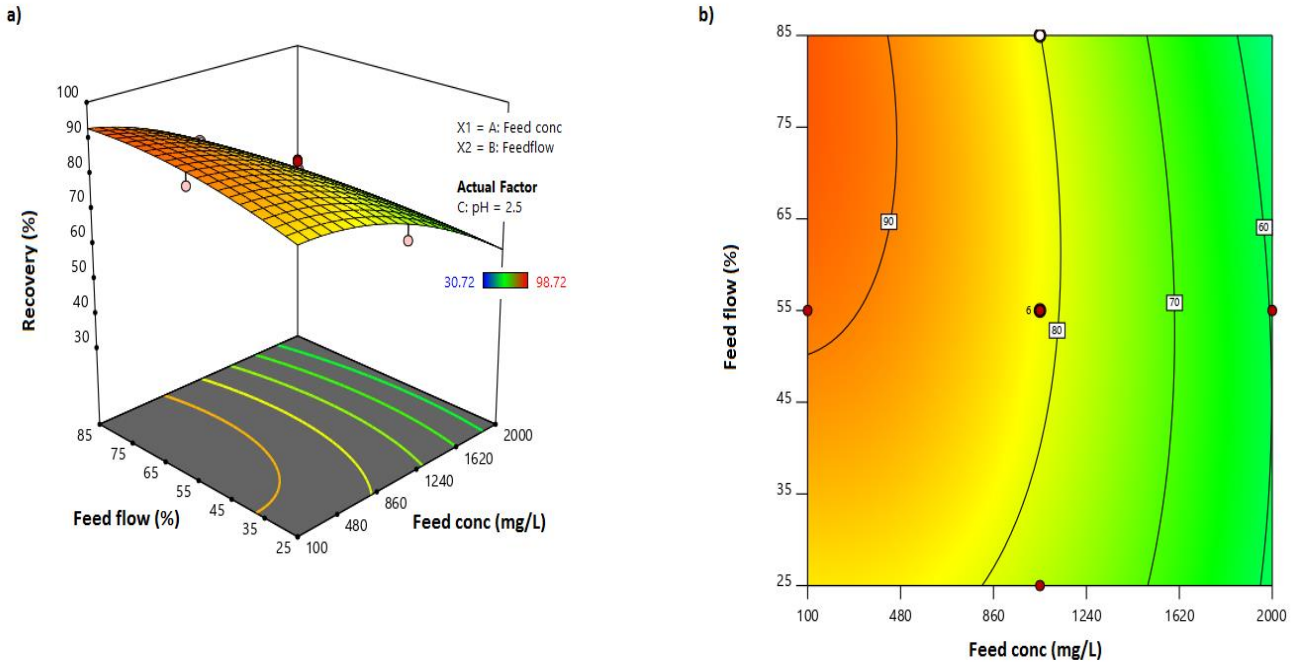

Figure 4-13: Effect of feed concentration and feed flowrate on Al-recovery; a) 3D plot, b) contour plot

Figure 4-14 represents the Al-recovery profile at constant feed flowrate of 55% with varied pH and feed concentration. The upward curvature on the pH axis reveals the extent of impact of an increasing pH against the decreasing nature of feed concentration on recovery. Changing pH affects the hydrolysis product formed and this might have an effect on the Al species which consists of aqua ligands and sulfate terminal ligands (Sarpola et al., 2007). As such, these species would have an effect on the type of Al transport detected as Al^{3+} by the MP-AES. Admitting to not focusing on the complexes, the highest recovery was found to be 96%. Operating with a pH range of 2.5-3.7 would result in a greater than 80% recovery for a feed concentration range of 100-1100 mg/L. The recovery decreases from 80% to 60% when the pH decreased from 2.5 to 1.3 for the same feed range and reduced by 20-25% for a feed concentration of 1270- 2000 mg/L. Therefore, to increase recovery at high feed concentration (> 1200 mg/L), the pH has to be

increased at a reduced feed flowrate due to the linear impact of the feed flowrate. The effect of the pH explains the 70% Al-recovery observed by Prakash and SenGupta (2003) with a starting feed concentration of 2400 mg/L at 3-3.5 pH.

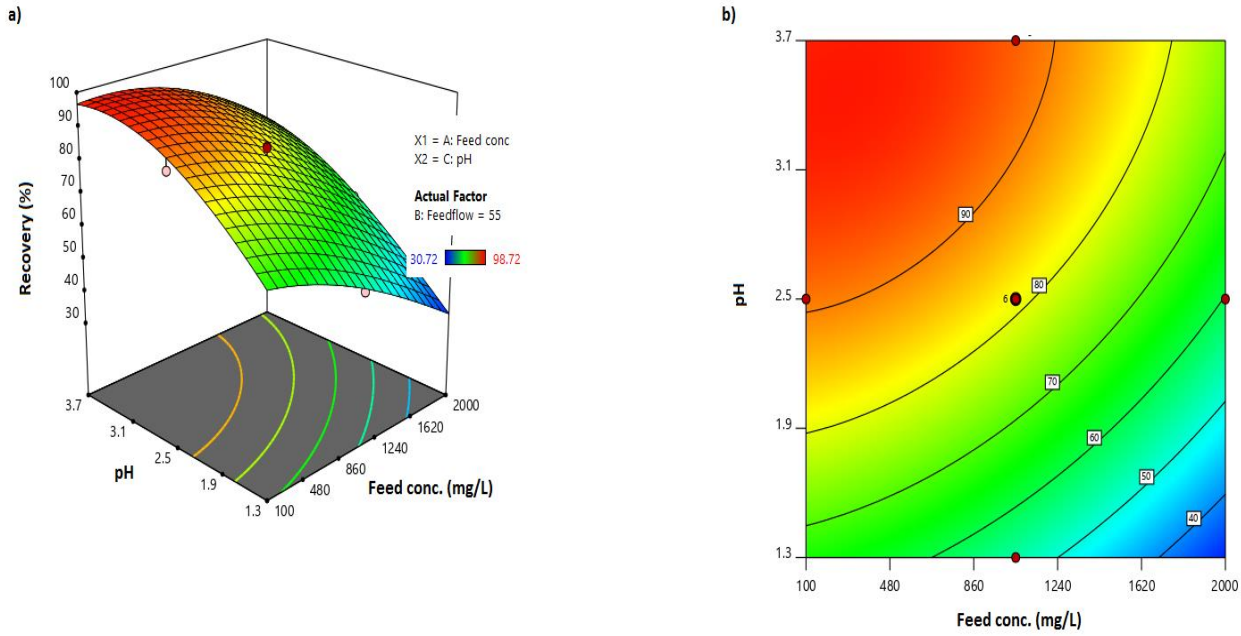

Figure 4-14: Effect of feed concentration and pH on Al recovery; a) 3D plot b) contour plot

4.5.4 Optimization of acidification transport

The widely used desirability method, a non-linear programming technique, was applied due to its simplicity and flexibility in realizing a multi-objective optimization for responses. The Al-recovery is subjected to desirability transmutation with a range of $0 \leq d_i \leq 100$. Using the Design Expert software, a three star importance was assigned by the software to the various terms. Out of 95 solutions produced by the software, the first five solutions are presented in Table 4-8 for a 70%

recovery target. The selected recommendation by the software with a desirability of 100% achieves the 70% target with a high feed concentration at a pH of 2.52. In terms of energy, bulk distribution of Al-ions on membrane surface, selectivity and transmembrane transport, 1.56 mLs^{-1} representing 59.84% is the best. Although increasing the pH would allure to chemical cost, this would pay off in obtaining a high recovery. From this, any feed concentration with respect to PWTR that does not exceed 1610 mg/L for this set up would achieve 70% and more recovery within the feed flowrate limits at a pH range of 2.5-3.7.

The experimental results for three runs conducted at two days intervals is presented in Figure 4-15. Using the optimum condition settings, it was observed that, the recovery was 6.15% less than the predicted value. The recovery mean of 63.85% was in agreement with the predicted recovery by the model. The difference between both values can be considered as an error and it is less than 7.0%

Table 4-8: Al-recovery optimization solution

Number	Feed concentration (mg/L)	Feed flowrate (%)	pH	Al-Recovery (%)	Desirability (%)
1	1606.55	59.84	2.52	70	100
2	1672.50	58.85	2.61	70	100
3	1576.96	28.23	2.57	70	100
4	1525.77	25.44	2.53	70	100
5	1940.08	73.61	3.25	70	100

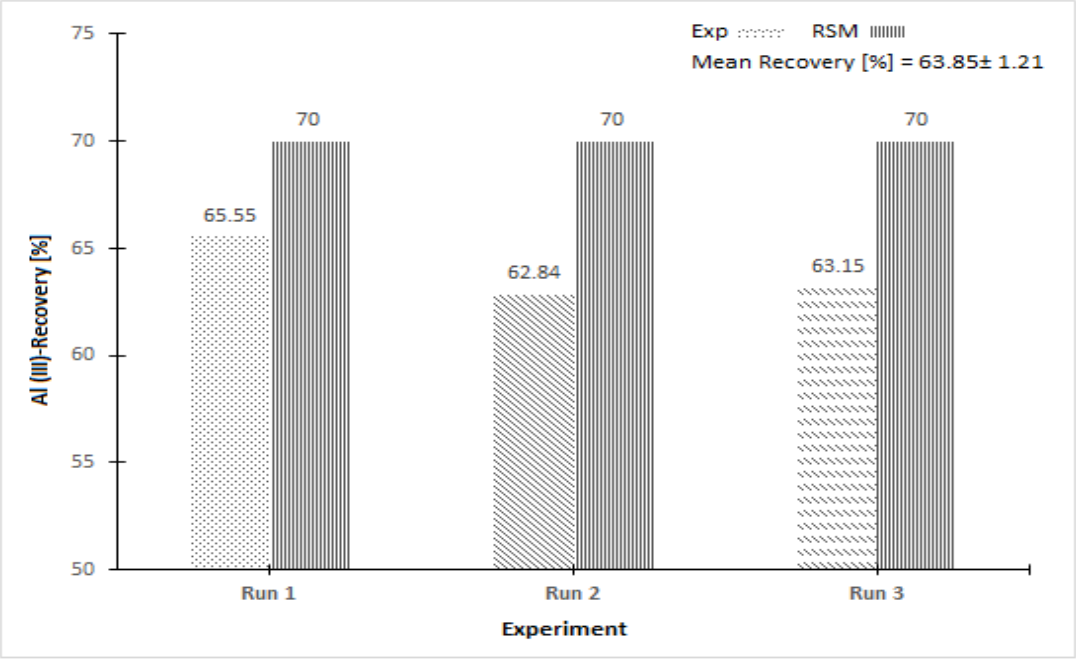

Figure 4-15: Acidification route validation Runs for Predicted recovery

4.5.5 Summary of acidification transport

Acid digestion of PWTR before Donnan dialysis is the surest path to achieve high recovery due to high solubilization of Al. This study focused on the three factors, feed concentration (100-2000 mg/L), feed flowrate (25-85%), pH (1.3-3.7), sweep flowrate (55%) and sweep concentration (0.75 N). A statistical model that can be seen below was generated to predict Al-recovery using the actual values:

$$Al\ (III)_{\ 28hrs}(\%) = (4.20225 - 0.00034X_1 + 0.032107X_2 + 2.68182X_3 - 6.23319 \times 10^{-6}06X_1X_2 + 0.000260X_1X_3 - 0.001633X_2X_3\ - 4.3502810^{-7}X_1^2\ -\ 0.000171X_2^2 - 0.382560X_3^2)^2 \qquad 4.6$$

The model was tested for its significance and accuracy by plotting a predicted Al-recovery against the experimental data. After the fitting of a straight line, an actual R^2 value of 0.9966 was found, which showed that the experimental data fitted well to the model. The model was significant with a P-value less than 0.05 as well as independent factors also being significant. The P-values were <0.0001, 0.0436 and <0.0001 for feed concentration, feed flowrate and pH, respectively. Subsequently, a response surface plot navigating through the significant interactions of feed concentration and feed flowrate; feed concentration and pH was drawn. In general, increasing feed concentration decreases recovery on the back of an almost insignificant effect from the feed flowrate. The pH improves recovery even at high feed concentration and most suitably operating from a pH range of 2.5-3.7 for a low to medium feed concentration.

The optimum conditions to achieve a 70% recovery at a 100% a desirability was found to be 1606.55 mg/L for the feed concentration, 59.84% feed flowrate and a pH value of 2.52. The confirmational runs showed that a 63.85% Al can be recovered using optimum settings assigned by the statistical tool.

4.6 Metal Permeation

The composition of metals in a PWTR varies if and how they inhibit the recovery of aluminium is crucial. The selectivity of the DD and Nafion 117 towards metal impurities was tested in a 1:1 head to head transport with aluminium. Results from the previous section guided in selecting a range for this study by using a random selection for the starting concentration in the feed phase from a low to medium range. The feed and sweep phase flowrates were kept at 50% with the sweep phase acid concentration at 0.75 N. This section looks at the inhibition of 6 metals at a starting

concentration of 400 mg/L. The choice of the divalent metals was based on the physicochemical composition of PWTR reviewed by Ahmad et al. (2016a). Furthermore the choice of 400 mg/L was handpicked from a selectivity balloting process for the concentration between the low and medium range (100–1000 mg/L).

Different factors control the transport of ions in solution. The membrane's selectivity and transport of ions is reflected by the inherent differences in velocity of diffusion for charged species undergoing electrostatic interaction and binding strength of the ions in exchange. Essentially, for an equimolar condition, diffusion of ions across the membrane will depend on the charge and ionic size in solution. Under these premises, the kinetics of a multi-cationic solution is analyzed for 20 hrs at the feed phase.

4.6.1 Group Two elements

Magnesium from magnesium sulphate heptahydrate and calcium from calcium sulphate dehydrate was studied individually with aluminium in a solution. Figure 4-16 shows that transport of aluminium against Mg and Ca. Comparing the aluminium recovery in the Al-Ca transport line to the Al-only, the inhibition is clear with a reduction in transport by the introduction of Ca. In the period 0-8 hrs, the recovery reduced by 6.40% to about 17.10% from an actual recovery of 29.40% at 4 hrs and 44.70% at 8 hrs, respectively for Al-only. The highest reduction occurred at 16 hrs where the difference in Al-only and Al-Ca was 23%. Without Ca, the inhibition would increase by 17.50% from 54.78% in an Al-Ca to obtain the recovery in Al-only at 20 hrs. Similarly, the presence of Mg inhibits Al-recovery as displayed in Figure 4-16. As a cation in solution, Mg will equally exchange with hydrogen by the electrochemical potential difference. Comparing the Al transport in the presence of Mg in Al-Mg to Al transport in Al-only, the reduction by Mg is between 10% to 17.40%, with the highest occurring at 16 hrs. The gradual increases in reduction

tappers off after 20 hrs to obtain a recovery of 59.50% in Al recovery in Al-Mg transport which represents a 12.80% reduction from the Al-only kinetics at the same period.

However, monitoring the effect of Ca and Mg on Al transport, the ionic transport of Ca is higher than Mg in their respective Al mix. The Ca recovery was 27.6% and 52.20% at 4 hrs and 12 hrs, respectively. These recoveries were 2.1 and 3.1% higher than Mg recovered. However, the transport of Mg increases to obtain a final recovery of 69.60% recovery as compared to 63.10%. This phenomenon is similar to Mg and Ca studies by Wiśniewski and Rózańska (2007) accounted that the initial phase flux of Ca was higher than Mg. The hydration radius, 0.41 nm for Ca^{2+} and 0.43 nm for Mg^{2+} explains the faster diffusion of Ca^{2+} over Mg^{2+} despite having the same ionic charge (Wang et al., 2010).

However, the increase in Mg ions over Ca ions after 16 hrs could be attributed to the higher hydration energy and higher ionic charge densities. The ionic radius of Mg^{2+} of 0.070 nm gives it a higher ionic charge density over Ca^{2+} with 0.100 nm ionic radius. Essentially, a higher ionic charge density results in higher electrostatic repulsion with positively charged ion-exchange groups (Cheng et al., 2018). Alternatively, a higher ionic charge would result in a stronger binding of the ion of concern with the negative sulfonic groups of the Nafion 117. As such, despite lower velocity of diffusion of Mg^{2+}, the Mg ion binds stronger hence the lower recovery difference compared to the Ca ion. Additionally, Mg^{2+} holds adjoining water molecules stronger than Ca^{2+} due to the hydration energy of -1830 kJ mol^{-1} and -1505 kJ mol^{-1}, respectively. As water transport is inevitable in a DD system and hydration of membrane structure increases permeation, within the zone of an osmotically driven mechanism, it would be expected to have Mg^{2+} increase in transport with these attributes. For this and other solubility conditions, the recovery of Mg^{2+} was higher than Ca^{2+} (Wang et al., 2010).

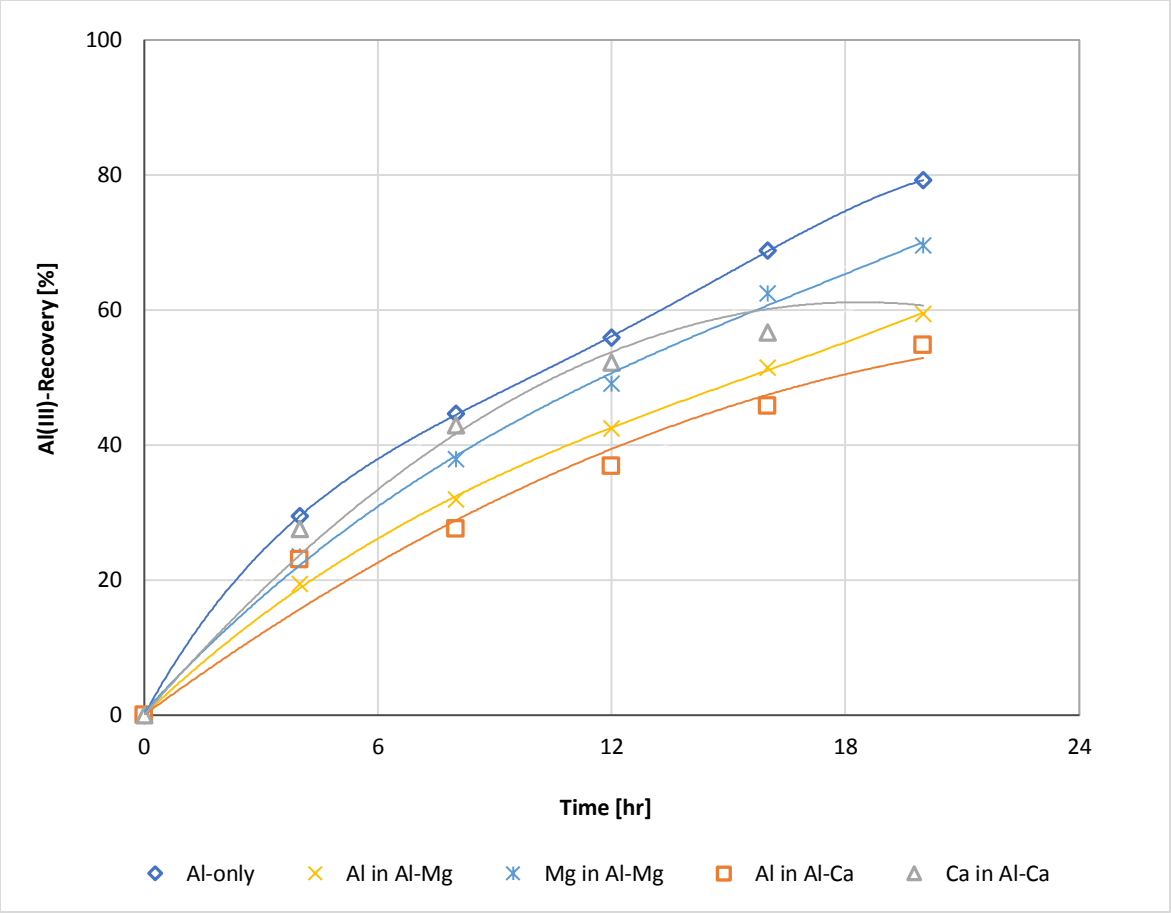

Figure 4-16: Ca and Mg inhibition to Al for 20 hrs

4.6.2 Multi group element

The specific binary transport of aluminium and other group elements, mainly Cu (II) of group 11, Fe (II) of group 8, Mn (II) of group 7 and Zn (II) of group 12 using $CuSO_4.5H_2O$, $FeH_{14}O_{11}S$, $MnSO_4.H_2O$ and $ZnSO_4.7H_2O$, respectively was investigated. The inhibition plots have been categorized in Figure 4-17a and Figure 4-17b. Figure 4-17a consists of the binary runs of Cu and Zn while Figure 4-17b has that of Fe and Mn. In each Figure, the Al-only run was compared to Al in their respective binary runs.

Figure 4-17a revealed that Al^{3+} transport across the membrane is reduced in the binary transport with Cu^{2+}. Using Al-only as reference line, the Al reduced in an increasing range of 1.75- 4.15% for the period 4 to 12 hrs. However, the effect of Cu on Al transport reduced to have an Al/Cu at 68.70% and 68.80%, a difference of 0.10%. Subsequently, the presence of Cu increased the transport of Al in the binary solution. Confirming that observation was the increase in recovery by 4.69% more than Al-only at 20 hrs. While there was an increase in recovery of Ca and Mg in the binary transport with Al in Figure 4-16, it did not increase Al in the binary run. However, a Cu increase affects Al in the Al/Cu transport as the Cu recovery is 3.30% and 5.20% higher than Al-only at 16 and 20 hrs, respectively, while on the other hand Cu recovery is 3.34% and 0.5% higher than Al in Al-Cu. This is because, although the hydration energy for Al is more than twice that of Cu, -4665 $KJmol^{-1}$ and -2110 $KJmol^{-1}$, respectively, it does not correspond to a higher transport of Al^{3+} as ions with higher valence diffuse slowly due to their strong hydration and bigger size (Chung, 2020; Wang et al., 2010). The hydration radius of Cu^{2+} is 0.41 and Al^{3+} is 0.48 (Geise et al., 2013), hence, Cu ion will diffuse at a faster rate than Al ion even though mono and divalent cations have less binding strength than polyvalent ions. Therefore, the balance to have a high Al recovery could be attributed to its high binding strength with the sulfonic anionic group of the membrane.

Similarly, the presence of Zn negatively influenced the recovery of Al as illustrated in Figure 4-17a. The kinetic plot of Al in Zn and Al-only indicated that the range of reduction for the entire study period was 7.28–19.25%. Recovery reduction at 8 hrs was twice the reduction at 4 hrs. However, the difference in reduction increased by 2.94 – 3.07% within 12-16 hrs. The recovery at 20 hrs was 56.03%, which is 16.23% less than the recovery recorded for Al-only. From the

hydration radius of Zn^{2+} (0.43 nm) (De Carvalho Izidoro et al., 2012), it is expected to have a higher diffusional velocity than Al^{3+}.

The recovery profile of Al-only, Al in Al/Fe and Al in Al/Mn in Figure 4-17b demonstrates that the presence of Fe in the binary recovery studies results in achieving an Al recovery lower than 50% and greater than 70% in the presence of Mn. The hydration radius of Fe^{2+} (0.43 nm) is greater than the 0.48 nm of Al^{3+} (Geise et al., 2013), hence, its high diffusional velocity. Although Fe^{2+} is expected to be in solution, the possibility of Fe^{3+} complexes forming in solution cannot be overlooked as the low recovery could also be attributed to an inhibitive polyvalent complex. The hydration energy and ionic radius of Fe^{2+} and Fe^{3+} are -1946 $KJmol^{-1}$; 0.07 nm and -4430 $KJmol^{-1}$ 0.06 nm respectively. Compared to the hydration energy and 0.053 nm ionic radius of Al^{3+}, the binding strength of Al ion and Fe^{3+} are similar, which would potentially result in similar binding characteristics with the sulfonic group of Nafion 117. Therefore, Fe recovery inhibits Al-recovery to observe the low recovery trend. Independent recovery of Fe from Fe-PWTR achieved 76% recovery after 24 hrs as compared to 72% for Al-PWTR by Prakash and SenGupta (2003) confirms the high Fe recovery over Al in the binary run. However, Fe transport is the lowest amongst the other ions owing to the recovery of 13% at 4 hrs and 53% after 20 hrs. Also, the highest transport would be credited to Mn as recovery was recorded as 30% at 4 hrs and ended at 77% at 20 hrs. The observation can be attributed to the high diffusional velocity.

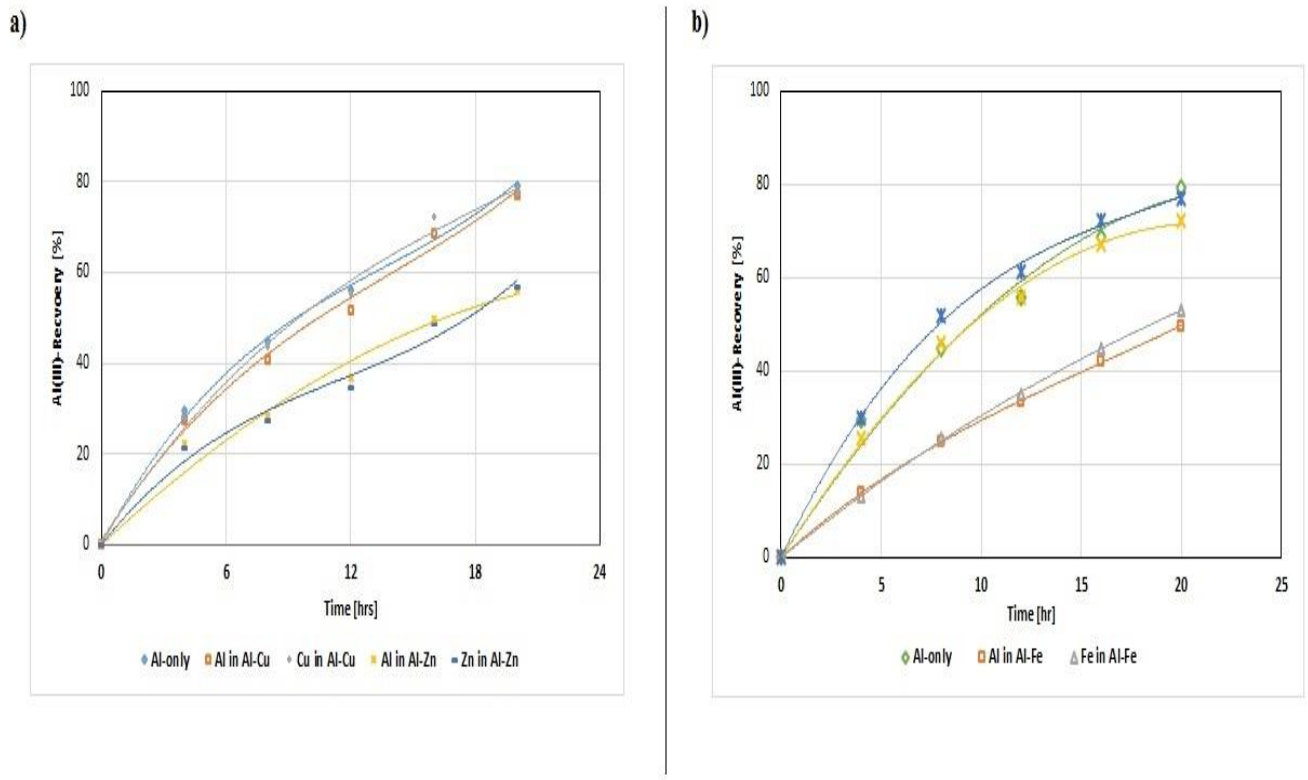

Figure 4-17: a) Cu and Zn inhibition to Al for 20 hrs; b) Fe and Mn inhibition to Al for 20 hrs

Both Figures, 4-17a and 4-17b establishes that during all binary runs, the recovery of Ca, Mg, Cu. Zn, Fe and Mn exceeds the transport of Al in their competitive runs. Although the high valence of Al should contribute to higher recoveries in such competitive run, the lower hydration radius gives the other metals in solution a transport edge over Al. The diffusional velocity drives the ions in the kinetics (0-6 hrs) and DD driven (6-20 hrs) zones, as such, there would be depletion in H^+ for exchange with Al^{3+}. Additionally, Al^{3+} would remain in solution at the feed phase before diffusing at the solution-membrane interface at the feed phase, then through to the membrane matrix and membrane-solution interface at the sweep phase due to its high hydration energy. High free energy metals prefer to remain in solution (De Carvalho Izidoro et al., 2012). The order of inhibition from the 1:1 study in descending order is Fe > Ca > Zn > Mg > Cu > Mn.

The trace transport of Fe, Cu, Zn and As to the sweep side observed by Prakash and SenGupta (2003) could only be attributed to the large Al ion population at the solution-membrane surface at the feed phase for selectivity and transport. The composition of PWTR used consisted of 1000-3000 mg/L Al, 100-300 mg/L Fe, < 10 mg/L Cu, < 30 mg/L Ca and < 20 mg/L Zn (Prakash et al., 2004). Comparing the PWTRs composition of the other metals to Al and the outcome from the binary inhibition run, it is understandable to have trace permeation. Additionally, the trace transport of organic compounds would serve as a carrier of the ions due to the solubility organo-metallic complexes formed during primary digestion of PWTR.

4.6.3 Summary of inhibition transport

Inhibition study of binary transport of Aluminium with Ca, Mg, Cu, Zn, Fe and Mn through Nafion 117 membrane was performed at constant feed and sweep phase conditions. Using established conditions, the feed and sweep flowrate were set at 50% and the sweep concentration at 0.75 M. Using a random selection system, the starting concentration for all ions under the 1:1 stoichiometric run was 400 mg/L.

While the standard run of Al-only achieved a 72.30% recovery, the binary runs of Al and their metals of study, 59.50% Ca, 69.90% Mg, 77.50% Cu, 57.10% Zn, 72.20% Fe and 76.95% Mn was recovered. The order of impact of these metals on Al^{3+} were Fe > Ca > Zn > Mg > Cu > Mn. In the transport of Al in Cu and Al in Mn, Al recovery was higher than that achieved in the standard run at different time zones. The conditions of hydration radius, ionic radius and hydration energy to analyze the observation showed that diffusional velocity which is attributed to hydration radius was the most dominating factor that led to having high transport for the other metals than polyvalent Al. As such, trace amounts of these metals would transport across the Nafion 117 membrane as long as they exist in the PWTR due to their hydration radius.

4.7 Donnan Dialysis on real Potable Water Treatment Residue

The purpose of this section was to investigate the recovery of aluminium from a PWTR and if recoveries would be as high as recovery obtained using the synthetic feed. Also, the investigation proceeded to find out if organics would penetrate through the Nafion 117 membrane from the feed phase to the sweep phase. The PWTR was obtained from the potable water treatment plant. Although it would have been prudent to take the residue from the settling tanks after coagulation, the residue was taken from the first stage of the dewatering pond. This was as a result of the process design at the treatment plant. The collection, storage and digestion of feed with HCl is presented in sub section 3.3.4.2.

4.7.1 Set-up

The feed solution obtained from the digestion of PWTR at the 0.05 M and 0.5 M concentration was to quantify the effect of acid concentration on aluminium and organics released from the PWTR matrices during digestion. The feed solutions were operated at a 1.43 mL/s feed and sweep flowrate. The sweep acid was 0.75 M HCl in a 2:1 feed phase and sweep phase volume ratio. The set-up for the PWTR in the feed phase against HCl in the sweep phase is shown in Figure 4-18.

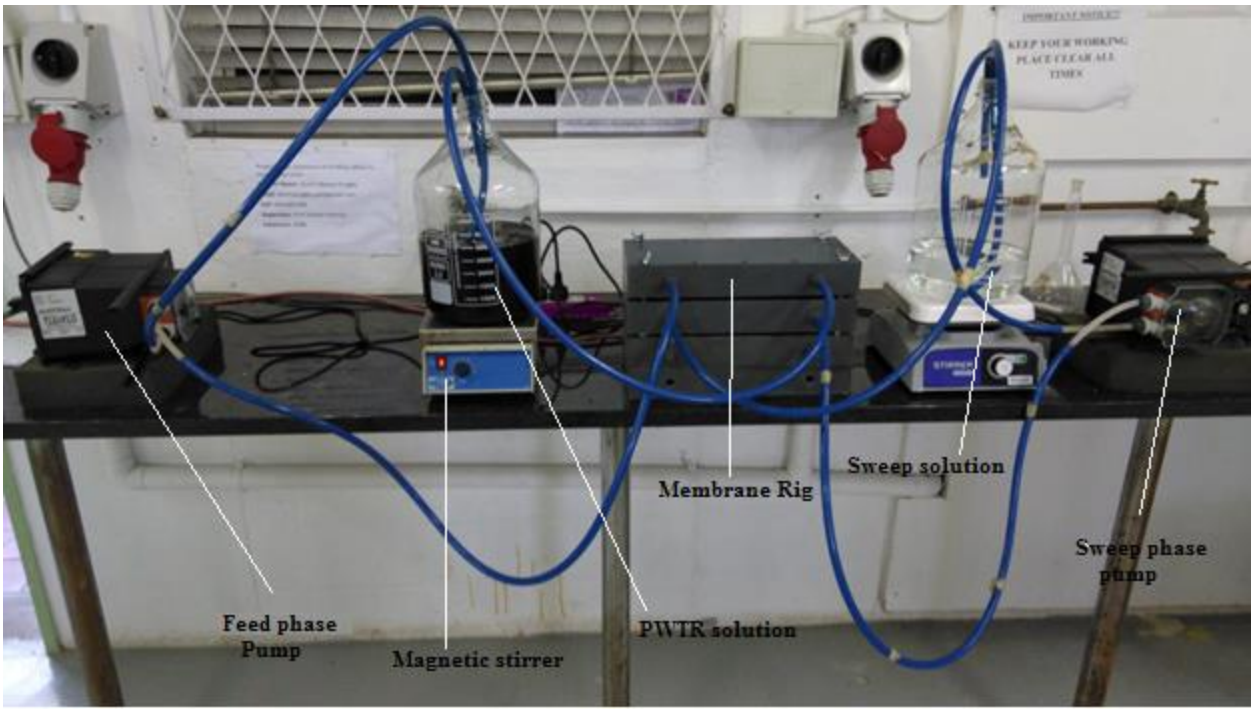

Figure 4-18: Al recovery set-up for PWTR feed

4.7.2 Aluminium recovery

Analysis of the total aluminium concentration in the leachate from the primary digestion of PWTR with HCl at 0.05 M and 0.05 M obtained an Al concentration of 300 mg/L and 700 mg/L, respectively. This indicates that, increasing the concentration of acid used in primary digestion increases the aluminium released from the residue into the solution. From this acidification, increasing the magnitude of concentration resulted in more than doubling the Al extracted. The decreasing Al in feed phase as a function of time and its respective recovery (%) in the Donnan dialysis process is illustrated with a dot plot in Figure 4-19.

Starting with a feed concentration of 700 mg/L, less than half of the Al was recovered after 32 hrs. In terms of recovery, 46.50% of the starting feed was recovered as illustrated in the Al-recovery (%) plot. This low transport can be attributed to the high hydrogen ions in the feed phase. This, therefore, reduces the exchange capabilities due to concentration gradient. The kinetics therefore becomes slow. However, the concentration of feed digested with 0.05 M had almost all Al transporting to the sweep side. From Figure 4-19, about 84-97% of Al had transported between 20-28 hrs. This is due to the high gradient exisiting between the two solutions.

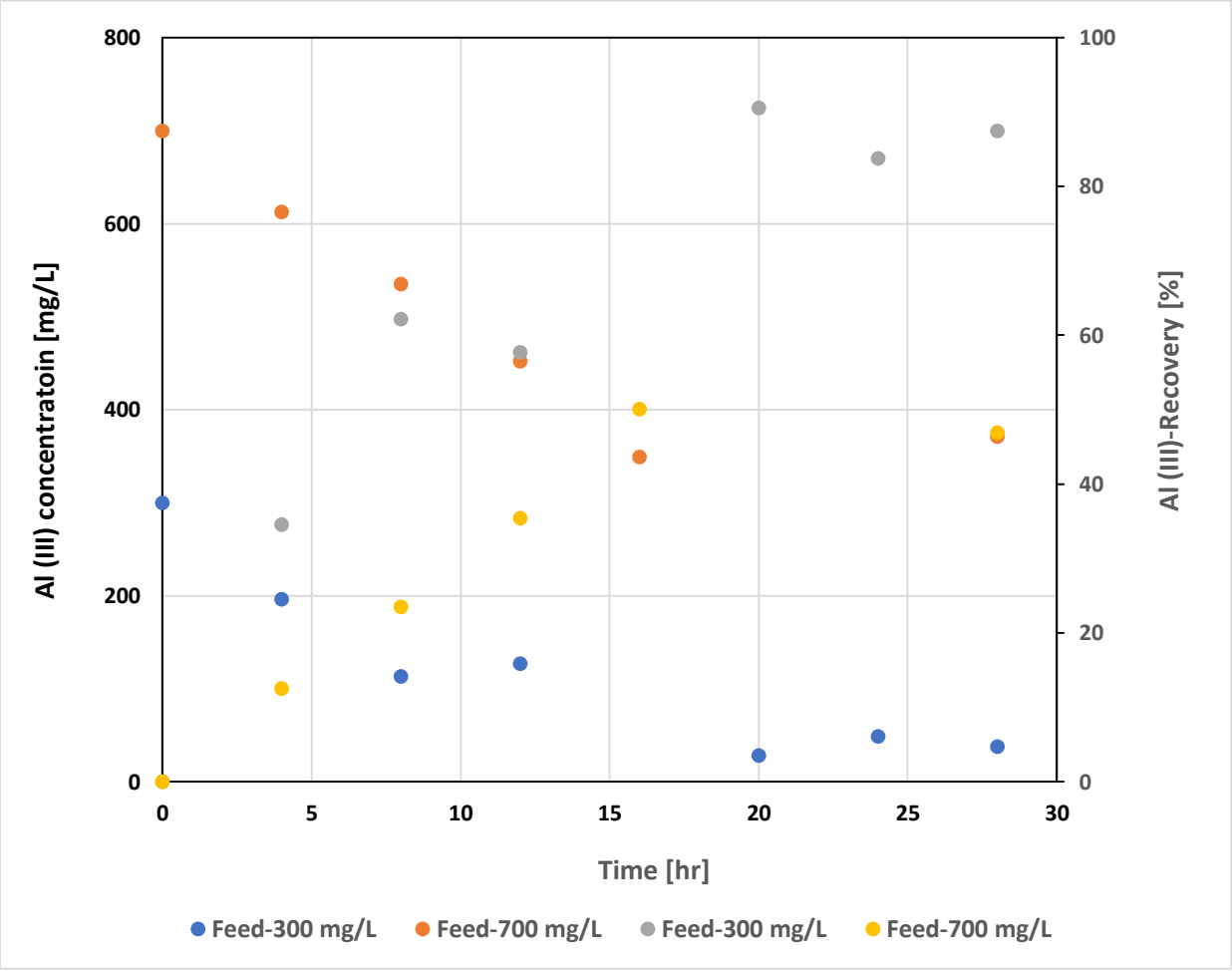

Figure 4-19: Al-PWTR transport in concentration [mg/L] and percentage recovery

4.7.3 Organics Permeation

The UV analyzer used determine the organics present in the feed and sweep phase was set at a wavelength of 254 nm. The relative change in organics is shown in Figure 4-20. From the onset, it can be seen that increasing the acid concentration for digestion increases the organic solubilization into the leachate. This will potentially lead to high organometallic composition in the leachate.

The relative organics at the feed phase for 300 mg/L and 700 mg/L were quantified as 20.14 abs/cm and 25.5 abs/cm, respectively, at time 0 hrs. A 4.35% decrease in organics for 700 mg/L was observed between 24-32 hrs whilst a 5.78% was recorded for 300 mg/L. This would have increased if recovery in section 4.7.2 was continued. However, since it was not so, ending the experiment at 28 hrs would result in a 2.4% and 1.99% decrease in organics at the feed phase.

Also, since the UV analyzer determines other compounds aside humic and organic compounds, the sweep phase absorbance can be standardized as zero due to the absence of organics at the start. From Figure 4-20, although there was a 4.35% decrease in organics at the feed phase, 1.22 abs/cm organics permeated through the Nafion 117 for 700 mg/L feed phase after 32 hrs. Similarly, 0.92 abs/cm organic increase was found at the sweep phase of the 300 mg/L.As such, 0.85 abs/cm and 0.11 abs/cm organics were within the membrane-membrane interface as that had not transported for the 700 mg/L run and 300 mg/L run, respectively.

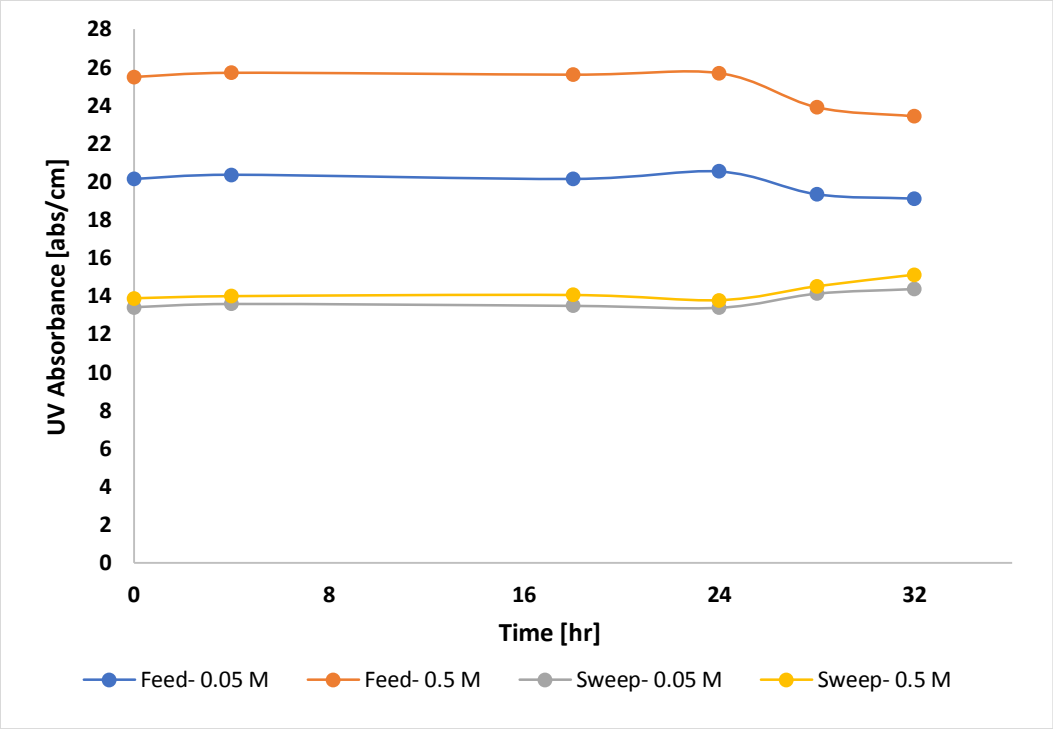

Figure 4-20: UV relative quantification of organics for 0.05 M and 0.5 M PWTR digestions

4.7.4 Summary of real PWTR DD treatment

Acidification of PWTR was done with 0.05 M and 0.5 M HCl to obtain 300 mg/L and 700 mg/L aluminium concentration. Having had Al leached increase with an increase in acid concentration for acidification, organic solubilization followed a similar trend.

After 32 hrs of DD, 42.44% of 700 mg/L feed was recovered and 97.5% at the same period for 300 mg/L. The difference in recoveries could be attributed to the low concentration gradient between the feed phase and sweep phase at 700 mg/L. Acidification of PWTR with high acid concentration reduced the ion exchange kinetics.

The determination of relative organics showed that Nafion 11 rejected 97.6 % organics at 700 mg/L run and 96.01% organics at 300 mg/L after 28 hrs. This was further reduced by 1.95% and

1.12% at each concentration, respectively. It would therefore be a step in the right direction to have a recovery study within 24-32 hrs to avoid further decrease in aluminium recovery and an increase in organic permeation through the membrane into the sweep side. Lastly, it would ensure less water transport across the membrane.

CHAPTER 5

CONCLUSIONS AND RECOMMENDATIONS

The significant findings are summarized in this chapter. Also, recommendations for further research and decision-making is provided. Investigation on the optimum range of operating variables for the recovery of alum with Donnan dialysis was performed by OFAT and statistical modelling with RSM data-driven approach using synthetic and potable water treatment residue (PWTR) sourced from a local potable water treatment plant in Durban, South Africa.

The objectives were:

1. To investigate the effect of flow rate and concentration of the feed phase and sweep phase on the recovery of aluminium.
2. To evaluate the combined effect of pH, optimal flow and concentration conditions on aluminium transport.
3. To investigate the inhibition of heavy metals in a binary transport with aluminium.
4. To evaluate the mechanistic pathway for aluminium recovery using PWTR solution and the efficiency of organic rejection by Donnan dialysis.

5.1 Conclusions

Based on analytical observation of experimental results, modelling and numerical optimization techniques employed in this research, the following findings were drawn from the study:

- After establishing the hydrodynamic effect of hydrochloric acid and sulfuric acid, hydrochloric acid was selected as the electrolytic solution for the sweep phase. The

maximum concentration for HCl was 1 M and the maximum range of concentration for aluminium after the OFAT studies for the feed phase was set at 100 to 2000 mg/L. Concentration of aluminium in the sweep solution was found to decrease after 32 hrs hence all experiments were conducted for a maximum period of 32 hrs.

- The most significant factors in ascending order was feed flowrate, sweep concentration and feed concentration. The sweep flowrate had an insignificant effect on Al-recovery. Furthermore, the significant interdependent interactions were the feed flowrate-feed concentration and the sweep concentration-sweep flowrate. A high feed concentration corresponded to low recovery. However, an increase in sweep concentration increased the recovery. The model generated showed a good correlation between the actual and predicted response R^2.
- With the effect of feed concentration, feed flowrate and pH on recovery, all factors were statistically significant. The feed concentration was found to be highly inter-twined with the pH. A medium to high pH range increased recovery. The flowrate had a linear effect on the recovery at constant sweep phase conditions. Therefore, the significant interaction was feed concentration and feed flowrate; feed concentration and pH. The model generated was statistically significant with $p < 0.05$.
- Using the hydration radius, ionic radius ad hydration energy to interpret trends of 1:1 metal inhibition on Al recovery, the order of impact was $Mn^{2+} < Cu^{2+} < Mg^{2+} < Zn^{2+} < Ca^{2+} < Fe^{2+}$. Due to the diffusional velocity dominating all factors, permeation of other metal ions is inevitable in DD transport even if these ions are in small concentrations in a digested residue.
- Acidification of PWTR resulted in high solubilization of aluminium and organics at

increasing acid concentrations. The concentration of Al released PWTR digested with 0.05 M and 0.5 M HCl was 300 mg/L and 700 mg/L, respectively. The recovery yielded 42.44% for 0.5 M acid digested feed and 98% for 0.05 M acid digested feed.

- Finally, UV 254 analysis showed that, 96-98% organics was rejected by Nafion 117 during the entire run. However, rejection rate could reduce further beyond 32 hrs.

Donnan dialysis can be used to recover aluminium in both synthetic and real PWTR residue. In synthetic feeds, 70 to 98% recovery can be achieved with an initial Al feed concentration of 100-1610 mg/L at a pH range of 2.5 to 3.7 for a wide range of feed flowrates and sweep phase conditions. For acidified leachate of PWTR, a high recovery of 98% can be achieved. However, the aluminium recovered cannot be directly used in a treatment plant due to trace amounts of other metals. Also, the aluminium in the sweep solution needed to be further concentrated.

5.2 Recommendations

The following recommendations are suggested based on the research findings on the DD module:

- Future investigations must focus on acidification route using a range of acid concentrations in synthesized aluminium feed as it was done for the pH range at the feed phase. That, in a way would aid in understanding the kinetics and recovery from acidified PWTR.
- Future studies could focus on the integration of IEM with high affinity to divalent ions to examine the extent of pure Al recovery that could be achieved. Furthermore, the integration of Donnan dialysis with chelating agents and nanofiltration to increase flux, recovery and concentrating of Al at sweep phase could be included.
- The effect of flow patterns and its effect of Al deposition on the membrane surface can be further understood with the aid of scanning electron microscopy (SEM) to analyze the Nafion 117 surface. This future study would help establish ion transport channels at active

sites and potential dead zones.

- Lastly, the non-fouling hypothesis of DD and the membrane must be evaluated in future studies through longer recovery with PWTR in order to establish industrial feasibility.

REFERENCES

Agarwal, C., Cattrall, R.W. and Kolev, S.D. 2016. Donnan dialysis based separation of gold(III) from electronic waste solutions using an anion exchange pore-filled membrane. Journal of. Membrane. Science. 514: 210–216.

Agarwal, C., Chaudhury, S., Pandey, A.K. and Goswami, A. 2012. Kinetic aspects of Donnan dialysis through Nafion-117 membrane. Journal of Membrane Science. 415–416: 681–685.

Agarwal, C. and Goswami, A. 2016. Nernst Planck approach based on non-steady state flux for transport in a Donnan dialysis process. Journal of Membrane Science. 507: 119–125.

Ahmad, T., Ahmad, K. and Alam, M. 2016a. Sustainable management of water treatment sludge through 3'R' concept. Journal of Cleaner. Production. 124: 1–13.

Ahmad, T., Ahmad, K. and Alam, M. 2016b. Characterization of Water Treatment Plant's Sludge and its Safe Disposal Options. Procedia Environmental Science. 35: 950–955.

Akoto, O., Gyamfi, O., Darko, G. and Barnes, V.R. 2017. Changes in water quality in the Owabi water treatment plant in Ghana. Applied Water Science. 7: 175–186.

Akretche, D.-E. 2000. Donnan dialysis of copper, gold and silver cyanides with various anion exchange membranes. Talanta. 51: 281–289.

Andrada, H.E., Franzoni, M.B., Carreras, A.C., Chávez, F.V., 2018 Dynamics and spatial distribution of water in Nafion 117 membrane investigated by NMR spin-spin relaxation. International Journal of Hydrogen Energy. 43: 8936–8943.

Antony, J. 2014. Fundamentals of Design of Experiments. In: Design of Experiments for Engineers and Scientists. Elsevier.7–17.

Ariono, D. and Khoiruddin, 2017. Improving Ion-Exchange Membrane Properties by the Role of Nanoparticles, in: International Conference on Engineering, Science and Nanotechnology 2016 (ICESNANO 2016). AIP Publishing.

Asante-Sackey, D., Rathilal, S., Pillay, L. and Tetteh, E.K. 2019. Effect of ion exchange dialysis process variables on aluminium permeation using response surface methodology. Environmenatl Engineering. Research. 52 (5): 714-721.

Asante-Sackey, D., Rathilal, S., V. Pillay, L. and Kweinor Tetteh, E. 2020. Ion Exchange Dialysis for Aluminium Transport through a Face-Centred Central Composite Design Approach. Processes, 8 (2): 160.

Babatunde, A.O. and Zhao, Y.Q. 2007. Constructive Approaches Toward Water Treatment Works Sludge Management: An International Review of Beneficial Reuses. Critical Reviews in Environmental Science and Technology. 37 (2): 129–164.

Babu, J.D., King, P. and Prasanna Kumar, Y. 2019. Optimization of Cu (II) biosorption onto sea urchin test using response surface methodology and artificial neural networks. International Journal of. Environmental Science and Technology. 16: 1885–1896.

Baker, R.W. 2012. Membrane Technology and Application,3rd ed, Membrane Technology. John Wiley & Sons Ltd, West Sussex-UK.

Barton, R.R. 2013. Response Surface Methodology, in: Gass, S.I., Fu, M.C. (Eds.), Encyclopedia of Operations Research and Management Science. Springer US. Boston. MA.1307–1313.

Bashir, M.J.K., Aziz, H.A., Aziz, S.Q. and Amr, S.A. 2012. An overview of wastewater treatment processes optimization using response surface methodology (RSM). 4th International. Engineering Conference. 15–16.

Ben Hamouda, S., Touati, K. and Ben Amor, M. 2017. Donnan dialysis as membrane process for nitrate removal from drinking water: Membrane structure effect. Arabian Journal of Chemistry. 10: S287–S292.

Berdous, D. and Akretche, D.E. 2002. Recovery of metals by Donnan dialysis with ion exchange textiles. Desalination. 144: 213–218.

Brandt, M.J., Johnson, K.M., Elphinston, A.J., Ratnayaka, D.D., Brandt, M.J., Johnson, K.M., Elphinston, A.J. and Ratnayaka, D.D. 2017. Storage, Clarification and Chemical Treatment. Twort's Water Supply. 323–366.

Bratby, J. 2016. Coagulation and Flocculation in Water and Wastewater Treatment. 3rd ed. IWA Publishing, London.

Bryjak, M., Poźniak, G. and Kabay, N. 2007. Donnan dialysis of borate anions through anion exchange membranes: A new method for regeneration of boron selective resins. Reactive and Functional Polymer. 67: 1635–1642.

Çengeloğlu, Y., Kir, E., Ersöz, M. 2001. Recovery and concentration of Al(III), Fe(III), Ti(IV), and Na(I) from red mud. Journal of Colloid and Interface Science. 244 (2). 342–346.

Çengeloğlu, Y., Kir, E., Ersoz, M., Buyukerkek, T. and Gezgin, S. 2003. Recovery and concentration of metals from red mud by Donnan dialysis. Colloids and Surfaces A:Physicochemical and Engineering Aspects. 223 (1-3). 95–101.

Cevheroğlu Çira, S., Dağ, A. and Karakuş, A. 2016 Application of Response Surface Methodology and Central Composite Inscribed Design for Modeling and Optimization of Marble Surface Quality. Advances in Materials Science and Engineering. 2016: 13.

Chandra, A., E, B. and Chattopadhyay, S. 2019. Physicochemical interactions of organic acids influencing microstructure and permselectivity of anion exchange membrane. Colloids and Surfaces A: Physicochemical and Engineering Aspects. 560: 260–269.

Chen, Y.J., Wang, W.M., Wei, M.J., Chen, J.L., He, J.L., Chiang, K.Y. and Wua, C.C. 2012. Effects of Al-coagulant sludge characteristics on the efficiency of coagulants recovery by acidification, In: Environmental Technology. Hong Kong SAR-P.R. China. 617–622.

Cheng, W., Liu, C., Tong, T., Epsztein, R., Sun, M., Verduzco, R., Ma, J. and Elimelech, M. 2018. Selective removal of divalent cations by polyelectrolyte multilayer nanofiltration membrane: Role of polyelectrolyte charge, ion size, and ionic strength. Journal of Membrane Science. 559: 98–106.

Cheng, W.P., Chen, P.H., Tian, D.R., Yu, R.F. and Fu, C.H. 2016a. Use of nanofiltration membranes to concentrate and recover leached aluminum from acidified water treatment sludge. Environmental Protection Engineering. 42: 19–32.

Cheng, W.P., Chi, F.H., Yu, R.F. and Tian, D.R. 2016b. Application of nanofiltration membrane in the recovery of aluminum from alkaline sludge solutions. Advances in environmental research. 5(2): 141–151.

Chung, P.C. 2020. Hydration. LibreText. available on, https://chem.libretexts.org/Bookshelves/Physical_and_Theoretical_Chemistry_Textbook_Maps/Supplemental_Modules_(Physical_and_Theoretical_Chemistry)/Thermodynamics/Ener

gies_and_Potentials/Enthalpy/Hydration. (Accessed 5 July 2020).

Cornwell, D.A., Roth, D.K. and Brown, R.A. 2010. Minimizing Water Treatment Residual Discharges to Surface Water. Water Research Foundation.USA, Denver-Colorado.

da Silva Biron, D., dos Santos, V. and Zeni, M. 2018. Ceramic Membranes Applied in Separation Processes, Topics in Mining, Metallurgy and Materials Engineering. Springer International Publishing, Cham. 7-29.

David Kuo, H.W. and Xagoraraki, I. 2016. Contaminants Associated with Drinking Water, in: International Encyclopedia of Public Health. Elsevier Inc. 148–158.

Davis, T.A. 2000. Donnan Dialysis, in: Membrane Separations. Academic Press, Annandale-NJ. 1701–1707.

De Carvalho Izidoro, J., Fungaro, D.A. and Wang, S. 2012. Zeolite synthesis from Brazilian coal fly ash for removal of Zn 2+ and Cd2+ from water. in: Advanced Materials Research. 356-360: 1900–1908.

Debora, J., Theodoro, P., Lenz, G.F., Zara, R.F. and Bergamasco, R. 2013. Coagulants and Natural Polymers : Perspectives for the Treatment of Water. Plastic and Polymer Technology. 2 (3): 55–62.

Duan, Q., Wang, H. and Benziger, J. 2012. Transport of liquid water through Nafion membranes. Journal of Membrane Science. 392–393 (393): 88–94.

Eikerling, M. 1998. Phenomenological Theory of Electro-osmotic Effect and Water Management in Polymer Electrolyte Proton-Conducting Membranes. Journal of The Electrochemical Society. 145 (8): 2684–2699.

Emelko, M.B., Silins, U., Bladon, K.D. and Stone, M. 2011. Implications of land disturbance on drinking water treatability in a changing climate: Demonstrating the need for "source water supply and protection" strategies. Water Research. 45: 461–472.

Ersöz, M., Çengelolu, Y., Kir, E., Koyuncu, M. and Yazicigil, Z. 2001. Transport of Cu(II) ions through charged cation-exchange membranes. Journal of Applied Polymer Science. 81 (2): 421–427.

Ersoz, M. and Kara, H. 2000. Cobalt(II) and Nickel(II) Transfer through Charged Polysulfonated Cation Exchange Membranes. Journal of Colloid and Interface Science. 232: 344–349.

Evuti, A.M. and Lawal, M. 2011. Recovery of coagulants from water works sludge : A review. Advances in Applied Science. Research. 2 (6): 410–417.

Finkbeiner, P., Redman, J., Patriarca, V., Moore, G., Jefferson, B. and Jarvis, P. 2018. Understanding the potential for selective natural organic matter removal by ion exchange. Water Research. 146: 256–263.

Frías, M., Vigil De La Villa, R., De Soto, I., García, R. and Baloa, T.A. 2014. Influence of activated drinking-water treatment waste on binary cement-based composite behavior: Characterization and properties. Composite. Part B Engineering. 60: 14–20.

Garmes, H., Persinb, F., Sandeauxb, J. and Pourcellyb, G. 2002. Defluoridation of groundwater by a hybrid process combining adsorption and Donnan dialysis. Desalination, 145: 287–291.

Geise, G.M., Paul, D.R. and Freeman, B.D. 2014. Fundamental water and salt transport properties of polymeric materials. Progress in Polymer Science. 39 (1). 1–42.

Goldbold, P., Lewin, K., Graham, A. and Barker, P. 2003. The potential reuse of water utility

products as secondary commercial materials final report. In: WRc technical report series. No UC 6081. WRc plc, Swindon, Wiltshire-UK,

Hassanvand, A., Wei, K., Talebi, S., Chen, G.Q. and Kentish, S.E. 2017. The role of ion exchange membranes in membrane capacitive deionisation. Membranes (Basel). 7(3): 1-23.

He, Z., Lan, H., Gong, W., Liu, R., Gao, Y., Liu, H. and Qu, J. 2016. Coagulation behaviors of aluminum salts towards fluoride: Significance of aluminum speciation and transformation. Separation and Purification Technology. 165: 137–144.

Ho, C.C., Jan, D.S.ans Tsai, F.N. 1993. Membrane diffusion-controlled kinetics of ionic transport. Journal of Membrane Science. 81 (3): 287–294.

Huang, C.H. and Wang, S.Y. 2013. Application of water treatment sludge in the manufacturing of lightweight aggregate. Construction and Building Materials. 43: 174–183.

Iben Nasser, I. and Ahmed, C. 2015. Application of donnan dialysis for cyanide removal from aqueous solutions. Internatinal Journal of Environmental Research. 9 (2): 505–510.

Ippolito, J.A., Barbarick, K.A. and Elliott, H.A. 2011. Drinking Water Treatment Residuals: A Review of Recent Uses. Journal of Environmental Quality. 40 (1): 1-12.

Jeswani, H.K., Gujba, H., Brown, N.W., Roberts, E.P.L. and Azapagic, A. 2015. Removal of organic compounds from water: life cycle environmental impacts and economic costs of the Arvia process compared to granulated activated carbon. Journal of Cleaner Production. 89: 203–213.

Jung, K.W., Hwang, M.J., Park, D.S. and Ahn, K.H. 2016. Comprehensive reuse of drinking water treatment residuals in coagulation and adsorption processes. Journal of Environmental

Management. 181: 425–434.

Kawahara, M. and Kato-Negishi, M. 2011. Link between Aluminum and the Pathogenesis of Alzheimer's Disease: The Integration of the Aluminum and Amyloid Cascade Hypotheses. International Journal of Alheimer's Disease. 2011: 1–17.

Keeley, J., Jarvis, P. and Judd, S.J. 2014a. Coagulant Recovery from Water Treatment Residuals: A Review of Applicable Technologies. Critical Reviews in Environmental Science and Technology. 44 (24): 2675–2719.

Keeley, J., Jarvis, P. and Judd, S.J. 2012. An economic assessment of coagulant recovery from water treatment residuals. Desalination. 287: 132–137.

Keeley, J., Jarvis, P., Smith, A.D. and Judd, S.J. 2016. Coagulant recovery and reuse for drinking water treatment. Water Research. 88: 502–509.

Keeley, J., Smith, A.D., Judd, S.J. and Jarvis, P. 2014b. Reuse of recovered coagulants in water treatment: An investigation on the effect coagulant purity has on treatment performance. Separation and Purification Technology. 131: 69–78.

Kleijnen, J.P.C. 2015. Response surface methodology. International Series in Operations Research and Management Science. 216: 81–104.

Koleva, M.N., Styan, C.A. and Papageorgiou, L.G. 2017. Optimisation approaches for the synthesis of water treatment plants. Computers and Chemical Engineering. 106: 849–871.

Koseoglu, T.S., Kir, E., Ozkorucuklu, S.P. and Karamizrak, E. 2010. Preparation and characterization of P2FAn/PVDF composite cation-exchange membranes for the removal of Cr(III) and Cu(II) by Donnan dialysis. Reactive and Functional Polymers. 70(11): 900–907.

Ladewig, B. and Al-Shaeli, M.N.Z. 2017. Fundamentals of Membrane Processes. In: Fundamentals of Membrane Bioreactors, Materials, Systems and Membrane Fouling. Springer Nature Singapore Pte Ltd, Singapore. 13–37.

Levenstein, R., Hasson, D. and Semiat, R. 1996. Utilization of the Donnan effect for improving electrolyte separation with nanofiltration membranes. Journal of Membrane Science. 116(1): 77–92.

Li, X.F. and Mitch, W.A. 2018. Drinking Water Disinfection Byproducts (DBPs) and Human Health Effects: Multidisciplinary Challenges and Opportunities. Environmental Science and Technology. 52(4): 1681–1689.

Liu, S., Lim, M., Fabris, R., Chow, C., Drikas, M. and Amal, R. 2009. Comparison of photocatalytic degradation of natural organic matter in two Australian surface waters using multiple analytical techniques. Organic Geochemistry. 41: 124–129.

López Días, V., Hoang, H.Q., Martínez-Carreras, N., Barnich, F., Wirtz, T., McDonnell, J.J. and Pfister, L. 2019. The use of Nafion membranes to measure 2H/1H and 18O/16O isotopic ratios in water. Journal of Membrane Science. 572: 128–139.

Luis, P. 2018. Introduction, in: Fundamental Modelling of Membrane Systems:Membrane and Process Performance. Elsevier. 1–23.

Luo, J., Wu, C., Xu, T. and Wu, Y. 2011. Diffusion dialysis-concept, principle and applications. Journal of Membrane Science. 366(1-2): 1–16.

Luo, T., Abdu, S. and Wessling, M. 2018. Selectivity of ion exchange membranes: A review. Journal of Membrane Science. 555: 429–454.

Maiden, P., Hearn, M.T.W., Boysen, R.I., Chier, P., Warnecke, M. and Jackson, W.R. 2015. 100S-042 Alum sludge re-use investigation. GHD and Centre for Green Chemistry (Monash University) for the Smart Water Fund, Victoria, ACTEW Water & Seqwater, Victoria-Australia.

Mark, H. and Workman, J. 2018 Experimental Designs, Part 1: Introduction, in: Chemometrics in Spectroscopy. Elsevier. 57–61.

Marzouk, I., Chaabane, L., Dammak, L. and Hamrouni, B. 2013a Application of Donnan Dialysis Coupled to Adsorption onto Activated Alumina for Chromium (VI) Removal. American Journal of Analytical Chemistry. 4: 420–425.

Marzouk, I., Dammak, L., Chaabane, L. and Hamrouni, B. 2013b. Optimization of Chromium (Vi) Removal by Donnan Dialysis. American Journal of Analytical Chemistry. 4: 306–313.

Masschelein, W.J., Devleminck, R. and Genot, J. 1985. The feasibility of coagulant recycling by alkaline reaction of aluminium hydroxide sludges. Water Research. 19(11): 1363–1368.

Matilainen, A., Gjessing, E.T., Lahtinen, T., Hed, L., Bhatnagar, A. and Sillanpää, M. 2011. An overview of the methods used in the characterisation of natural organic matter (NOM) in relation to drinking water treatment. Chemosphere. 83(11): 1431–1442.

McTigue, N.E. and Cornwell, D.A. 2009 Water Treatment Residuals Management for Small Systems. Water Research Foundation, USA, Denver-Colorado.

Mekonnen, M.M. and Hoekstra, A.Y. 2016. Four billion people facing severe water scarcity. Science Advances. 2(2):1-6.

Miroslav, K. 2008. Opportunity for water treatment sludge re-use. GeoScience Engineering. 54(1):

11–22.

Miyoshi, H. 1998. Diffusion coefficients of ions through ion excange membrane in Donnan dialysis using ions of different valence. Journal of Membrane Science. 141(1): 101–110.

Miyoshi, H. 1997. Diffusion coefficients of ions through ion-exchange membranes for Donnan dialysis using ions of the same valence. Chemical Engineering Science. 52(7): 1087–1096.

Mohammad, A.W., Teow, Y.H., Ang, W.L., Chung, Y.T., Oatley-Radcliffe, D.L. and Hilal, N. 2015. Nanofiltration membranes review: Recent advances and future prospects. Desalination. 356: 226–254.

Mohapatra, T., Sahoo, S.S. and Padhi, B.N. 2019. Analysis, prediction and multi-response optimization of heat transfer characteristics of a three fluid heat exchanger using response surface methodology and desirability function approach. Applied Thermal Engineering. 151: 536–555.

Montgomery, D.C. 2017. Design and analysis of experiments,9th ed. John Wiley & Sons.

Mortula, M., Bard, S.M., Walsh, M.E. and Gagnon, G. A. 2009. Aluminum toxicity and ecological risk assessment of dried alum residual into surface water disposal. Canadian Journal of Civil Engineering. 36(1): 127–136.

Nair, A.T. and Ahammed, M.M. 2017. Influence of sludge characteristics on coagulant recovery from water treatment sludge: a preliminary study. Journal of Material Cycles and Waste Management. 19(3): 1228–1234.

Nair, A.T. and Ahammed, M.M. 2014. Coagulant recovery from water treatment plant sludge and reuse in post-treatment of UASB reactor effluent treating municipal wastewater.

Environmental Science and Pollution Research. 21(17): 10407–10418.

Nair, A.T., Makwana, A.R. and Ahammed, M.M. 2014. The use of response surface methodology for modelling and analysis of water and wastewater treatment processes: A review. Water Science and Technology. 69(3): 464–478.

Napoli, L., Lavorante, M.J., Franco, J., Sanguinetti, A. and Fasoli, H. 2013. Effects on nafion® 117 membrane using different strong acids in various concentrations. Journal of New Materials for Electrochemical Systems. 16(3): 151–156.

Niquette, P., Monette, F., Azzouz, A. and Hausler, R. 2004. Impacts of substituting aluminum-based coagulants in drinking water treatment. Water Quality Research Journal of Canada. 39(3): 303–310.

Oehmen, A., Valerio, R., Llanos, J., Fradinho, J., Serra, S., Reis, M.A.M., Crespo, J.G. and Velizarov, S. 2011. Arsenic removal from drinking water through a hybrid ion exchange membrane – Coagulation process. Separation and Purification Technology. 83(1): 137–143.

Okada, T., Xie, G., Gorseth, O., Kjelstrup, S., Nakamura, N. and Arimura, T. 1998. Ion and water transport characteristics of Nafion membranes as electrolytes. Electrochimica Acta. 43(24): 3741–3747.

Okuda, T., Nishijima, W., Sugimoto, M., Saka, N., Nakai, S., Tanabe, K., Ito, J., Takenaka, K. and Okada, M. 2014. Removal of coagulant aluminum from water treatment residuals by acid. Water Research. 60: 75–81.

Ooi, T.Y., Yong, E.L., Din, M.F.M., Rezania, S., Aminudin, E., Chelliapan, S., Abdul Rahman, A. and Park, J. 2018. Optimization of aluminium recovery from water treatment sludge using

Response Surface Methodology. Journal of Environmental Management. 228: 13–19.

Pal, P. 2017. Water Treatment by Membrane-Separation Technology. In: Industrial Water Treatment Process Technology. Elsevier. 173–242.

Paull, B. and Nesterenko, P.N. 2013. Ion Chromatography. Liquid Chromatography. Elsevier. 157–191.

Pessoa-Lopes, M., Crespo, J.G. and Velizarov, S. 2016. Arsenate removal from sulphate-containing water streams by an ion-exchange membrane process. Separation and Purification Technology. 166: 125–134.

Petruzzelli, D., Limoni, N., Tiravanti, G. and Passino, R. 1998. Aluminum recovery from water clarifier sludges by ion exchange. Reactive and Functional Polymers. 38(2-3): 227–236.

Petruzzelli, D., Volpe, A., Di Pinto, A. and Passino, R. 2000a. Conservative technologies for environmental protection based on the use of reactive polymers. Reactive and Functional Polymers. 45(2): 95–107.

Petruzzelli, D., Volpe, A., Limoni, N. and Passino, R. 2000b. Coagulants removal and recovery from water clarifier sludge. Water Research. 34(7): 2177–2182.

Ping, Q., Abu-Reesh, I.M. and He, Z. 2015. Boron removal from saline water by a microbial desalination cell integrated with donnan dialysis. Desalination. 376: 55–61.

Powers, L. and Gonsior, M. 2019. Non-targeted screening of disinfection by-products in desalination plants using mass spectrometry: A review. Current Opinion in Environmental Science and Health. **7**: 52–60.

Prakash, P., Hoskins, D. and SenGupta, A.K. 2004. Application of homogeneous and

heterogeneous cation-exchange membranes in coagulant recovery from water treatment plant residuals using Donnan membrane process. Journal of Membrane Science. 237 (1-2): 131–144.

Prakash, P. and SenGupta, A.K. 2005. Modeling Al3+/H+ ion transport in Donnan membrane process for coagulant recovery. AIChE Journal. 51 (1): 333–344.

Prakash, P. and SenGupta, A.K. 2003. Selective Coagulant Recovery from Water Treatment Plant Residuals Using Donnan Membrane Process. Environmental Science & Technology. 37 (19): 4468–4474.

Pyrzynska, K. 2006. Preconcentration and Recovery of Metal Ions by Donnan dialysis. Microchimica Acta. 153 (3-4) 117–126.

Ran, J., Wu, L., He, Y., Yang, Z., Wang, Y., Jiang, C., Ge, L., Bakangura, E. and Xu, T. 2017. Ion exchange membranes: New developments and applications. Journal of Membrane Science.. 522: 267–291.

Ring, S., Hasson, D., Shemer, H. and Semiat, R. 2015. Simple modeling of Donnan separation processes. Journal of Membrane Science. 476: 348–355.

Rózańska, A. and Wiśniewski, J. 2009. Modification of brackish water composition by means of Donnan dialysis as pretreatment before desalination. Desalination. 240: 326–332,

Rozanska, A., Wisniewski, J. and Winnicki, T. 2006. Donnan dialysis with anion-exchange membranes in a water desalination system. Desalination. 198: 236–246.

Şahin, M., Görçay, H., Kir, E. and Şahin, Y. 2009. Removal of calcium and magnesium using polyaniline and derivatives modified PVDF cation-exchange membranes by Donnan dialysis.

Reactive and Functional Polymers. 69 (9): 673–680.

Sahoo, P. and Barman, T.K. 2012. ANN modelling of fractal dimension in machining. In: Mechatronics and Manufacturing Engineering. Elsevier. 159–226.

Santoro, C., Arbizzani, C., Erable, B. and Ieropoulos, I. 2017. Microbial fuel cells: From fundamentals to applications. A review. Journal of Power Sources. 356: 225–244.

Sarpola, A., Hellman, H., Hietapelto, V., Jalonen, J., Jokela, J., Rämö, J. and Saukkoriipi, J. 2007. Hydrolysis products of water treatment chemical aluminium sulfate octadecahydrate by electrospray ionization mass spectrometry. Polyhedron. 26 (12): 2851–2858.

Sata, T. 2007. Ion Exchange Membranes: Preparation, Characterization, Modification and Application. 1st ed. Royal Society of Chemistry, Cambridge.

Singh, R. 2015. Water and Membrane Treatment, in: Membrane Technology and Engineering for Water Purification. Elsevier. 81–178.

Sonoc, A.C., Jeswiet, J., Murayama, N. and Shibata, J. 2018. A study of the application of Donnan dialysis to the recycling of lithium ion batteries. Hydrometallurgy. 175: 133–143.

Strathmann, H. 2004. Ion-exchange membrane separation processes. Elsevier, Amsterdam, Netherlands.

Szczepański, P. and Szczepańska, G. 2017. Donnan dialysis − A new predictive model for non−steady state transport. Journal of Membrane Science. 525: 277–289.

Tanaka, Y. 2015. Donnan Dialysis, In: Ion Exchange Membranes. Elsevier. 445–457.

Tang, H. and Pan, M. 2015. Nafion. In: Encyclopedia of Polymer Science and Technology. John Wiley & Sons, Inc.

Teh, C.Y. and Wu, T.Y. 2014. The potential use of natural coagulants and flocculants in the treatment of urban waters, In: Yong, J., Liew, P.Y., Klemes, J.J., Varbanov, P.S. (Eds.). Chemical Engineering Transactions. AIDIC: Italian Association of Chemical Engineering, Prague. 1603–1608.

Tetteh, K.E. and Rathilal, S., 2019. Application of Organic Coagulants in Water and Wastewater Treatment. Organic. Polymer. DOI: http://dx.doi.org/10.5772/intechopen.84556

Toms, D., Deardon, R. and Ungrin, M. 2017. Climbing the mountain: experimental design for the efficient optimization of stem cell bioprocessing. Journal of Biological Engineering. **11 (1):** 35.

Turki, T. and Amor, M. B. 2017. Nitrate removal from natural water by coupling adsorption and Donnan dialysis. Water Science and Technology: Water Supply, 17 (3): 771–779.

U.S. EPA. 2011. Drinking Water Treatment Plant Residuals. Management Technical Report. Summary of residuals generation, treatment and disposal at large community water systems. United State Environmental Protection Agency (U.S.EPA). ISBN: EPA 820-R-11-003.

Ulmert, H. and Särner, E. 2005. The ReAl Process – A combined membrane and precipitation process for recovery of Aluminum from waterwork sludge. Vatten. 61. 273–281.

Uysal, A., Tuncer, D., Kir, E. and Koseoglu, T.S. 2017. Recovery of nutrients from digested sludge as struvite with a combination process of acid hydrolysis and Donnan dialysis. Water Science and Technology. 76 (10): 2733-2741.

Vanoppen, M., Stoffels, G., Demuytere, C., Bleyaert, W. and Verliefde, A.R.D. 2015. Increasing RO efficiency by chemical-free ion-exchange and Donnan dialysis: Principles and practical

implications. Water Research. 80: 59–70.

Velizarov, S. 2013. Transport of arsenate through anion-exchange membranes in Donnan dialysis. Journal of Membrane Science. 425–426: 243–250.

Wagner, J.R., Mount, E.M. and Giles, H.F. 2014. Design of Experiments, In: Extrusion. Elsevier. 291–308.

Wang, Q., Lenhart, J.J. and Walker, H.W. 2010. Recovery of metal cations from lime softening sludge using Donnan dialysis. Journal of Membrane Science. 360 (1-2): 469–475.

Warsinger, D.M., Chakraborty, S., Tow, E.W., Plumlee, M.H., Bellona, C., Loutatidou, S., Karimi, L., Mikelonis, A.M., Achilli, A., Ghassemi, A., Padhye, L.P., Snyder, S.A., Curcio, S., Vecitis, C.D., Arafat, H.A. and Lienhard, J.H. 2018 A review of polymeric membranes and processes for potable water reuse. Progress in Polymer Science. 81: 209–237.

Watson, D.W. 2018. How It Works: Ion-Exchange SPE. available on, http://www.chromatographyonline.com/how-it-works-ion-exchange-spe. (Accessed 12 December 2018)

Weng, L., Temminghoff, E.J.M., Van Riemsdijk, W.H. 2002. Aluminum speciation in natural waters: Measurement using Donnan membrane technique and modeling using NICA-Donnan.. Water Research. 36: 4215–4226.

Wenten, I.G. 2016. Recent developments in heterogeneous ion-exchange membrane: preparation, modification, characterization and performance evaluation. Journal of Engineering Science and Technology. 11 (7): 916–934.

Wiśniewski, J. and Rózańska, A. 2007. Donnan dialysis for hardness removal from water before

electrodialytic desalination. Desalination. 212: 251–260.

Wiśniewski, J. and Różańska, A. 2006. Donnan dialysis with anion-exchange membranes as a pretreatment step before electrodialytic desalination. Desalination. 191: 210–218.

Wiśniewski, J.A., Kabsch-Korbutowicz, M. and Łakomska, S. 2014. Ion-exchange membrane processes for Br − and BrO 3 − ion removal from water and for recovery of salt from waste solution. Desalination. 342: 175–182.

Xie, G. and Okada, T. 1995. Water Transport Behavior in Nafion 117 Membranes. Journal of The Electrochemical Society. 142 (9): 3057.

Xu, T. 2005. Ion exchange membranes: State of their development and perspective. Journal of Membrane Science. 263. 1–29.

Xue, T., Longwell, R.B. and Osseo-Asare, K. 1990. Mass transfer in Nation membrane systems: Effects of ionic size and charge on selectivity. Journal of Membrane Science. 58 (2): 175–189.

Zhao, B., Zhao, H., Dockko, S. and Ni, J. 2012. Arsenate removal from simulated groundwater with a Donnan dialyzer. Journal of Hazardous Materials. 215–216: 159–165.

Zhao, B., Zhao, H. and Ni, J. 2010. Modeling of the Donnan dialysis process for arsenate removal. Chemical Engineering Journal. 160 (1): 170–175.

APPENDIX

Appendix A: Materials of Construction and set-up

The appendix on materials of construction and set-up elaborates on the materials, quantity and purpose of usage as cited in Table A-1. The procedure to used to mount the laboratory scale set-up is also considered.

Table A- 1: Material of construction DD cell

Material	Description	Quantity	Usage
PVC Block	35 cm x 15.10 cm x 4 cm	2	Houses the membrane
Peristatlic pump	Maximum flow: 2.6 mL/s	2	Transport feed and sweep phase electrolytic solution
Nafion 117 Membrane	30 cm x 10 cm	1	Ion exchange medium
PTFE tubing	1 cm inner Diameter 8 m long	1	Transportation of feed and sweep solutions
Nozzels	1 cm	4	Connects tubing to membrane block
Glass vessels	5000 mL	2	Storage of feed and sweep solution
Magnetic stirrers	-	2	For homegeinity of solutions
Bolts and wing nuts	M8x 120mm s/s	14	Clamping of PVC blocks
Silicon rubber	336.3 cm^2	1	Seals PVC block and membrane

Hose clips	-	8	Keep tubes well fitted to nozzels

Quality assurance steps were taken to ensure that the PVC blocks have been properly extruded to accommodate the nozzles with no transport blockagae and bolt holes. The front view of the two blocks (unclamped) in Figure A-1, the opened view in Figure A-2a and the top view of the membrane blocks in Figure A-2b.

Figure A- 1: Front view of membrane block

a) b)

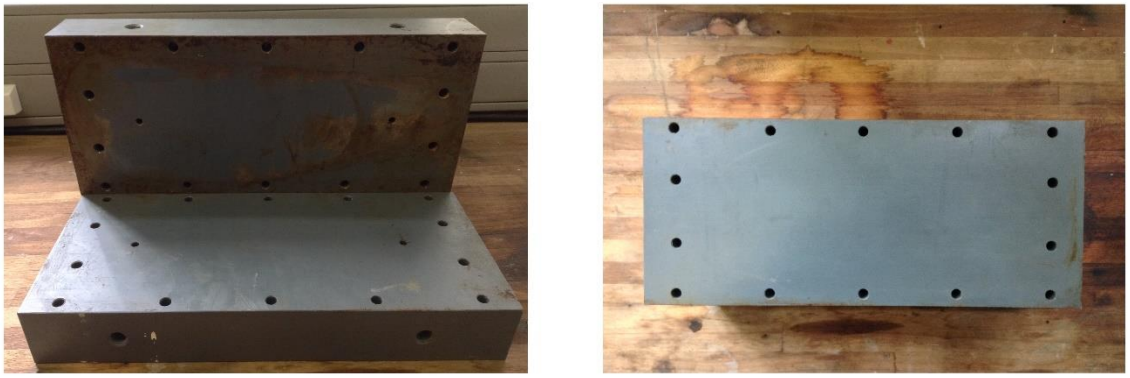

Figure A- 2: a) opened membrane rig showing two inner channels; b) Top-view of closed membrane rig

The nozles showin Figure A-3a are wrapped with Teflon tapes and then screwed into the PVC membrane block as illustrated in Figure A-3b The PVC block making the rig is opened and the treated membrane is on a silicon rubber support as in Figure A-3c. The support ensures that the blocks are clamped tightly without any leaks.

Figure A- 3: a) nozzels for block to pipe connection; b) screwed nozzles; c) Nafion membrane on silicon rubber support

The other block is clamped with stainliness steel bolts and wig-nuts and tubes connected are demonstrated in Figure A-4. Four blue Teflon tubes, two on the top block and the remaining on the down blocks are connecrted to feed the membrane with electorlyteic solutions for the counter transport of Al^{3+} - H^{+}.

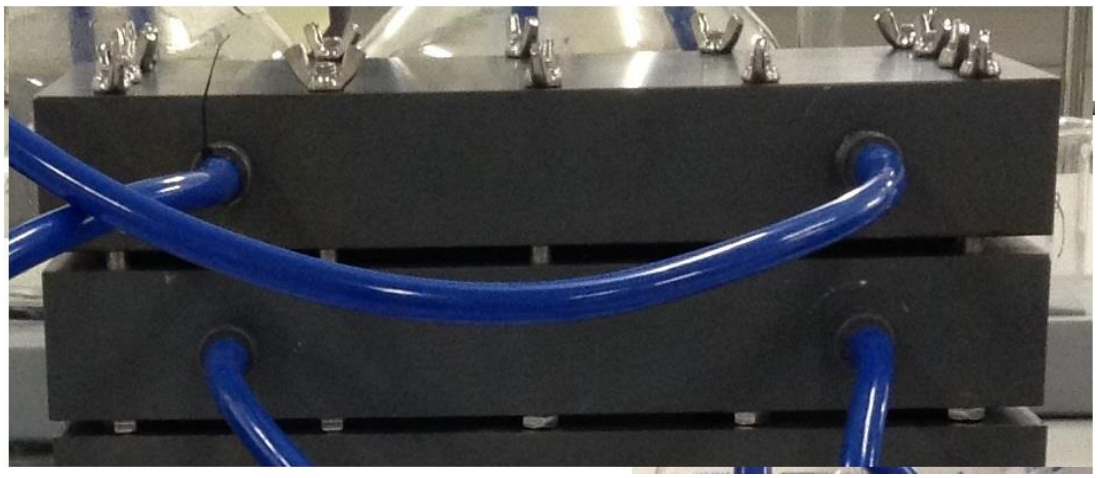

Figure A- 4: Completed Donnan dialysis membrane block cell.

The blue Teflon tubing is then connected to two 5L glass vessels that have been placed on magnetic stirrers for contious agitiation of feed and sweep solutions to improve homogeneity. The glass vessels are for the feed and sweep phase. The feed solution flows on top of the membrane whilst the sweep solution flows beheath. The tubes are also connected to respective feed and sweep phase pumps in Figure A-5. The pump has adaptors that help to connect the tubes to the pump without any leaks. The final set-up is shown in Figure 3-4.

Figure A- 5: Peristaltic pump

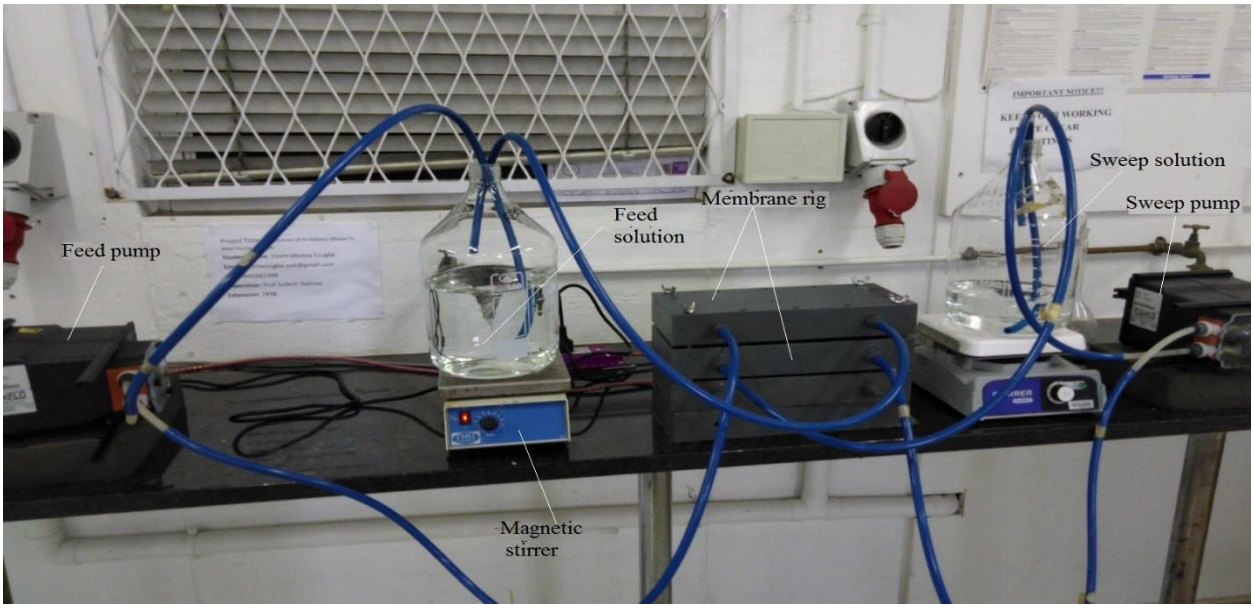

Figure 3-4: Actual Experimental set-up

Appendix B: Quality checks and Analytical Protocol

Appendix B-1: Leak Test

The quality of this experiment is a function of leakage, such that any leak from either phases invalidates the results obtained. Prestart checks are made on sealings,Teflon pipes to the pumps and inner tubing of the peristaltic pump for any tear. The placement of rubber seals in between the PVC block and membrane must align. Furthermore, tear in the membrane is check since its availability affects efficient counter exchange of ions and causes solution permeation.

After assembling the rig, the feed and sweep phase vessels were filled with 3L of water and tubes immersed in vessels correctly. The feed phase pump was switched on to operate for an hour. Observingly, there was no change in volume at the feed and sweep phases. A change in sweep phase volume would possibility be attributed with membrane tear. If reduction in feed phase volume did not contribute to change in sweep phase volume, the leak would be attributed to less tightening of PVC blocks and nozzeles or possible tear along the tubes.

Appendix B-2: Micro-plasma atomic emission spectrophotometer

The Agilent MP-AES, MY 18379001 was used to quantify the ions in solution as metals. The start-up and shut-down process are provided below.

<u>Start-up:</u>

- Pre-checks on intake and exhaust lines, connecting gas lines and all other tubings are well connected.

- The exhaust system was switched on followed by the switching on of the nitrogen generator to warm up the MP-AES for about 10 mins. The connecting computer and other peripherals were then switched on.
- The MP-AES was then turned on and Plasma switched on. The settings used were 3 sec read time, -10 viewing position and nebulizer flow of 0.9 l/min.
- The MP-AES was calibrated with four standards of aluminium and other metals of concern. The standards were 2 ppm, 10 ppm, 25 ppm and 50 ppm. It is known that calibration of aluminium above 50 ppm deviates a straight line. The R-square was between 0.98- 0.99.
- Samples collected at time intervals were diluted between 5 to 100 times with 1% wt HNO_3 to volume.

Shut down

- The spray chamber was rinsed with aspirating water and extinguish the Plasma by choosing the Plasma off from the buttom drop-down arrow.
- The nitrogen gas was left to flash through the system for about 5 mins.
- The MP-AES was switched off.

Appendix B-3: Ultra violet visible spectrophotometer

The UV-vis used for quanitification of relative organics was switched on and the lamps are left to warm up for 12 hrs in order to stabilize. Two quartz cuvettes were wiped with cloth to remove an fingerprint traces. One of the cuvette is filled with distilled water to serve as the blank. The cuvette with the blank was inserted and aligned properly. The lid was covered to prevent the enterance of

ambient light. The equipment was then initialized to have the deionized water as reference point and zeroed.

The lid was opened and the cuvette with the PWTR sample from feed and sweep phase of DD system taken at time intervals were inserted along side the blank. The wavelength of 250 nm was selected and samples analyzed. The cuvette was removed, rinsed with deionized water and wiped clean. This process was followed for all samples.

After all the samples had ben analyzed, the cuvettes were removed, rinsed and wiped clean. The UV-vis was switched off.

Appendix C: Raw Data collected

Appendix C provides the data collected from the experiments performed in research which includes, pump calibration (Table C-1), Validation and error analysis, mass balance, and the four key objectives.

The data for validation and error analysis conducted in section 4.2 of the thesis is provided in Table C-2 using a starting condition of 200 mg/L Al feed concentration, 0.625 mL/s feed and sweep flowrate and 0.5 M HCl sweep concentraton

Table C- 1:Repeatability runs for feed phase

Time	0	4	8	12	16	20	24	28
Main Run, Feed (mg/L)	200	192	161.40	130.50	130	120	105.25	84
Repeat 1 Feed (mg/L)	200	180	155	133.80	129	124	82.5	81.20
Repeat 2 Feed (mg/L)	200	175	158	128	135	117	109	100.9

Table C-3 provides the data for Al^{3+} mass balance verification investigated in section 4.2.1 of the thesis.

Table C- 2: Mass balance and verification studies

Time (hrs)	Feed (mg/L)	Sweep (mg/L)
0	3256	0
4	3009.10	675.10
8	2818	1035
16	2144	2400
20	1608.70	2920

24	1311.18	3500
28	1129.40	4240
32	1019.50	4950
36	998.40	6698.50
44	910	6340
48	899.73	6160

Table C-4 provides the data points for OFAT studies investigated at 24 hrs in section 4.4

Table C- 3:Al recovery limit data

Number	Condition [Feed flowrate- Sweep flowrate]	Al concentration in Feed solution at t=24 hrs		
		2000 mg/L	3000 mg/L	3300 mg/L
1	Low -Low	861	1872	2219.58
2	High -High	966	1593.6	1855.92
3	High-Low	715	1662	1662
4	Low-Low	768	1776	2145

Table C-5 cites the data for Face centered central composite design for the significant studies on feed concentration, feed flowrate, sweep concentration and sweep flowrate in section 4.6, whilst Table C-6 shows the data for inhibition studies in section 4.11. Table C-7 provides the aluminium DD recovery in feed and sweep concentration for 0.05 M and 0.5 M HCl acidification of the PWTR in section 4.13.2. Table C-8 give the data points on the UV assessment of organics in both feed and sweep PWTR samples in section 4.13.3.

Table C- 4: FC-CCD for significant effect

Condition at t=0 Feed conc (mg/L)/ feedflowrate (%)/ sweep conc. (M)/ sweep flowrate (%)	Time (hrs)	Feed conc (mg/L)
2000/25/0.25/25	4	1941
	8	1909
	12	1533.50
	16	1509.50
	20	1445.50
	24	1436.40
	28	1358.50
	32	1282.
2000/25/1/85	4	1617
	8	1617
	12	1344.50
	16	1180.50
	20	974
	24	872
	28	760.5
	32	637.50

2000/85/1/85	4	1671.50
	8	1500.50
	12	1415
	16	1246
	20	1077
	24	969.05
	28	855
	32	723
2000/25/1/25	4	1691
	8	1486.50
	12	1363.50
	16	1125.50
	20	1001
	24	845
	28	776.50
	32	653.50
2000/85/0.25/25	4	1715
	8	1674
	12	1658.50
	16	1483
	20	1448
	24	1310
	28	1325.50
	32	1309.50

2000/85/0.25/85	4	1738.5
	8	1670.5
	12	1549.5
	16	1569
	20	1523
	24	1298.5
	28	1114.5
	32	1054.5
2000/25/0.25/85	4	1782
	8	1655.50
	12	1548
	16	1510
	20	1392.5
	24	1369
	28	1314
	32	1288.50
2000//55/0.625/55	4	1839
	8	1655.5
	12	1624.5
	16	1238.5
	20	1094.5
	24	980.5

	28	871.5
	32	813.5
	4	1727
	8	1501
200/85/1/25	12	1359
	16	1079
	20	958
	24	723
	28	669.5
	32	553
100/25/1/25	4	84.275
	8	66.8
	12	56.775
	16	45.725
	20	37.8
	24	30.425
	28	23.4
	32	22.3
	4	74.275
	8	59.825
	12	47.975

100/85/0.25/25	16	37.825
	20	32.5
	24	24.075
	28	19.275
	32	15.5
100/25/0.25/85	4	75.95
	8	64.2
	12	54.4
	16	48.6
	20	44.75
	24	41.6
	28	40.625
	32	38.1
100/85/1/85	4	63.9
	8	49.35
	12	42.5
	16	28.7
	20	20.05
	24	13.15
	28	8.2
	32	6.35

100/25/0.25/25	4	81.225
	8	69.5
	12	61.775
	16	52.375
	20	48.425
	24	40.95
	28	36.8
	32	33.95
100/85/1/25	4	71.83
	8	54.675
	12	38.6
	16	27.13
	20	18.75
	24	12.6
	28	8.65
	32	5.18
	4	73.2
	8	52.875
	12	38.9
	16	30.6
	20	23.8

100/85/0.25/85	24	18.95
	28	14.075
	32	10.3
100/25/1/85	4	82.9
	8	73.43
	12	63.83
	16	57.30
	20	49.70
	24	41.48
	28	35.85
	32	31.15
100/55/0.625/55	4	76.025
	8	52.95
	12	44.575
	16	31.325
	20	23.55
	24	12.85
	28	10.725
	32	7.625
	4	877.5
	8	707.50
	12	598

1050/55/0.625/55	16	488.50
	20	419
	24	219.50
	28	287.45
	32	147
1050/55/0.625/55	4	824.5
	8	647
	12	475
	16	380.5
	20	309.5
	24	222.6
	28	204
	32	169.5
1050/25/0.625/55	4	850.25
	8	649
	12	551
	16	418.25
	20	357.75
	24	498.5
	28	479.75
	32	417

1050/50/0.625/50	4	827.25
	8	616.75
	12	457.25
	16	362.25
	20	277.75
	24	227
	28	194.5
	32	149.3
1050/55/1/55	4	829
	8	638
	12	481.75
	16	391.5
	20	254.25
	24	171.75
	28	110.55
	32	102.75
1050/55/0.625/25	4	820.25
	8	593.5
	12	462.75
	16	352.25
	20	276

	24	221.50
	28	178.75
	32	148.5
	4	846.5
1050/55/0.625/85	8	690.75
	12	565
	16	492.25
	20	425
	24	345.75
	28	310
	32	235.25
1050/85/0.625/55	4	1014
	8	737.25
	12	637.75
	16	508
	20	412.25
	24	290.5
	29	261.75
	32	201
	4	941.25
	8	800.5

1050/55/0.25/55	12	741.75
	16	668.75
	20	606.75
	24	536.5
	28	505.5
	32	475
1050/55/0.625/55	4	816.25
	8	645
	12	473
	16	378.25
	20	308.5
	24	222.475
	28	205
	32	158
1050/55/0.625/55	4	877.5
	8	707.5
	12	598
	16	488.5
	20	419
	24	219.5
	28	287.5

	32	147

Table C- 5: Binary Inhibition transport

Time (hrs)	Feed of Al-only	Feed of Al/Ca (mg/L)		Feed of Al/Mg (mg/L)		Feed of Al/Cu (mg/L)	
		Al	Ca	Al	Mg	Al	Cu
0	400	400	400	400	400	400	400
4	282.28	307.80	289.60	322.50	306.10	289.30	288.80
8	221.40	289.60	228.10	272.30	248.30	237.20	225.40
12	176.16	252.60	191.20	230.20	203.60	192.60	178.30
16	124.84	216.70	173.10	194.10	150.00	125.40	111.50
20	82.96	180.90	147.60	162.10	121.80	92.20	80.20
Time (hrs)		Feed of Al/Zn (mg/L)		Feed of Al/Mn (mg/L)		Feed of Al/Fe (mg/L)	
		Al	Zn	Al	Mn	Al	Fe
0		400	400	400	400	400	400
4		311.40	313.40	297.50	280.00	344.40	348.20
8		286.10	252.40	216.50	193.30	301.00	298.10
12		252.40	260.40	177.40	154.90	266.60	259.40

16	201.80	203.80	131.50	110.40	232.00	220.40
20	175.90	171.80	111.30	92.20	201.40	188.20

Table C- 6: Aluminium feed concentration for 0.05 M and 0.5M acidification DD recovery

Time (hrs)	Al concentration (mg/L)- Feed solution	
	0.05 M	0.5 M
0	300	700
4	196.32	612.50
8	113.4	535.50
12	126.81	451.92
16	-	349.30
20	28.20	-
24	48.63	-
28	37.5	371.42
32	7.5	403.92

Table C- 7:UV-vis analysis of PWTR

Time (hrs)	Feed solution		Sweep solution	
	0.05 M	0.5 M	0.05 M	0.5 M
0	20.15	25.50	13.42	13.89
4	20.37	25.72	13.59	14.00

18	20.15	25.62	13.49	14.06
24	20.54	25.70	13.39	13.79
28	19.35	23.91	14.13	14.52
32	19.12	23.43	14.37	15.13

Appendix D: Sample Calculations

The section of the appendix provides sample calucations for the error analysis and percentage recovery in the entire Chapter 4. For the sample calculation on the validation and error analysis, the sweep phase Al concentration is shown.

Table D- 1: Repeatability runs for sweep phase

Time	0	4	8	12	16	20	24	28
Main Run, Sweep (mg/L)	0	75.4	150	193	220	274.9	285	84
Repeat 1 Sweep (mg/L)	0	66.70	150	183	215	279	265	334
Repeat 2 Sweep (mg/L)	0	82.70	154	193	209	273	269	325

- The mean and standard deviation at each time intercval was calculated from Table …

Using datat points at t= 4hrs, the mean = $\frac{75.4+66.70+82.70}{3}$ = 74.93 mg/L

- The standard deviation is then provided as,

std dev= $\sqrt{\frac{((75.4-74.93)^2+(66.70-74.93)^2+(82.70-74.0)^2))^2}{3}}$ = 6.5403 mg/L

- The calculated mean is deducted from each run value (main and repeated) and the average of the results is the calculated. The average obtain at the considered time level is converted into percentage by dividing the average by the mean.

  Taking t=4hrs as an example: $\frac{(75.4-74.93)+(66.70-74.93)+(82.70-74.93)}{3}$ = 5.49 mg/L

The average percentage deviation (avg dev. %) for at 4 hrs is given by

$= \frac{\frac{75.4+66.70+82.70}{3}}{\frac{(75.4-74.93)+(66.70-74.93)+(82.70-74.93)}{3}}$ = 7.33%

The mean, standard deviation and average mean and average percentage deviation for each time interval is provided in Table D-2. The final table was presented in Table 4-1 of section 4.2

Table D- 2: Mean, standard deviation, average and average deviation for validation and error analysis

Time	0	4	8	12	16	20	24	28
Mean (mg/L)	0	74.93	151.33	189.67	214.67	275.63	273.00	332.00
Std dev	0	6.45	1.89	4.71	4.49	2.50	8.64	5.10
Average of (run-mean) (mg/L)	0	5.49	0.89	4.44	3.78	2.24	5.33	4.67
Avg dev.(%)	0	7.33	0.59	2.34	1.76	0.81	1.95	1.41

- The Al recovery and other recovery values (%) is calculated using the equation:

$$Al - recovery\ (\%)_{t=final}\ \frac{Feed\ conc_{t=0} - Feed\ conc_{t=final}}{Feed\ conc._{t=0}} \times 100 \qquad \text{D1- 1}$$

Taking condition in Table D-3, the data points are placed into the equation.

Table D- 3: Feed concentration for DD experiment

condition	100 mg/L Feed concentration, 85% feed and sweep flowrate and 1 M HCl								
Time (hrs)	0	4	8	12	16	20	24	28	32
Conc	100	64.75	50.13	42.83	28.93	20.15	13.10	8.20	6.4

Recovery at time,12 hrs, Al-rec (%)=$\frac{100-42.83}{100} \times 100$= 57.17%

Same is applied at each time interval to obtain recovery. Table D-4 provides the recovery at each time.

Table D- 4: Al-recovery for condition under consideration

Time (hrs)	0	4	8	12	16	20	24	28	32
Al-rec (%)	0	35.25	49.88	57.18	71.08	79.85	86.90	91.80	93.60